Biomarkers and cell phenotypes in TB patients with minimal or persisting lung inflammation post-anti-TB treatment and *ex-vivo* atorvastatin immunomodulatory effects on *M. tuberculosis*-infected PBMC

By

Bongani Motaung

[B.Sc. Hons (Microbiology), M.Sc. (Molecular Biology)]

Thesis submitted for the Degree of DOCTOR OF PHILOSOPHY (Ph.D.) to the Department of Pathology, Faculty of Health Science, University of Cape Town.

Supervisor: Prof. Reto Guler

Co-supervisors: A/Prof. Friedrich Thienemann and Dr. Mumin Ozturk

Cytokines and Disease Group,
International Centre for Genetic Engineering & Biotechnology (ICGEB), Cape Town Component, IIDMM, Division of Immunology,
Faculty of Health Sciences, University of Cape Town,

February 2024

Declaration

I, Bongani Motaung, hereby declare that the work on which the thesis is based, is my original work (except where acknowledgments indicate otherwise) and that neither the whole work nor any part thereof is being, has been, or is to be submitted for another degree in this or any other University.

I empower the University of Cape Town to reproduce for the purpose of research either the whole or any portion of the contents in any manner whatsoever.

……

Bongani Motaung

12 February 2024

Dedication

This thesis is dedicated to my late mother, Nomsombuluko Emily Motaung, and my late grandmother, Nomvula Miriam Motaung.

Acknowledgments

I would like to extend my sincere gratitude to the following individuals, institutes, and funding bodies who have made enormous contribution to the execution of this thesis.

Firstly, I wish to thank my supervisor Prof. Reto Guler, for affording me the opportunity to join his research team under his supervision. I further wish to commend my supervisor for the immeasurable support through the years and enormous contribution to my growth within the research field. Thank you for your teaching patience, availability, encouragement, and providing funding to execute this research project.

A special thanks to my co-supervisors Dr Mumin Ozturk and A/Prof. Friedrich Thienemann for their enormous support, troubleshooting, and constructive suggestions throughout the research program.

I wish to extend my thankfulness to Prof. Frank Brombacher, International Centre for Genetic Engineering and Biotechnology (ICGEB), and the University of Cape Town (UCT) for providing suitable research facilities to facilitate the execution of this study.

I would like to sincerely thank all the study participants around Cape Town, South Africa for their courage and selflessness in providing biological samples which made this project a success.

A special thanks to Dr. Solima Sabeel and Miss Wendy Green for being the greatest laboratory partners daily and for ensuring a smooth operational flow of things from procurement to sample processing and storage.

Thank you to our General Medicine and Global Health (GMGM) clinical team; Dr Sandra Mukasa, Dr Karen Wolmarans, Nosipho Portia Mkuzangwe, Ndilisa Siwela, Richard Luvuyo Valela, Phila Mawu, Antoneta Mashinyira, Siphokazi Khonkwane, and Nolusindiso Thelma Lokruzo for all the hard work ranging from participant recruitment to sample collection and sample delivery to the laboratory. Your efforts are greatly appreciated.

A special thanks to my colleagues from the Brombacher Group (Cytokine and Disease group) for all the assistance offered in times of need, friendliness which made the lab habitable, encouragements, suggestions in times of confusion and critical discussions around scientific procedures; Dr. Mumin Ozturk, Dr. Sabelo Hadebe, Dr. Suraj Parihar, Miss Sibongiseni Poswayo, Miss Nontobeko Mthembu, Dr. Solima Sabeel, Dr. Bernard Osero, Dr. Shandré

Pillay, Miss Lwanda Ndwandwe, Miss Noxolo Ntuli, Dr. Lorna Gcanga, Mr. Robert Rousseau, Dr. Rudranil Hazra, Mr. Paul Ikwegbue.

I am grateful to EDCTP and NRF for providing financial assistance during this research work.

Finally, I wish to humbly thank my family; my aunt Sibongile Motaung, and my siblings Thabiso Motaung, Siboniso Mndaweni, Nonhlanhla Pretty Ngwenya, Silindile Motaung, and Thembeka Kubheka for the support during this period and mostly thank my partner Portia Manngo and my son Bonginkosi Motaung for standing with me and being always the pillar of strength. Your words of wisdom and encouragement will forever be cherished.

Publication contributions

Published and accepted manuscripts, with notable contributions

Authors: Solima Sabeel*, **Bongani Motaung***, Mumin Ozturk, Sandra Mukasa, Andre Pascal Kengne, Dirk Blom, Karen Sliwa, Emmanuel Nepolo, Gunar Günther, Robert J. Wilkinson, Claudia Schacht, Friedrich Thienemann, Reto Guler

Title of contribution: Protocol for systematic review and meta-analysis: impact of statins as immune-modulatory agents on inflammatory markers in adults with chronic diseases.

Journal, Date: BMJ Open, 2020

Publisher: BMJ Publishing Group

Format: Protocol

DIO: 10.1136/bmjopen-2020-039034

***Joint first authors**

Authors: Reto Guler, Mumin Ozturk, Solima Sabeel, **Bongani Motaung**, Suraj P Parihar, Friedrich Thienemann, Frank Brombacher

Title of contribution: Targeting Molecular Inflammatory Pathways in Granuloma as Host-Directed Therapies for Tuberculosis.

Journal, Date: Frontiers in Immunology, 2021

Publisher: Frontiers Media SA

Format: Review

DIO: 10.3389/fimmu.2021.733853

Authors: Cosnet L Rametse, Emily L Webb, Carolina Herrera, Berenice Alinde, Asiphe Besethi, **Bongani Motaung**, Tshepiso Mbangiwa, Lloyd Leach, Shorok Sebaa, Azure-Dee A P Pillay, Thabiso B Seiphetlo, Boitshoko Malhangu, Stefan Petkov, Laura Else, Susan Mugaba, Patricia Namubiru, Geoffrey Odoch, Daniel Opoka, Jennifer Serwanga, Andrew S Ssemata, Pontiano Kaleebu, Saye Khoo, Limakatso Lebina, Neil Martinson, Francesca Chiodi, Julie Fox, Clive M Gray; CHAPS consortium

Title of contribution: A randomized clinical trial of on-demand oral pre-exposure prophylaxis does not modulate lymphoid/myeloid HIV target cell density in the foreskin.

Journal, Date: AIDS (London, England), 2023

Publisher: AIDS

Format: Original research

DIO: 10.1097/QAD.0000000000003619

Manuscripts under preparation, with notable contribution

Authors: Solima Sabeel†, **Bongani Motaung†**, Kim Nguyen†, Mumin Ozturk, Sandra Mukasa, Dirk J. Blom, Karen Sliwa, Emmanuel Nepolo, Gunar Günther, Robert J. Wilkinson, Claudia Schacht, Andre Pascal Kengne, Friedrich Thienemann*, Reto Guler*

Title of contribution: Impact of statins as immune-modulatory agents on inflammatory markers in adults with chronic diseases: A systematic review and meta-analysis.

Format: Meta-analysis

†Joint First Authors

*Authors contributed equally

Conferences

European and Developing Countries Clinical Trial (EDCTP): 11th EDCTP Forum, Partnering for Global Health Research Innovation and Impact in Africa, 7-10 November 2023, Paris, France. **Poster Presented.**

International Union of Immunology Societies (IUIS): 18th International Congress of Immunology, 27 November – 2 December 2023, Cape Town, South Africa. **Poster Presented.**

List of Abbreviations

APCs	Antigen Presenting Cells
ART	Antiretroviral Therapy
AUC	Area ROC Under Curve
BSA	Bovine Serum Albumin
BSL	Biosafety Level
CD	Cluster of Differentiation
CFU	Colony Forming Unit
cMBC	Classical memory B-cells
CM	Classical monocytes
CRP	C-reactive protein
DCs	Dendritic Cells
ddH_2O	double distilled water
DMSO	Dimethyl sulfoxide
DPI	Day Post Infection
DPI	days post-infection
EACS	European Aids Clinical Society
ELISA	Enzyme-Linked Immunosorbent Assay
EMB	Ethambutol
FACS	Fluorescence-Activated Cell Sorting
FBS	Fetal Bovine Serum
FDA	Food and Drug Administration
FDG	Fluorodeoxyglucose
FMO	Florescent Minus One

GCP	Good Clinical Practice
HDT	Host Directed Therapy
HIV	Human Immunodeficiency Virus
HLA-DR	Human Leukocyte Antigen-DR
HMG-CoA	Hydroxy-3-Methylglutaryl Co-A
HRP	Horseradish Peroxidase
IFN	Interferon
IL	Interleukin
INH	Isoniazid
iNKT	invariant natural killer T-cells
iNOS	inducible Nitric Oxide Synthase
IRIS	Immune Reconstitution Inflammatory Syndrome
LDL	Low-Density Lipoprotein
LTBI	Latent TB Infection
ManLAM	Mannosylated Lipoarabinomannan
MDM	Monocyte-Derived Macrophages
MDR-TB	Multi-Drug Resistant TB
MGIT	Mycobacteria Growth Indicator Tube
MHC	Major Histocompatibility Complex
MMP	Matrix Metalloproteinases
MOI	Multiplicity of Infection
Mtb	Mycobacterium tuberculosis
NCM	Non-classical monocytes
NFκβ	Necrosis Factor kappa beta

NK	Natural Killer
PAS	Para-aminosalicylic
PBMC	Peripheral Blood Mononuclear Cells
PD	Programmed Death
PTLD	Post-TB Lung disease
PET/CT	Positron Emission Tomography/Computed Tomography
PFA	Paraformaldehyde
PZA	Pyrazinamide
QFT	QuantiFERON
RIF	Rifampicin
ROC	Receiver Operating Characteristic
ROS	Reactive Oxygen Species
SD	Standard Deviation
SI	Staining Index
SUV	Standardized Uptake Value
TB	Tuberculosis
TLG	Total Lung Glycolysis
TLR	Toll-like Receptor
WHO	World Health Organisation
XDR-TB	Extensively Drug Resistant TB

Table of Contents

List of Figures

Chapter 1

Chapter 2

Chapter 3

List of Tables

Chapter 2

Chapter 3

Abstract

Unresolved lung inflammation post-anti-TB treatment necessitates the evaluation of additional host-directed therapies (HDT). Statins, recognized for their pleiotropic effects, show potential as immunomodulators to reduce post-TB lung inflammation. The ongoing StatinTB clinical trial utilizes a double-blind, randomized, placebo-controlled approach post-anti-TB treatment to assess the safety and efficacy of atorvastatin in reducing post-TB lung inflammation. At the end of TB treatment, Mtb culture-negative participants were stratified into minimal (Arm A, Total Lung Glycolysis (TLG) < 50 SUV) or persisting (Arm B/C, TLG ≥ 50 SUV) lung inflammation using Positron Emission Tomography/Computed Tomography (PET/CT) scan. Arm B/C received atorvastatin (40mg/day) or placebo for 12 weeks, and this data remains currently blinded. Study participants were evaluated for hematological, biochemical, and inflammatory parameters where ALP, proBNP, vitamin D, and CRP showed significant increases in Arm B/C compared to Arm A at the end of TB treatment. Serum biomarkers were evaluated at different time points using Luminex multiplex assay in 71 participants stratified by lung inflammation and HIV status post-anti-TB treatment and in 28 healthy participants stratified by QuantiFERON-TB gold assay. In a panel of 48 biomarkers, 33 were identified, with 19, 18, and 16 biomarkers showing significant upregulation in Arm B/C when compared to Arm A at week 0, 12, and 24, respectively. Furthermore, 10 biomarkers were significantly upregulated in TB patients after completion of anti-TB treatment when compared to healthy participants. Fourteen biomarkers showed the potential to discriminate between minimal and persisting lung inflammation, while 13 biomarkers correlated with lung inflammation post-anti-TB treatment. Cell phenotype analysis post-anti-TB treatment using flow cytometry revealed significantly reduced memory B-cells and classical monocytes, while non-classical monocytes were significantly increased in Arm B/C compared to Arm A. Atorvastatin's immunomodulatory effects were evaluated *ex-vivo* using PBMCs, where cytokines were measured using ELISA at 1, 3, and 6 days post-infection (DPI) following infection with three different Mtb stains (H37Rv, HN878, and CDC1551). At 1DPI and 6DPI, IL-1β showed significant reduction following atorvastatin stimulation in all three Mtb strains, while IL-6 and IL-8 showed inconsistent regulation. Evaluation of cell phenotype showed a reduction in B-cell, DCs, and monocyte subsets, while activated NK cell subsets and M2-like monocytes were upregulated in atorvastatin-stimulated, Mtb-infected PBMCs. In conclusion, TB patients remain with persistent inflammation post-anti-TB treatment, and atorvastatin may be a promising intervention for modulating inflammatory responses.

Chapter 1: Literature Review and Introduction

1.1.Host immune response to Mycobacterium tuberculosis (Mtb) infection and granuloma dissemination

TB disease develops from Mtb infection; this pathogen enters its host through the inhalation of aerosol particles containing the Mtb bacilli [1]. Upon inhalation, the Mtb bacteria are taken up by antigen-presenting cells (APCs), such as alveolar macrophages, lung macrophages, and dendritic cells lining the airways through phagocytosis, which facilitate their migration across the epithelial cells to the lung tissues [2, 3]. Infected APCs prime immunological responses through the secretion of chemokines and cytokines, which serve as chemo-attractants for the recruitment of immune cells to the site of infection, and further enhance cell activation, differentiation, and proliferation [3]. Continued recruitment of immune cells to the site of infection aids in the containment of the invading Mtb bacilli through the development of a highly organized containment structure known as the granuloma (Figure 1.1.) [4]. The granuloma structures prevent the rapid spread of the Mtb bacilli to other host organs. These structures are composed of Mtb-infected macrophages at the center of the granuloma, surrounded by other immune cells, including uninfected macrophages, foamy macrophages, neutrophils, dendritic cells, monocytes, natural killer cells, T-cells, B-cells, and multi-nucleated giant cells (Figure 1.1.) [4, 5]. This infection phase is widely known as Latent TB Infection (LTBI), and it is characterized by protective granuloma structures [6]. Even though Mtb bacteria are contained, they have been reported to slowly replicate within the granuloma, leading to unbalanced immune regulation and necrotic death of infected cells. The continued replication and immune imbalance through manipulation of CD4+ T-cells, subsequently result in disseminated granuloma, tissue destruction, and progression to active TB phase [4, 7].

1.2.Mtb bacilli establishes chronic pathogenesis by suppressing host immune responses and antigen presentation

Mtb establishes its pathogenesis by evading destruction by host immune responses. Several host mechanisms have been described as being exploited by Mtb infection for its survival, including inhibition of MHC class II antigen presentation by infected APCs [3]. The inhibition of the MHC class II complex has been shown to depend on Toll-like receptor-2 (TLR-2) signaling. Despite protective immunity, such as apoptosis induction and bactericidal

effect against Mtb, being mediated through TLR-2, Mtb manipulates this mechanism through the induction of TLR-2 response. It does this by secreting various Mtb lipoproteins such as LpqH, LprG, PhoS1, and LprA, which are known to be agonists of TLR-2. This further inhibits the MHC class II antigen presentation to T-cells, allowing Mtb to evade the immune system and establish chronic infection [3, 8, 9]. The reduced functionality of the MHC class II molecule during the early stages of Mtb infection and granuloma formation delays the onset of acquired immune responses which has been reported to be preceded by the appearance of the bacteria in the draining lymph node [7]. Mtb further inhibits phagolysosome maturation and acidification through the expression of its virulent factor, mannosylated lipoarabinomannan (ManLAM). Furthermore, this bacillus is known to secrete a 6-kilodalton (kDa) early secreted antigen target (ESAT-6) protein that can be stabilized into a heterodimeric complex with 10-kDa culture filtrate protein (CFP-10) to evade phagosome containment into the cytoplasm of infected cells, where it further suppresses the onset of innate immunity [10].

1.3.Host lipids enhance survival of intracellular Mtb

Upon infection, Mtb survival depends on its ability to extract and utilize essential nutrients from its host, specifically lipids such as fatty acids and cholesterol [11]. It has been reported that during early infection, Mtb uses fatty acids as its primary source of carbon rather than carbohydrates [12]. This phenomenon was demonstrated using a mouse model in which Mtb respiration was strongly stimulated by fatty acids but was unresponsive to carbohydrates [13]. Furthermore, cholesterol has been shown to be an essential component for Mtb persistence [14]. However, mycobacterium itself lacks the enzymes squalene monooxygenase and oxidosqualene cyclase, which are essential for sterol biosynthesis [15]. Hence, Mtb obtains its cholesterol diet from the host; this has been shown to be transported into the mycobacterium through mammalian cell entry-4 (*mce*4) operons [14]. The alteration of host lipid synthesis and sequestration may be associated with the transition from latent to active TB disease in infected individuals. Particularly, foamy macrophages have been shown to promote Mtb persistence, leading to tissue pathology, which is a hallmark of lesion formation and facilitates the escape of the bacilli [16].

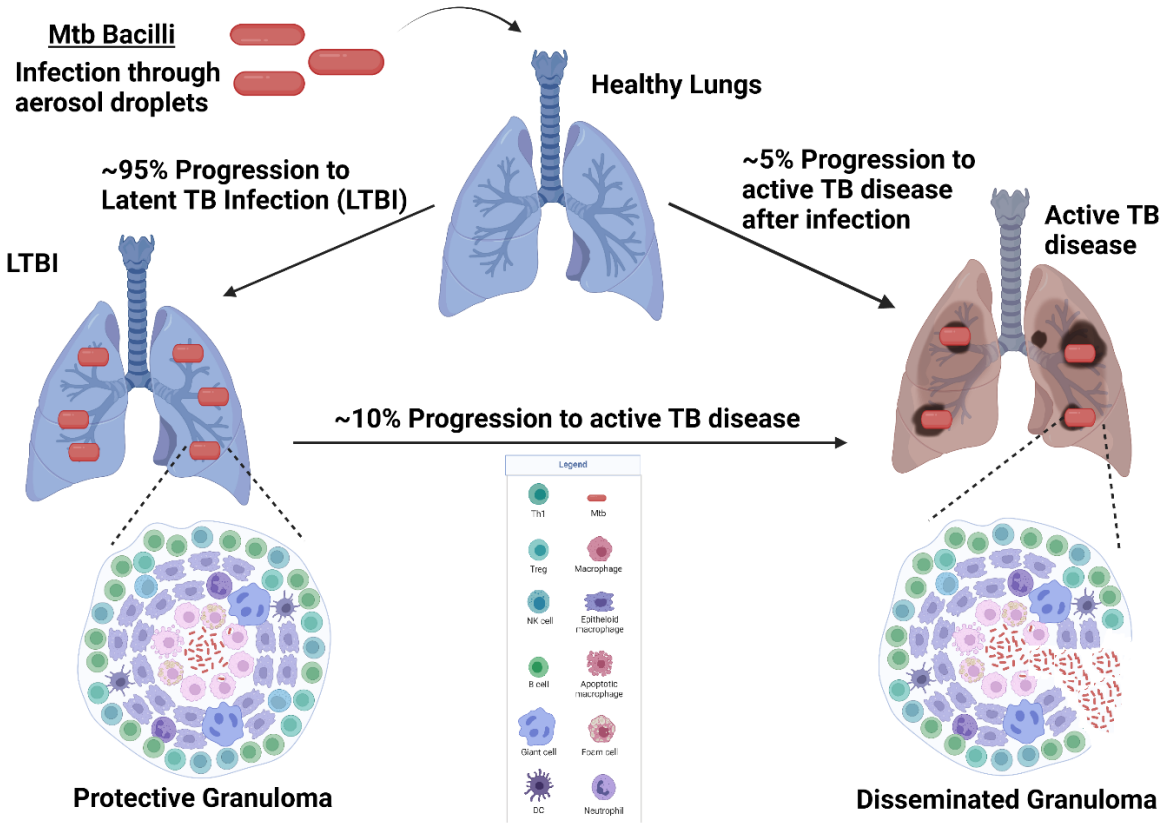

Figure 1.1. Active pulmonary tuberculosis disease occurs through inhalation of aerosol particles containing the Mtb bacilli. A 95% estimation of infected individuals develop Latent TB Infection (LTBI) which is characterized by stable granuloma structures containing the Mtb pathogen whereas 10% of these may develop active TB disease which is characterized by unstable/disseminated granuloma leading to lung tissue pathology. Image adapted from Rook et al. (2005) and modified using BioRender.com [17, 18].

1.4.Cellular immunity mediates Mtb infection and progression to active TB disease

Controlling Mtb infection and the development of active TB disease requires a balanced interaction between innate and adaptive immune cells [19]. Innate immune cells involved in TB infection include macrophages, dendritic cells (DCs), neutrophils, and natural killer cells, which initiate immune responses through the recognition of Mtb pathogen-associated molecular patterns (PAMPs) [20]. In contrast, adaptive immune responses during TB infection are mainly associated with T-cell and B-cell activation.

1.4.1. Mtb manipulates lymphocyte cell population to establish chronic infection

Activation of CD4+ (helper) T-cells by APCs during Mtb infection has been reported to be of prime importance in host resistance to Mtb through increased production of interferon-gamma (IFN-γ) [3]. These cells are known to be involved in a variety of functions during

Mtb infection, such as enhancing antibody response by B-cells, stimulating cytokine production by APCs, and maintaining CD8+ (cytotoxic) T-cell responses. Additionally, activation of CD8+ T-cells results in increased cytokine secretion and direct killing of infected cells. Recently, a population of innate lymphoid-like cells, such as γ^{δ}T-cells and invariant natural killer T-cells (iNKT), has been reported to play a critical role in early responses against pulmonary infection including TB [21]. A study by Veenstra et al. (2006) reported a significant reduction in the absolute numbers of circulating lymphocyte populations, which include T-cells, B-cells, and NK cells in TB patients at diagnosis compared to healthy controls, however, these cells were shown to be reconstituted by the end of anti-TB treatment [22]. Additionally, active TB patients were shown to have a reduced frequency of both CD4+ and CD8+ T-cells compared to healthy and treated TB patients, suggesting an association between active TB disease and reduced T-cell population [23]. On the other hand, B-cells are known to present antigens to T-cells and mount an antibody response against invading pathogens, including Mtb. However, characterization of B-cell subtypes during and after TB treatment has been limited. A study by Joosten et al. (2016) showed that TB patients have a reduced number of circulating B-cell populations compared to healthy and LTBI individuals [24]. This further suggests that Mtb bacilli establish their chronic infection through the reduction of important lymphocyte populations. However, lymphocyte cells are known to generate immunological memory against pathogens, and this enhances efficient immune responses during subsequent infections. Both B-cells and T-cells have been shown to be capable of generating immune memory, which can be classified based on CD27+ expression within the B-cell population and CCR7+ expression within both CD4+ and CD8+ T-cells [21, 24, 25].

1.4.2. Monocyte activity in response to Mtb infection and TB disease

Monocytes are leukocyte cells characterized by the expression of CD14. These cells can be classified into three subgroups, including 1) classical monocytes, described as $CD14^{+}CD16^{-}$, 2) intermediate monocytes, $CD14^{+}CD16^{+}$; and 3) non-classical monocytes, $CD14^{dim}CD16^{+}$ [26]. Upon encountering Mtb antigens, the monocyte population has been shown to differentiate into antigen-presenting cells (APCs) such as macrophages and dendritic cells to facilitate the rapid clearance of the invading pathogen [27, 28]. APCs mediate phagocytic functions and activation of immune responses, which in turn leads to phenotype changes through upregulation or down-regulation of both cell surface and intracellular markers. Phagocytic uptake of Mtb bacilli by APCs is facilitated through cell surface receptors, such

as mannose receptor, CD14, TLR-2, and Fcγ receptors [8]. These receptors recognize the Mtb ManLAM, resulting in the activation and polarization of monocyte cells to either M1 or M2 macrophages. Macrophage polarization can lead to either inflammatory (M1 macrophages) or immunosuppressive responses (M2 macrophages) [29, 30]. Inflammatory macrophages (M1) mediate pro-inflammatory responses, characterized by elevated expression of cytokines such as tumor necrosis factor-alpha (TNF-α) and interleukin (IL)-1β [31]. This macrophage sub-population highly expresses CD80 and CD86 and lacks the expression of scavenger receptor CD163 and the mannose receptor CD206 [29]. M1 macrophages mediate the killing of internalized pathogens through the induction of free radicals such as reactive oxygen species (ROS), reactive nitrogen intermediates, superoxidases, and upregulation of inducible nitric oxide synthase (iNOS). These mediators are generally associated with Mtb pathology through exacerbation of tissue damage and necrosis [32]. In contrast, immunosuppressive macrophages (M2) regulate inflammatory responses during Mtb infection and TB disease. M2 macrophages are characterized by the expression of CD163, CD206, and increased expression of arginase (Arg)-1, as well as elevated secretion of IL-10 [33]. Particularly, the frequency of the circulating total monocyte population has been shown by Castano et al. (2011) to increase during Mtb infection [34]. Additionally, the monocyte population was shown to be significantly increased in TB patients at diagnosis compared to healthy controls. However, continued monitoring showed a significant reduction of monocyte cells during the active TB disease and treatment phases, and these cells remained significantly reduced at week 26 of anti-TB treatment [22].

1.5.Cytokines and chemokines enhance lung tissue damage during TB disease and anti-TB therapy

Even though blood soluble mediators are beneficial in protecting the host against any invading pathogens, excessive or uncontrolled secretion of pro-inflammatory cytokines such as TNF-α, IL-12p40/ 12p35, IFN-γ, IFN-α, and IFN-β may negatively affect the host through tissue damage, toxicity, and the activation of permissive macrophages [35]. Similarly, increased chemokine receptor and ligand expression during Mtb infection are both beneficial (such as CCR2 which facilitates recruitment of DC, T-cells, and NK-cells) [36] and detrimental to the host (such as CXCL-5, which has been shown to increase Mtb susceptibility) [37]. Mtb bacteria are known to evade these host immune responses through various mechanisms, which involve modulation of antigen presentation on infected macrophages, thus escaping the activation of $CD4^+$ helper T-cells [38] and suppression of

phagolysosome formation, which further enhances its persistent intracellular survival [10, 38]. Seven soluble mediators, which include SAA1, PCT, IL-1β, IL-6, CRP, PTX-3, and MMP8, were reported to strongly correlate with baseline disease severity during TB disease, where lung involvement was above 50% with a smear grade above 2 and lung cavitation above 4cm [39]. However, these were strongly modulated by anti-TB treatment in TB patients who had sputum conversion at month 2, except for MCP-1, MCP -4, and osteocalcin, which remained elevated following anti-TB treatment [39].

1.6. Host immunological factors and anti-TB treatment may contribute to persisting TB disease, lung inflammation, and recurrent TB

Active TB disease is treated with first-line anti-TB regimens comprised of isoniazid (INH), rifampicin (RIF), pyrazinamide (PZA), and ethambutol (EMB) [40]. Successful anti-TB treatment is administered over a course of 6 months, which is categorized into 2 months of intensive treatment with all 4 regimens followed by 4 months of treatment with INH and RIF only (Figure 1.2.). Recently, epidemiological studies have defined antimicrobial resistance in Mtb strains which may be classified as mono-drug-resistant TB [41], multidrug-resistant TB (MDR-TB) or extensively resistant TB (XDR-TB) [41, 42]. Drug-resistant Mtb strains require an extended anti-TB treatment phase and these are treated with second-line anti-TB regimens, which include para-aminosalicylic acid (PAS), ethionamide, cycloserine, amikacin and capreomycin [40]. Despite the availability of anti-TB treatment, studies have shown varying percentages of recurrent TB globally and this has been associated with region-specific TB burden. Figure 1.2 highlights the standard treatment period for active drug-sensitive TB disease and different factors that may be associated with the growing percentage of recurrent TB, including drug resistance in Mtb leading to treatment failure, reinfection with a different Mtb strain [43], and persistent lung inflammation [44].

Recurrent TB represents a growing threat globally. Various factors such as geographic location, age, and co-infection with HIV have been reported to contribute to the growing global percentage of 2-3% at varying scales [45]. A study by Vree et al. (2007) reported an estimation of up to 8.6% TB relapse of all treated cases in Vietnam, whereas up to 24.4% in HIV co-infected individuals was reported by Glynn et al. (2010) [46, 47]. These estimates are driven by factors such as regional TB burden and drug susceptibility of the Mtb strain, where patients with drug-susceptible TB were reported with a recurrent rate of 35 cases per 1000 treated patients. However, this rate was higher in patients with drug-resistant TB, whereby 65 cases per 1000 treated patients were noted in the study by Sun et al. (2017) [48].

Additionally, it is reported that about 88% of recurrent TB cases occur through Mtb re-infection in HIV-positive patients and only 9% in HIV-negative patients [49]. The higher TB recurrence rate in HIV-positive patients is in part due to antiretroviral therapy (ART), which has been shown to lead to Immune Reconstitution Inflammatory Syndrome (IRIS). IRIS is characterized by aggressive immune responses from several immune factors ranging from immune cells, pro-inflammatory cytokines, chemokines, and toll-like receptors. These factors exacerbate lung inflammation and the formation of lung lesions, resulting in opportunistic occurrences of Mtb infection [50].

Development of lung cavities and persisting lung inflammation during pulmonary TB disease has been reported to be associated with poor treatment outcomes, anti-TB treatment relapse, a higher transmission rate, and the development of drug resistance [51]. Previous studies have defined these lung cavities through lung radiographic techniques such as X-rays and PET/CT scans [39, 44]. Various factors have been suggested to collectively contribute to the development of lung cavities and inflammation during active TB disease. These include biochemical mediators such as depletion of extracellular matrix, biophysical factors (proximity to airway), immunological factors involving both innate and adaptive responses, and microbiological processes through secretion of tuberculosis necrotizing toxin [51].

The influx of activated $CD4^+$ T-cells into the granuloma structures during TB disease enhances necrotic cell death, subsequently leading to disseminated granuloma and destruction of the lung tissues, forming lung lesions/cavities [7]. Various factors are implicated in granuloma dissemination, such as upregulation of Matrix Metalloproteinases (MMPs). In a mice model, Mtb has been shown to upregulate the expression MMP-1, which facilitates granuloma dissemination through collagen breakdown, thereby enhancing alveolar destruction [52]. Additionally, MMP-9 is another MMP that is implicated in local tissue destruction, shown to be upregulated in monocytes infected with Mtb. Furthermore, immunohistochemistry staining revealed MMP-9 to be localized in the center of the granuloma, adjacent to the caseous necrosis in the lymph nodes of Mtb-infected patients [53]. Through proteolytic cleavage, MMPs further regulate the functions mediated by both chemokines and cytokines such as IFN-γ, IL-1β, CCL7, TNF-α, and CXCL-8/IL-8 [54]. Lung cavitation/inflammation may further be exacerbated by uncontrolled neutrophil response. This is mainly driven by an altered Neutrophil Extracellular Trap (NET) network and elevated expression of inflammatory proteins associated with neutrophil-mediated responses, such as citrunillated histone H3 (cit-H3) [55]. Excessive secretion of host proteases, such as

MMPs and cathepsin by monocyte-derived cells, neutrophils, and stromal cells, further destroys lung parenchyma, leading to lesion formation [56]. These lung lesions represent Mtb-rich areas, which further enhance disease development and inter-host transmission, thus posing a greater risk of Mtb spread [7, 56]. Lung lesions are also associated with increased antibiotic resistance and antibiotic failure [56]. This was shown in a study by Malherbe et al. (2016), where TB patients presenting with persisting lung inflammation following successful anti-TB treatment showed the presence of Mtb mRNA in the lung cavities, implying the possibility of an ongoing bacilli transcription [44].

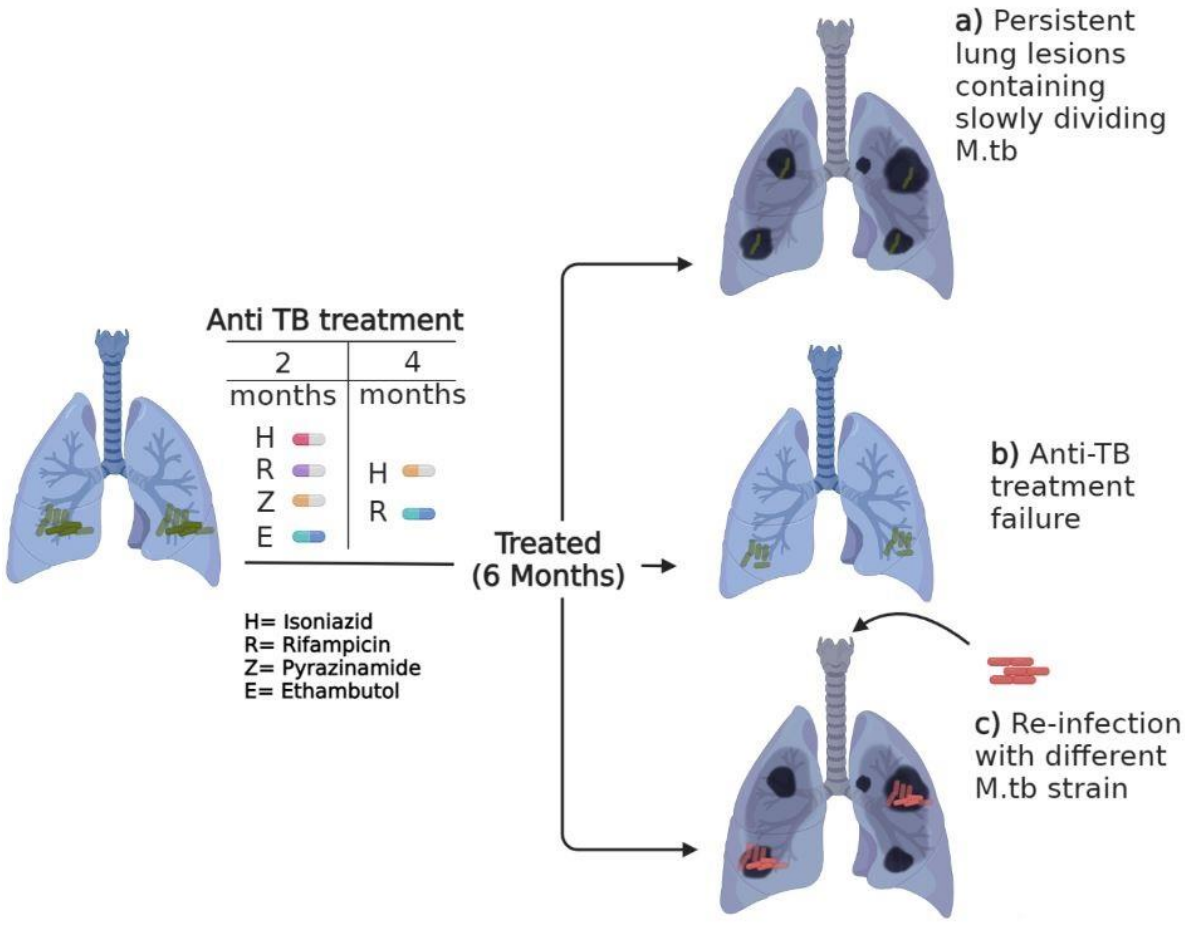

Figure 1.2. Drug-sensitive TB disease is treated over a standard period of 6 months. Treated TB patients may remain at risk of recurrent TB through various factors such as a) Persisting lung lesions containing slowly dividing Mtb, b) anti-TB treatment failure leading to Mtb reactivation, and c) Re-infection with different Mtb strain (image created with BioRender.com [17]).

1.7. Post-TB lung disease (PTLD) defines a new challenge for successfully treated TB patients

Despite the availability of anti-TB treatment, post-TB lung disease (PTLD) has been highlighted as an under-recognized global concern that leads to both morbidity and mortality in successfully treated TB patients [57, 58]. Currently, the identification of successfully treated TB patients who are at a higher risk of developing PTLD relies on chest radiography techniques such as chest X-ray, CT imaging, and PET/CT scans [58]. However, these techniques may be costly and unavailable in developing countries with high TB burden implying a continued risk of post-TB pulmonary complications in treated TB patients. Even though limited understanding is available on PTLD pathogenesis, it has been reported to be associated with tissue necrosis and impaired lung healing leading to long-term respiratory impairment following successful anti-TB treatment [57-59]. Various risk factors, which are linked to the interaction between host, pathogen, and environment such as repeated TB disease episodes, prevalence of drug-resistant TB, delayed TB diagnosis, and smoking, have been suggested to be major contributors to developing PTLD [57, 58, 60]. A study by Pasipanodya et al. (2007) reported pulmonary impairment in 59% of TB patients who had completed 20 weeks of anti-TB treatment whereas only 20% of pulmonary impairment was observed in LTBI patients, and this was more prevalent in cigarette smokers [60]. Even though immune-mediated mechanisms that contribute to PTLD in human TB remain understudied, pre-clinical and animal model studies have reported on immunological pathways that may be involved in the development of PTLD through unbalanced innate and adaptive immune responses [58]. Innate immune responses drive tissue injury and contribute to the development of PTLD through both cell-mediated and cytokine secretion leading to fibrotic TB granuloma. Macrophages have been reported to be classically activated during Mtb infection, thus promoting pro-inflammatory responses mediated through secretion of IL-1β, TGF-β, TNF-α, reactive oxygen species, and reactive nitrogen species, which in turn enhance tissue damage [61]. The cytokines IL-1β and TGF-β have been reported to be associated with the induction of fibrosis and lung damage [62-64] whereas TNF-α is known to maintain the structural integrity of TB granuloma and promote lung damage through necrosis [65]. Furthermore, neutrophil activation and recruitment exacerbate tissue injury through the release of Neutrophil Extracellular Traps (NET), which have been reported to be correlated with lung tissue damage measured by chest radiography [55]. Additionally, the secretion of metalloproteinases (MMP) has been implicated in exacerbating tissue damage and contributing to PTLD development through enhanced fibrosis [66]. Particularly, MMP-1

and MMP-8 have been reported to be elevated in TB patients with severe lung cavitation [67, 68]. On the other hand, adaptive immune responses promote fibrosis and the development of PTLD through the upregulated activity of Th2 cells which secrete pro-fibrotic cytokines such as IL-14 and IL-13 [69]. This phenomenon was observed in a study by Mazzarella et al. (2003) where TB patients with lung cavitation showed elevated levels of IL-4 compared to those without lung cavitation [70]. This shows that besides the invading pathogen, host immune responses play a significant role in tissue destruction and long-term pulmonary complications in successfully treated TB patients, indicating the importance of evaluating host-directed therapies with immunomodulatory properties.

1.8.Statins as host-directed therapy (HDT) agents to regulate systemic inflammation

HTD is a growing platform focusing on identifying biological agents that may lead to better disease outcomes. Chronic pulmonary TB disease leads to localization of inflammatory responses in the lungs resulting in the development of persistent lung inflammation following a successful anti-TB treatment period despite culture conversion from month 2 [44]. The presence of persisting lung inflammation in treated TB patients highlights the need to further explore host-directed agents that may enhance tissue healing through the induction of anti-inflammatory mediators to balance aggressive pro-inflammatory responses.

Statins are Food and Drug Administration (FDA) approved drugs that are widely known for their function in resolving cardiovascular diseases [71]. They are classified into two groups based on solubility; 1) hydrophilic statins which include pravastatin and rosuvastatin and display high hepatoselectivity, and 2) lipophilic statins which are characterized by passive diffusion into cells and include atorvastatin, simvastatin, lovastatin, fluvastatin, pitavastatin and cerivastatin [72, 73]. Statins are naturally acquired through fungal fermentation (lovastatin and pravastatin); however, they can be semi-synthetic such as simvastatin which is produced from alkylation of lovastatin, or fully-synthetic such as pitavastatin, rosuvastatin, fluvastatin, atorvastatin and cerivastatin which are synthesized from different substrates [72, 74, 75].

Statins exert their effect on the mevalonate pathway by directly blocking the enzyme 3-Hydroxy-3-Methylglutaryl Co-A (HMG-CoA) reductase which is crucial for converting HMG-CoA to L-mevalonate, thus inhibiting the biosynthesis of intracellular cholesterol [76]. Hepatocytes selectively take up statins; however, their uptake by other cells, including immune cells, highly depends on their chemical properties and expression of cell membrane

transport proteins [72, 77]. Inhibition of the mevalonate pathway by statins is known to lower extracellular low-density lipoproteins (LDL) levels by increasing cellular uptake through the upregulation of LDL receptors [10]. However, statins have been shown to have other lipid-independent pleiotropic effects on biological processes, such as protein prenylation, through inhibition of isoprenoid synthesis [78]. This activity alters other intracellular processes, such as cell membrane protein anchoring and protein-protein interaction [79]. Furthermore, statin therapy has been shown to reduce host inflammatory responses in a wide range of chronic disease conditions, including chronic obstructive pulmonary diseases (COPD), cancer, and tuberculosis, leading to better clinical outcomes and reduced disease-related mortality. Additionally, statins have been reported to reduce the levels of systemic C-reactive protein (CRP), which is regarded as a prime marker for innate inflammatory responses and is known to be upregulated in response to interleukin-6 (IL-6). Reduction of systemic inflammation by statins is achieved through regulating different immune response arms, including modulating expression of membrane-bound and soluble immunoglobulin and glycoproteins such as toll-like receptors (TLR), human leukocyte antigen-DR (HLA-DR), CC-chemokine receptor-2 (CCR-2), membrane-bound CD14, and soluble CD14 (sCD14) [80]. These compounds further regulate the secretion of pro-inflammatory cytokines, such as IL-6, IL-8, and IL-12 [81, 82]; chemokines secretion, including monocyte chemoattractant protein-1 (MCP-1) [83]; and inhibit the activity of transcription factor nuclear factor kappa beta (NFκβ) [81]. Statins enhance the anti-inflammatory profile by altering immune functions mediated by both monocytes and T-cells through targeting the lymphocyte function-associated antigen (LFA)-1 integrin molecules, which are involved in lymphocyte adhesion, migration and transduction of co-stimulatory signals during antigen presentation [84]. The immune regulatory properties mediated by statins may be key HDT targets to aid in resolving lung inflammation formed after successful anti-TB treatment.

1.9. Atorvastatin as a potential HDT to resolve pulmonary inflammation after successful anti-TB treatment in HIV-negative and HIV-positive adults

Atorvastatin is a full-synthetic lipophilic statin that is metabolized within the cell through cytochrome P450. The recommended dosage for atorvastatin ranges from 10 to 80 mg per day with a half-life of 14 hours, while its active metabolite has a half-life of 20-30 hours [85]. According to the European AIDS Clinical Society (EACS), atorvastatin shows no adverse interaction with antiretroviral therapy drugs in HIV-positive patients who are undergoing statin therapy. Furthermore, there are no drug-to-drug interactions reported with nucleoside

analog reverse transcriptase inhibitors (NRTIs) such as abicanir (ABC), non-nucleoside analog reverse transcriptase (NNRTIs) such as rilpivirine (RPV), and integrase inhibitors such as raltegravir (RAL). However, its interaction with protease inhibitors such as lipovanir+ritonavir (LPV/r) requires dose adjustment or close monitoring [86]. Anti-inflammatory response modulation by statins is shown to be dose and administration period-dependent, with atorvastatin documented to resolve lung inflammation in COPD patients. Atorvastatin administration for a period of 12 weeks was reported to reduce lung inflammation through various mechanisms which include a decrease in the number of CD45+ cells, a decrease in sputum neutrophil count, and downregulation of potent genes involved in inflammation, leukocyte activation, and immune responses [87].

1.10. Research gap in TB disease and study rationale

TB disease remains a global threat with an estimated 10.6 million infections globally in 2021 and 1.6 million deaths, with South Africa being listed among the countries with a high TB burden. Globally, TB treatment coverage was estimated at 61 % of all notified recurring or newly diagnosed TB cases in 2021 [88]. Recurrent TB following successful anti-TB treatment defines a new challenge in TB control and this has been reported both locally and internationally and this is further exacerbated by the increasing cases of drug resistance during TB treatment [89]. Host immune responses in Mtb-infected patients result in the formation of granuloma structures, which are considered as Mtb containment structures. However, these structures present with elevated levels of inflammatory mediators, which further lead to the destruction of host tissues within the lungs, causing cavities or inflammatory sites with a high burden of Mtb [90]. Despite the availability of anti-TB treatment, TB patients who have successfully completed their anti-TB therapy often experience persisting lung inflammation due to aggressive immune responses mediated during the active disease stage. Unresolved lung cavities/inflammatory sites after successful TB treatment have been reported to enhance opportunistic Mtb infection through re-infection by either a similar or different Mtb strain [44, 91]. TB patients co-infected with HIV are known to be at a higher risk of developing persisting lung inflammation and this is associated with uncontrolled immune responses primed by ART drugs. Thus, leading to lung tissue damage and increased risk of TB reactivation or re-infection in these patients. In particular, a study by Jo et al. (2014) reported about 1.9% of TB relapse or recurrent cases among a population of 137 HIV-negative participants within the first year after completing anti-TB treatment, which was further linked with positive sputum culture and development of lung

cavitation at month 2 [92]. The presence of Mtb mRNA and persisting lung inflammation were later reported in a study by Malherbe et al. (2016) in sputum samples of HIV-negative patients after 12 months post anti-TB treatment, indicating continued Mtb transcription and a risk of recurrent TB despite successful anti-TB treatment [44]. Untreated lung lesions, inefficiency of anti-TB treatment drugs to completely sterilize treated patients, and failure of host immune responses to properly contain and combat Mtb bacilli represent a growing challenge in reducing the percentage of recurrent TB in treated TB patients who are either co-infected with HIV or not.

Host-directed immunotherapy represents a promising platform for resolving inflammatory responses and control of disease outcomes. This can be achieved through targeting and enhancing specific host immune responses to promote self-healing. Despite the availability of anti-TB treatment, TB disease leads to persisting lung damage that increases the risk of recurrent TB in treated patients. The causative agent, Mtb, is known to reside in lipid-rich areas and survives by utilizing host-derived fatty acids and cholesterol [93]. Its survival within phagocytes depends highly on its ability to suppress phagosome maturation and phagolysosome formation. This highlights the need to explore biological and chemical agents that can better enhance Mtb control and resolve systemic and lung inflammation. Statins are widely known for their LDL reduction ability through blocking intracellular cholesterol synthesis. In addition, statin therapy modulates immune responses and reduces inflammatory responses. Recently, human PBMCs and MDMs isolated from familial hypercholesteremia (FH) patients treated with simvastatin showed resistance to Mtb infection. This resistance was characterized by reduced bacterial burden and increased phagosome maturation and autophagy, highlighted by upregulated early endosomal antigen-1 (EEA)-1 and lysosome-associated membrane protein (LAMP)-3, and light chain 3 (LC3)-II expression, respectively [94]. Although simvastatin has been reported to have no direct anti-mycobacterial activity, human PBMCs stimulated with simvastatin at varying concentrations and infected with H37Rv have shown reduced colony-forming unit (CFU) *in-vivo* and *in vitro* settings, which was further linked upregulated autophagy and apoptotic activity [94, 95]. Additionally, evaluation of immune regulation by simvastatin showed an increased frequency of natural-killer T-cells (NKT) and further promoted the expression of co-stimulatory molecules (CD80 and CD86) by monocytic cells with increased secretion of IL-1β, IL-12p40, and IL-10 [95]. Furthermore, evaluation of statin cytotoxicity in *ex-vivo* model using THP-1 cells and Vero cells, and *in-vivo* using mice models, showed no evidence of cytotoxicity induced by various

statins [96]. Additionally, in mice models, pravastatin and simvastatin were reported to have synergistic effects with standard anti-TB regimen in reducing lung bacterial burden [96, 97]. However, there is currently limited data evaluating the immune modulatory effects of atorvastatin post-anti-TB treatment.

1.11. Hypothesis

TB patients with persisting lung inflammation remain with elevated inflammatory mediators after completion of anti-TB treatment regardless of HIV status and *ex-vivo* stimulation of PBMC with atorvastatin may reduce pro-inflammatory cytokines.

1.12. Aims

1. To evaluate host serum biomarkers and cell phenotypes in TB patients presenting with minimal or persisting lung inflammation after completion of anti-TB treatment.

2. To assess the *ex-vivo* atorvastatin immunomodulatory effects on cytokines and cell phenotypes in Mtb-infected PBMC.

1.13. Objectives

Overall Objective

Evaluate differences in immune cell phenotype and soluble inflammatory mediators from TB patients presenting with or without persisting lung inflammation after anti-TB treatment completion and describe *ex-vivo* effects posed by atorvastatin stimulation in Peripheral Blood Mononuclear cells (PBMC) isolated from successfully treated TB patients.

Specific objectives

This study will be executed through the following specific objectives:

1. Collect blood samples from TB patients who have completed anti-TB therapy and classified into two study arms based on lung inflammation determined by Total Lung Glycolysis (TLG) measurement (study Arm A TLG < 50 Standardized Uptake Value (SUV) (Control) and study Arm B/C TLG ≥ 50SUV (Experimental groups).

2. Isolate serum and PBMC samples from collected blood samples at different time points identified as week 0, 2, 4, 8, 12, and 24 post anti-TB treatment.

3. Evaluate the expression of soluble biomarkers in serum samples isolated from successfully treated TB patients presenting with or without persisting lung inflammation at different time points using Luminex multiplex platforms.

4. Describe cell phenotype changes in PBMC samples isolated from successfully treated TB patients presenting with or without persisting lung inflammation at different time points using flow cytometer.

5. Define changes in cell phenotype and soluble inflammatory mediators in *ex-vivo* Mtb infection following atorvastatin stimulation using flow cytometer and Enzyme enzyme-linked immunosorbent Assay (ELISA), respectively.

Chapter 2: Materials and Methods

2.1. Ethics statement

This study forms part of the StatinTB clinical trial and was conducted in accordance with Good Clinical Practice (GCP) guidelines for the recruitment of successfully treated TB patients. The study protocol was reviewed and approved by the University of Cape Town Human Research Ethics Committee (UCT-HREC), Standard Operation Procedures, University of Cape Town, Version 7.0, April 2019 (HREC Ref. number 675/2019). Adverse events incurred during the clinical trial were reported to UCT HREC according to the HREC Standard Operating Procedures, University of Cape Town, version 7.0, April 2019; and to South African Health Products Regulatory Authority (SAHPRA) according to SAHPRA safety reporting during clinical trial in South Africa, Version2, August 2019. Study protocol for recruitment of healthy participants who are included in this study was reviewed and approved by the Human Ethics Committee, Faculty of Health Sciences, University of Cape Town, Cape Town (HREC Ref Number: 636/2015). All study participants who are included in this study provided written informed consent (StatinTB clinical Trial: NCT04147286).

2.2. Inclusion and Exclusion criteria

2.2.1. Successfully treated TB participant (StatinTB Cohort)

Included study participants were evaluated for sputum conversion and presented with negative sputum culture at months 4 and 6 of anti-TB therapy. Study participants were between the ages of 18 and 65 years, with body mass between 50 and 90 kg and willing to undergo HIV testing (Figure 2.1.). HIV-positive participants with CD4 counts ≥ 350 cells/µl within 30 days prior to enrolment were included in the study. Patients with any form of acute or chronic illness, known allergies, fever, evidence of extrapulmonary TB, drug-resistance TB, pregnancy, use of the investigational drug within the previous 3 months, and using immunosuppressive drugs were excluded from this study.

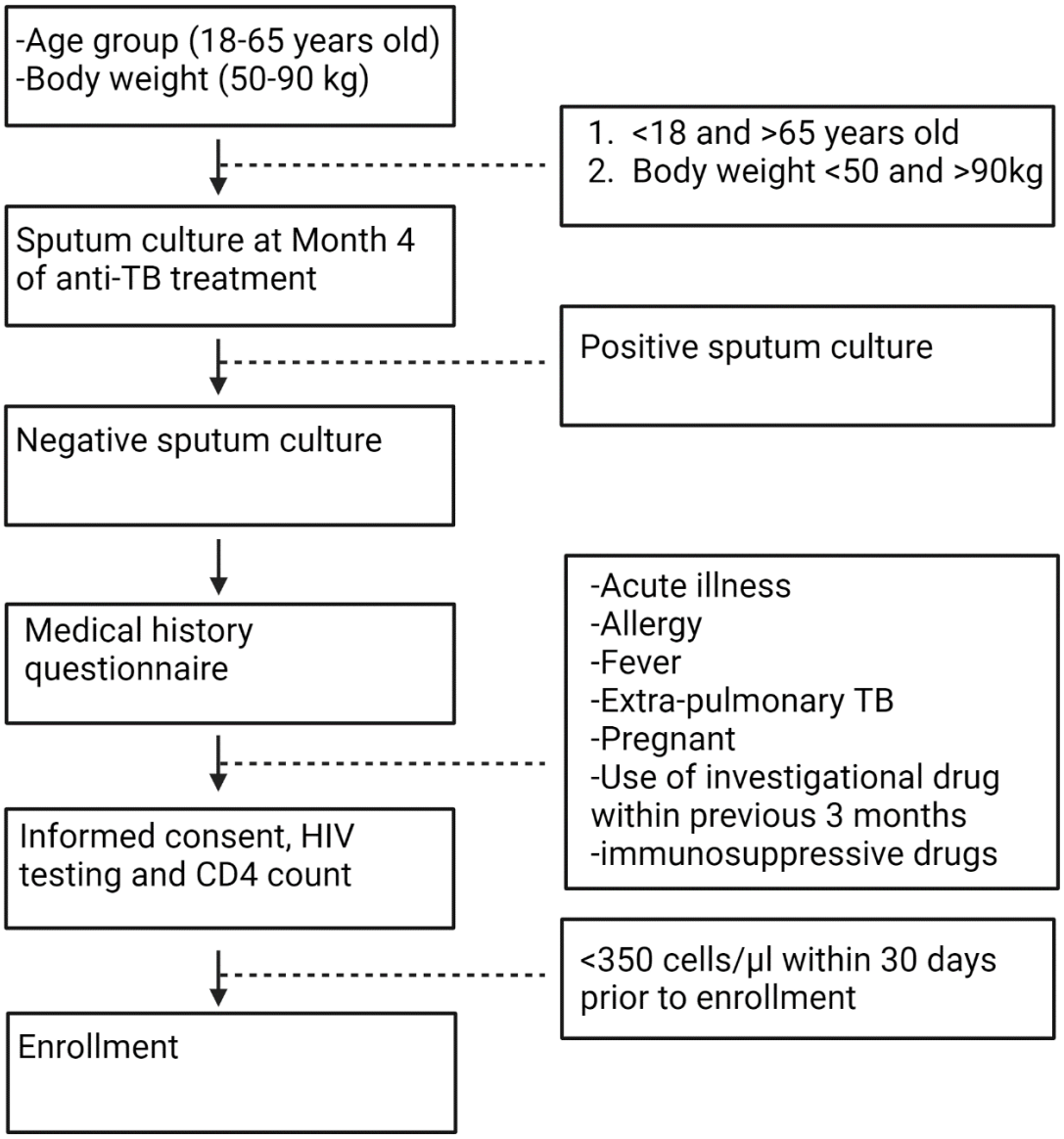

Figure 2.1. Schematic representation of participant enrolment for the StatinTB clinical trial.

2.2.2. Healthy participants

Healthy participants included in the study were between 18 and 50 years old. Study participants were recruited regardless of gender and had no history of active TB disease or contact with TB patients. All included participants were HIV-negative, non-smokers, and showed no evidence of chronic alcoholism. Furthermore, included participants had no detected acid-fast bacilli through negative sputum-smear results and displayed normal chest radiography on x-rays. The medical questionnaires of included participants indicated no history of chronic or other pulmonary diseases, and these participants were not on any immunosuppressive therapy. Participants who did not meet the above criteria, were not

willing to provide informed, consent, or did not undertake an HIV test were excluded from this study.

2.3. Participant demographics

2.3.1. StatinTB Cohort

Study participants were recruited from eight clinic facilities within the Western Cape, Cape Town, South Africa including the Langa clinic, Dunoon clinic, Albow Gardens clinic, Factreton clinic, Site B clinic, Vuyani clinic, Michael Mapongwana clinic, and Town 2 clinic. Participants were introduced to the study at month 4 of their anti-TB treatment. Upon providing written informed consent, study participants were subjected to a screening phase where sputum was collected for Mycobacteria Growth Indicator Tube (MGIT) culture and GeneXpert analysis. Enrolled study participants displayed negative MGIT and GeneXpert results and were followed up to month 6 of anti-TB treatment where sputum samples were collected for a second analysis. Participants with confirmed negative sputum results at month 6 of anti-TB treatment were then enrolled in the study and allowed a 1-week washout period. This was then followed by lung analysis using an FDG PET/CT scan at Groote Schuur Hospital, Cape Universities Body Imaging Centre (CUBIC). Participants with minimal lung inflammation, indicated by Total Lung Glycolysis (TLG) < 50 SUV were placed in study Arm A and regarded as the control group. Persisting lung inflammation was indicated by TLG ≥ 50 SUV and these participants were placed in study Arm B/C and regarded as the experimental group (Figure 2.2.). Study Arm B/C participants were randomized to receive atorvastatin (40 mg/day) or placebo in a double-blinded manner. All study participants were followed up for 24 weeks, consisting of 12 weeks of atorvastatin therapy and a 12-week observational period. Participants were monitored at different time points over the 24-week period where biological samples were collected for analysis.

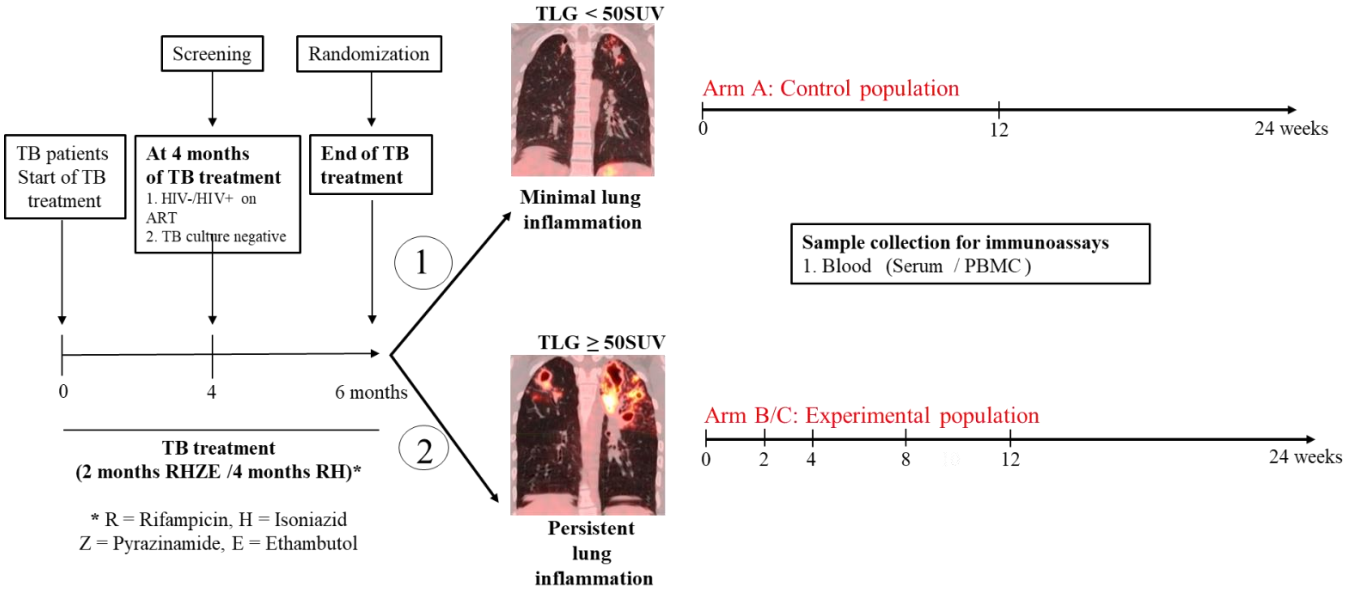

Figure 2.2. Description of study arms based on lung FDG PET/CT scan. Participants without persistent lung inflammation form study Arm A (TLG < 50 SUV) and participants with persistent lung inflammation form Arm B/C (TLG ≥ 50 SUV).

2.3.2. Healthy Participants

Healthy participants were recruited from two academic institutes within the Western Cape, Cape Town, South Africa, including the University of Cape Town and the University of Western Cape. Recruited participants were analysed for QuantiFERON (QFT) response at a single time point using the QuantiFERON®-TB Gold Plus assay, where detected levels of IFN-γ were used to distinguish between QFT- and QFT+ participants.

2.4. Sample collection and time point visits

Venous blood samples were collected from all enrolled study participants at the end of anti-TB treatment (week 0) for baseline analysis. Blood samples were collected at three time points for study Arm A (TLG < 50 SUV) participants, which were classified as week 0, week 12, and week 24. Study Arm B/C (TLG ≥ 50 SUV) participants had six time points for blood collection: week 0, week 2, week 4, week 8, week 12, and week 24. Blood samples were collected using different tubes for specific analysis, where 4 x 9ml sodium heparin tubes were collected for isolation of Peripheral Blood Mononuclear Cells (PBMC) only in the StatinTB cohort. Additional blood samples were collected in 1 x 4ml Serum Separating Tube (SST) was used to acquire serum samples from both the StatinTB cohort and healthy participants.

Table 2.1. Sample collection time point visits for StatinTB cohort. Blood samples were collected at 3-time point visits (week 0, 12, and 24) for study Arm A participants. Blood samples were collected in 6-time point visits (week 0, 2, 4, 8, 12, and 24) for study Arm B/C participants.

Time Point Visits	Arm A (TLG<50SUV)	Arm B/C (TLG≥50SUV)
Week 0 (end TB treatment)	X	X
Week 2		X
Week 4		X
Week 8		X
Week 12	X	X
Week 24	X	X

2.5. Blood processing

2.5.1. Serum collection

Serum samples were collected using a standardized protocol. Collected blood samples were allowed to clot completely (a minimum of 60 minutes from phlebotomy) at room temperature before processing. Clotted blood tubes were then processed by centrifugation at 1200 xg (rcf) for 10 minutes at room temperature with acceleration and braking at maximum. Resulting serum samples were aliquoted into 4 separate sterile, non-protein binding screw-cap tubes each containing approximately 350 µl of serum volume. These were then immediately frozen at -80^{o}C for downstream analysis.

2.5.2. PBMC isolation

PBMC isolation was performed through density gradient method, where blood processing commenced within two hours from phlebotomy for optimal cell recovery and viability. Collected blood samples were transferred from sodium heparin vacutainer tubes into sterile 50ml Falcon tubes. The blood samples were diluted with RPMI-1640 with L-glutamine at a 1:1 (v/v) dilution ratio and layered onto Ficoll Paque Plus. Tubes were centrifuged at 1000 xg (rcf) for 20 minutes at room temperature with acceleration at maximum and brakes off. A visible layer of PBMC between the plasma and Ficoll Paque density medium was aspirated using a sterile Pasteur pipette into sterile 50ml Falcon tubes. Collected PBMCs were washed twice with RPMI-1640 with L-glutamine at 120 xg (rcf) at room temperature for 10 minutes, with maximum acceleration and brakes off. Resulting cell pellets were re-suspended in 1 ml of RPMI-1640 with L-glutamine and cell counts were performed manually using a

hemocytometer. Cell viability was assessed using the trypan blue exclusion method. The cell suspension was then mixed with an equal volume of cryo-preservation media containing 80% Fetal Bovine Serum (FBS) and 20 % dimethyl sulfoxide (DMSO) and transferred into separate sterile 2 ml cryo-preservation tubes each containing 1 ml of cell suspension, and immediately transferred to ice. Cryo-preservation tubes were transferred into a Coolcell container and immediately stored at -80^{o}C overnight, then transferred to liquid nitrogen for long-term storage and downstream analysis.

2.6. PBMC thawing for flow cytometer and *ex-vivo* studies

Stored PBMC vials were recovered from a liquid nitrogen biorepository and fast-thawed at 37^{o}C. Briefly, 9ml of thawing media composed of RPMI-1640 with L-glutamine and 10% FBS was aliquoted into a sterile 50ml Falcon tube and pre-warmed to 37^{o}C. Frozen PBMC vials were fast-thawed in a water bath until little ice was visible inside the tubes. These were transferred into the biosafety cabinet, where 1 ml of pre-warmed media was slowly dispensed onto the cell suspension and mixed gently. This was followed by transferring the entire cell suspension from cryo-tubes into 50ml Falcon tubes containing pre-warmed thawing media and centrifuged at 120 xg (rcf) with maximum acceleration and brakes off to wash out residual cryo-preservation media. The resulting cell pallets were further washed a second time with 20 ml of thawing media under similar centrifugation conditions. To allow cells to rest, recovered cell pellets were re-suspended in 5 ml of thawing media and incubated for two hours at 37^{o}C and 5% CO_2, with humidity above 60%. Following cell resting, they were centrifuged at 120 xg (rcf) with maximum acceleration and brakes off for 10 minutes. The resulting pallets were then re-suspended in 1m of thawing media and cell recovery was determined through manual count using a hemocytometer, where trypan blue exclusion method was used to evaluate cell viability.

2.6.1. *Ex-vivo* Mtb infection of atorvastatin stimulated PBMC

Optimal *ex-vivo* stimulation conditions were evaluated using PBMCs from healthy participants where thawed PBMCs were plated at a density of 5 x 10^5 cells/well in a 96-well plate. These were stimulated in a Biosafety Level-2 (BSL-2) laboratory with different atorvastatin concentrations which included 50µM, 100µM and 200µM for 24hrs at 37^{o}C and 5% CO_2. Culture plates then were transferred to the BSL-3 laboratory where cells were infected with different Mtb strains including H37Rv, CDC1551, and NH878 at a Multiplicity of Infection (MOI) of 0.5 and further incubated at 37^{o}C and 5% CO_2 for 6 days. Culture supernatants were collected at specific time points (1-, 3- and 6-days post-infection (dpi)) and

filtered using MultiScreen filter plates, then analysed for cytokine secretion through ELISA. Cell pellets were harvested, stained with monoclonal antibodies, fixed using paraformaldehyde (PFA), and acquired on flow cytometry to evaluate cell phenotype changes. Subsequent *ex-vivo* studies (StatinTB cohort) were conducted using 10µM atorvastatin stimulation, and a single Mtb strain (HN878) at MOI=0.5. Cell phenotype changes were evaluated using flow cytometry at 1 dpi.

2.7. Flow cytometric analysis

2.7.1. Antibody panels and cell staining

Flow cytometry panels were designed to analyse differences within lymphocyte and monocyte cell populations (Table 2.2.). Optimal antibody concentrations were determined through a serial dilution method, after which the optimal Staining Index (SI) was determined for each antibody using FlowJo v10.7.1. Briefly, thawed PBMCs were seeded at a density of 5 x 10^5 cells/well and centrifuged at 300 xg (rcf) for 5 minutes. The resulting cell pellets were washed twice by re-suspending in 200 µl of cell staining buffer (BioLegend. United States) and centrifuged at 300 xg (rcf) for 5 minutes. Non-specific binding was blocked by incubating the cells with 100µl of a 10 x diluted Human TruStain FcX (BioLegend. United States) solution for 15 minutes at room temperature. Following incubation, cells were washed once using cell staining buffer, and then PBMCs were stained with monoclonal antibodies at their determined optimal concentrations and incubated in the dark for 30 minutes at room temperature. Following staining, cells were washed twice by re-suspending the cells in 200 µl of cell staining buffer and centrifuging at 300 xg (rcf) for 5 minutes. Intracellular staining (FoxP3) was performed after cell surface staining using True-Nuclear Transcription Factor Buffer Set (BioLegend, United States) where cells were incubated in the dark with 1 x True-Nuclear Fix solution for 60 minutes at room temperature. These were then washed twice using 1 x True-Nuclear Perm buffer and centrifugation at 300 xg (rcf). Following the wash steps, resulting cell pellets were stained with FoxP3 monoclonal antibody diluted in 1 x True-Nuclear Perm buffer and incubated in the dark for 30 minutes. These were then washed twice using 1 x True-Nuclear Perm buffer and centrifugation at 300 xg (rcf). The resulting cell pellets were then re-suspended in 100 µl of cell staining buffer and acquired using flow cytometry.

Table 2.2. Targeted flow cytometer panels to evaluate cell phenotype changes in PBMC samples from recruited study participants. A. antibody panel for evaluating functional changes in T-cells and B-cells (n=12). **B.** antibody panel for evaluating changes in monocytes, dendritic cells (DC), Natural Killer (NK) cells, and γ^{δ}T-cells. CD= Cluster of Differentiation, PD= Programmed Death, HLA-DR= Human Leukocyte Antigen DR.

A) Panel for T-cells and B-cells phenotype (n=12)	**B) Panel for Monocyte, Dendritic cells, NK-cells, and γ^{δ}T-cells phenotype (n=13)**
CD3	CD1c
CD4	CD3
CD8	CD11b
CD19	CD11c
CD21	CD14
CD27	CD16
HLA-DR	CD56
CD45RA	CD86
CCR7 (CD197)	CD80
PD1 (CD279)	CD163
FoxP3	CD206
CD25	NKp46
	γ^{δ}TCR

2.7.2. Gating strategies

Gating strategies for all targeted cell populations were corrected using the Fluorescent Minus One (FMO) method. Lymphocyte gating was designed to target the memory phenotype in B-cells through the expression of CD21 and CD27. Memory phenotype in helper (CD4+) and cytotoxic (CD8+) T-cells were evaluated through the expression of CD45RA and CCR7, whereas the regulatory phenotype was determined by CD25 and FoxP3 expression within the CD4+ T-cell population (Figure 2.3A). Furthermore, the expression of Programmed Death (PD)-1 was evaluated in both the CD4 and CD8 T-cell populations (Figure 2.3B). A subset of γ^{δ}T-cells was evaluated based on the γ^{δ}TCR expression (Figure 2.3C). Additionally, NK cell populations were evaluated through CD56 and CD16, where the activated subset was shown by NKp46 expression (Figure 2.3D). The dendritic cell population was gated based on CD1c and CD11c where active subsets were indicated by CD11b expression (Figure 2.3E).

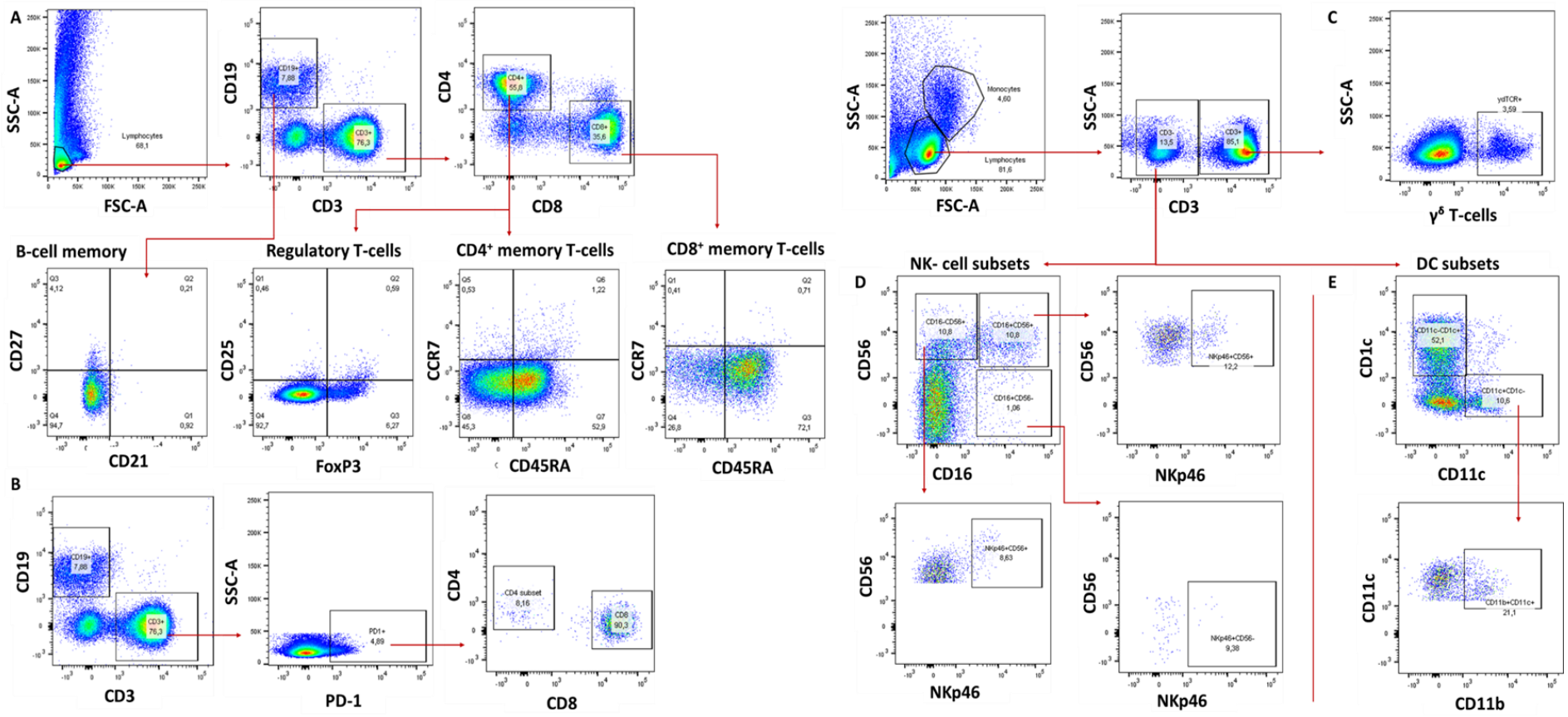

Figure 2.3. Gating strategy used to define changes in lymphocyte sub-populations. A. Evaluation of memory B-cells (CD19+) subsets characterized as naïve (CD19+CD21+CD27-), classical memory (CD19+CD21+CD27+) and activated memory (CD19+CD21-CD27+); regulatory T-cells (Tregs) defined as conventional Tregs (CD25+FoxP3+) and unconventional Tregs (CD25-FoxP3+); memory T-cells evaluated in both CD4+ and CD8+ T-cells based on CD45RA and CCR7 expression. **B.** Evaluation of Programmed cell death protein- 1 (PD-1) expression in CD4+ and CD8+ T-cells. **C.** γ^{δ}T-cells evaluation based on γ^{δ}TCR expression. **D.** Natural Killer (NK) cells subsets defined based on CD16 and CD56 expression where activation is indicated by NKp46 expression **E.** Evaluation of dendritic cells (DC) subsets based on CD1c and CD11c expression where CD11b expression indicates activation in CD1c-CD11c+ DC.

Different monocyte populations were classified based on CD14 and CD16 expression where activation was determined based on the expression of CD80 and CD86 co-stimulatory molecules (Figure 2.4.).

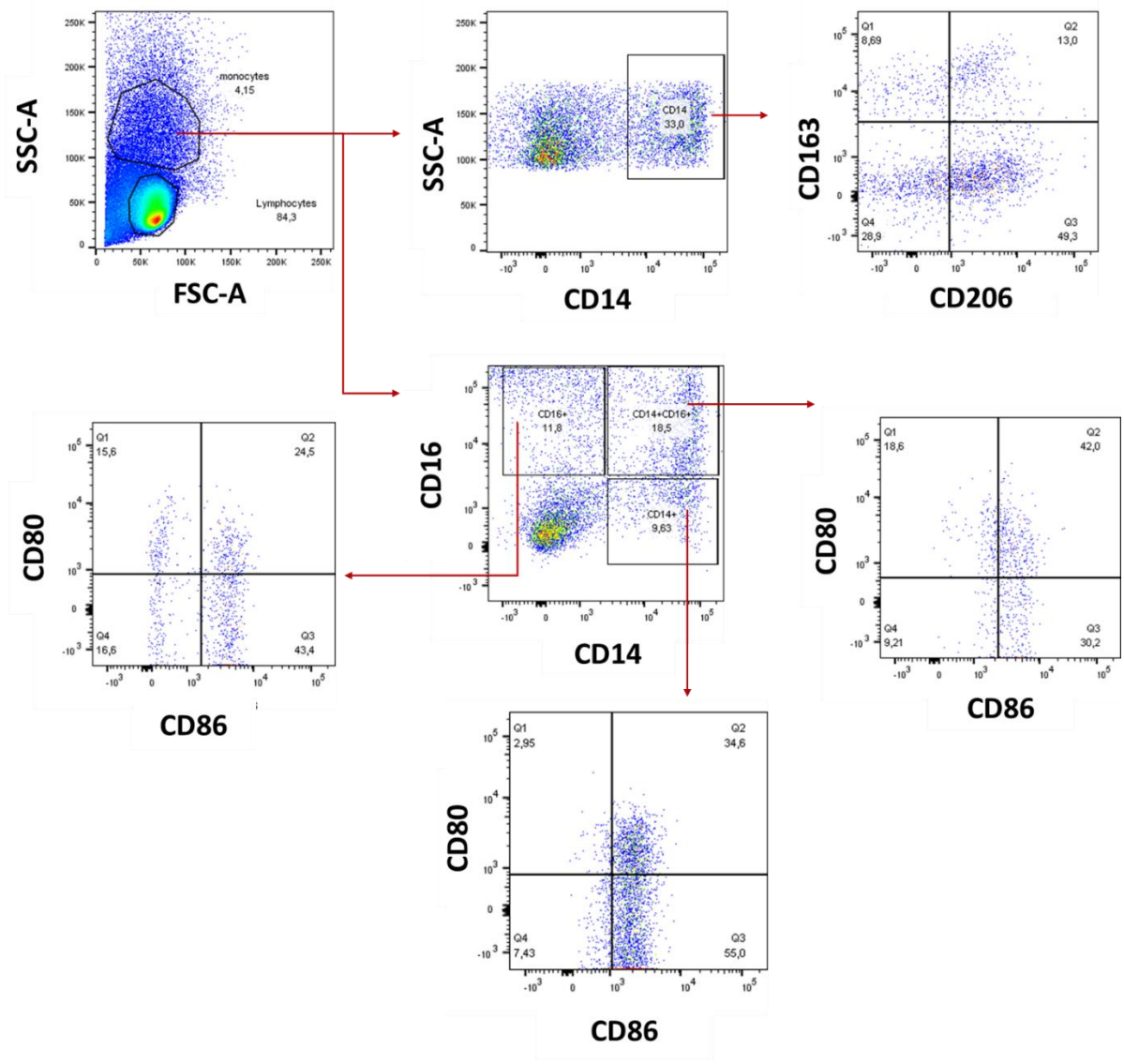

Figure 2.4. Gating strategy for defining changes in monocyte subsets. Expression of CD14 and CD16 defines classical (CD14+CD16-), non-classical (CD14-CD16+), and intermediate (CD14+CD16+) monocytes. CD80 and CD86 co-stimulatory molecules indicate activation. M1/M2 class switching in monocytes is defined based on CD163 and CD206 expression.

2.8. Enzyme-Linked ImmunoSorbent Assay (ELISA)

ELISA was performed on *ex-vivo* culture supernatant samples to evaluate the expression of pro-inflammatory cytokines, including IL-1β, IL-6, and IL-8 following atorvastatin stimulation and Mtb infection. Briefly, 96-well flat-bottom ELISA plates were incubated with 50 µl of coating antibodies diluted in 1 x PBS with 1% Bovine Serum Albumin (BSA)

overnight at 4°C. Plates were washed 4 x with wash buffer (20g KCL, 800g NaCl, 20g $KH_2HPO_4.2H_2O$, 50 ml Tween-20; diluted 1:20 in double distilled water (ddH_2O)) and incubated with 200 µl of blocking buffer containing 2% BSA for 2 hours at 37°C. Following incubation, plates were removed from the incubator and washed 4 times using wash buffer, after which 50 µl of standard antibodies and culture supernatant samples were added per well and incubated at 4°C overnight. Thereafter, plates were thoroughly washed and 50µl of respective secondary biotinylated antibodies were added to each well and incubated for 2 hours at 37°C. Plates were then thoroughly washed with wash buffer and 50µl of diluted Horseradish Peroxidase (HRP)-labeled streptavidin conjugate was added to each well and incubated for 1 hour at 37°C. Following incubation, plates were thoroughly washed with wash buffer. To develop the plates equal volumes of substrate A (Tetramethylbenzidine (TMB) Peroxidase substrate) and substrate B (Peroxidase substrate) were mixed at room temperature and 50µl of the mixture was added in each well and incubated for 10-15 minutes at room temperature in the dark. The reaction was stopped using 50µl of 1M Phosphoric acid and plates were read within 15 minutes at 450nm using a VERSAmax microplate reader (Molecular devices, USA). Detected concentrations were extrapolated using five-parameter logistic (5-PL) standard curves.

2.9. Luminex multiplex analysis

A panel of 48 soluble biomarkers (Table 2.3.) was evaluated using the Bio-Plex Pro Human Cytokine Screening 48-Plex (Bio-Rad, US). Serum samples were retrieved from the biorepository and thawed at 4°C overnight. Thawed serum samples were centrifuged at 1000 xg (rcf) for 15 minutes at 4°C and diluted to 1:4 using kit-specific sample diluent. Lyophilized standards and controls were reconstituted to require concentration using standard diluent HB solution. A serial dilution of eight standard concentrations was performed from the stock solution and these were kept on ice. During the analysis, a 10x solution of antibody-coated magnetic beads was diluted to 1 x solution using kit assay buffer and 50 µl of diluted magnetic beads was added in each well of the 96-well Luminex plates. The plates were then washed two times using 100 µl/well of 1x bio-plex wash buffer solution in a magnetic plate washer (Bio-Rad, BioPlex Pro wash station), after which 50 µl of the standards, controls, and diluted serum samples were added onto the plate at respective wells. The plates were then sealed and incubated at room temperature on a shaker (850 rpm) for 30 minutes. Following incubation, plates were washed three times with 100µl/well of 1x bio-plex wash buffer solution in a magnetic plate washer. Detection antibodies were diluted to 1x using detection

antibody diluent HB and 25 µl diluted detection antibodies was added into each well and incubated at room temperature on a shaker (850 rpm) for 30 minutes. Plates were washed three times with 100µl/well of 1x bio-plex wash buffer solution in a magnetic plate washer. A 1x Streptavidin-Phycoerythrin (SA-PE) solution was prepared, and 50µl was added into each well, after which plates were incubated at room temperature on a shaker (850 rpm) for 10 minutes. Thereafter, plates were washed three times with 100 µl/well of 1x bio-plex wash buffer solution in a magnetic plate washer, and 125 µl of assay buffer was added in each well followed by a shaking the plate at 850 rpm for 30 seconds. Luminex plates were read using Bio-Plex 200 system (Bio-Rad, US). Biomarker concentration was determined using 5-PL standard curves, and detected control concentrations were within accepted range for all analytes.

Table 2.3. A panel of 48 soluble biomarkers was evaluated from serum samples collected from healthy and successfully treated TB patients who are stratified based on lung inflammation using the Luminex multiplex platform. Biomarkers were stratified based on function and included pro-inflammatory (n=20), anti-inflammatory (n=5), growth factors (n=11), chemokines (n=10) and pleiotropic mediators (n=2).

Pro-inflammatory	Anti-inflammatory	Growth factors	Chemokines	Pleiotropic mediators
IFN-γ	IL-1ra	FGF basic	Eotaxin	IL-9
IL-1β	IL-10	G-CSF	RANTES	LIF
IL-1α	MIF	GM-CSF	MIP-1α	
IL-2Rα	IL-13	M-CSF	MIP-1β	
IL-6	IL-4	GRO-α	IP-10	
TNF-α		MIG	MCP-1 (MCAF)	
TNF-β		PDGF-BB	MCP-3	
IL-12 (p40)		SCGF-β	VEGF	
IL-2		HGF	CTACK	
IL-7		β-NGF	SDF-1α	
IL-5		SCF		
IL-8				
IL-3				
IL-15				
IL-16				
IL-18				
IL-12 (p70)				
IFN-α2				
IL-17A				
TRAIL				

2.10. Statistical analysis

Data analysis was performed using GraphPad Prism 8.0 software (http://www.graphpad.com). The analysed data were summarised into tables, graphs, and heat-map formats, where mean±SD, AUC, percentages (%), and frequency (%) were indicated where necessary. Heat-map analysis was used to evaluate host serum biomarker profiles between the study arms, where data normalization was performed for each biomarker, with 100% (red colour) indicated by the highest value and 0% (green colour) indicated by the lowest value. The association between host serum biomarker profiles and TLG (SUV) was assessed through the Pearson correlation coefficient. The diagnostic potential of host serum biomarkers was evaluated through ROC curve analysis, where the

Wilson/Brown method was used to determine AUC. The sensitivity and specificity of diagnostic biomarkers were evaluated using Youden's J statistics. The Shapiro-Wilk test was used to evaluate data normality. Depending on data distribution, number of groups, and variables, statistical significance was evaluated using the Mann-Whitney t-test, Kruskal-Wallis test with Dunn's multiple comparisons, or two-way ANOVA followed by Dunnett's corrected multiple comparisons. Statistical significance was indicated by a p-value threshold which is equal to or below 0.05. Statistical significance was summarized as *($p \leq 0.05$), **($p \leq 0.01$), ***($p \leq 0.001$) and ****($p \leq 0.0001$) on graphs.

Chapter 3: Results

3.1. Study participant demographics

3.1.1. StatinTB cohort demographic information

Recruited study participants were all successfully treated for active TB disease through a standard anti-TB regimen. All included study participants provided written informed consent and were evaluated for HIV status. This project forms part of the StatinTB clinical which is a double-blind, randomized controlled clinical trial where participants in study Arm B/C are given atorvastatin or matching placebo for 12 weeks after completion of anti-TB treatment. StatinTB clinical trial enrolment is still ongoing and data unblinding for direct comparison of atorvastatin intervention against placebo or control population (study Arm A) cannot be achieved for StatinTB time points (week 12 and week 24). However, this thesis evaluated the expression profile of soluble biomarkers in a total of 71 study participants who have completed all StatinTB designated time point visits where study Arm B/C (TLG ≥ 50 SUV) is analysed as a collective study arm. As highlighted in Table 3.1, the overall age (years) of included study participants showed a mean±SD of 34.65±12.03. Study participants were recruited regardless of gender where the overall percentage of males was 67.60% and females were 32.39%. HIV status among all included study participants showed 80.28% HIV negative and 19.71% HIV positive participants. Enrolled study participants were stratified based on Total Lung Glycolysis (TLG), where study Arm A (control population) included participants with minimal lung inflammation indicated by TLG < 50 SUV, and study Arm B/C (experimental population) included participants with persisting lung inflammation and defined by TLG ≥ 50 SUV (Table 3.1.). Smoking habits were determined at 57.1% and 69.0% in study Arm A and study Arm B/C, respectively. A total of 42 study participants were analysed from study Arm A (TLG < 50 SUV) where age (years) (mean±SD), gender (%), and HIV status (%) displayed 33.10±11.83, 66.66% males vs 33.33% females, and 85.71% HIV negative vs 14.28% HIV positive, respectively. Study Arm B/C (TLG ≥ 50 SUV) included a total of 27 study participants where age (years) showed a mean±SD of 36.90±12.17 with male and female populations representing percentages of 68.96% and 31.03%, respectively. Participants included in study Arm B/C (TLG ≥ 50 SUV) showed 72.41% HIV negative and 27.58% HIV positive. There was no significant difference (p=0.1919) observed in age (years) between the study arms. Among the total study participants (n= 71) included in the study, 7 (9.85%) participants were shown to experience recurrent TB. Among the recurrent TB

participants, 1 participant was in study Arm A with a negative HIV status and 6 were in study Arm B/C (TLG ≥ 50 SUV) where 3 (50%) were HIV negative and 3 (50%) were HIV negative (Table 3.1.).

Table 3.1. StatinTB cohort demographic information where study Arm A (TLG < 50 SUV) shows participants with minimal lung inflammation and study Arm B/C (TLG ≥ 50 SUV) shows participants with persisting lung inflammation after completion of anti-TB treatment. Data is shown as total numbers (n), percentages (%), and mean±SD (age). TLG=Total Lung Glycolysis, SUV=Standardized Uptake Value, SD= Standard Deviation, HIV= Human Immunodeficiency Virus.

	All participants	**Arm A (TLG<50 SUV)**	**Arm B/C (TLG≥50 SUV)**
Participants, n	71	42	29
Age (years), mean ± SD	34.65 ± 12.03	33.10 ± 11.83	36.90 ± 12.17
Male n (%)	48 (67.60)	28 (66.66)	20 (68.96)
Female n (%)	23 (32.39)	14 (33.33)	9 (31.03)
Smoking n (%)	44 (61.97)	24 (57.1)	20 (69.0)
HIV- n (%)	57 (80.28)	36 (85.71)	21 (72.41)
HIV+ n (%)	14 (19.71)	6 (14.28)	8 (27.58)
Recurrent TB, n (%)	7 (9.85)	1 (2.38)	6 (20.68)
HIV- n (%)	4 (57.14)	1 (100)	3 (50)
HIV+ n (%)	3 (42.85)	0 (0)	3 (50)

3.1.2. Evaluation of biochemical, hematological, and inflammatory parameters after completion of anti-TB treatment

Enrolled study participants were screened for biochemical, hematological, and inflammatory indicators after completion of anti-TB treatment. Measured biochemical parameters were within normal range, and no significant differences were observed in liver function between study Arm A (TLG < 50 SUV) and study Arm B/C (TLG ≥ 50 SUV) as determined by alanine transaminase, aspartate aminotransferase, bilirubin, and gamma-glutamyl transferase tests (Table 3.2.). Although the alkaline phosphatase (ALP) test remained within the normal range after completion of anti-TB treatment, a significant difference (p=0.0029) with an increased detection of ALP in study Arm B/C (TLG ≥ 50 SUV) was observed (Table 3.2. and Figure 3.1A.). Evaluation of kidney function, muscle injuries, hemoglobin, and glycated hemoglobin were also detected at normal ranges following anti-TB treatment with no significant differences between the study groups as indicated by creatinine, creatine kinase, hemoglobin, and hemoglobin A1C tests, respectively. As highlighted in table 3.2, iron levels and iron metabolism were evaluated in enrolled participants where no significant differences

were observed between study Arm A (TLG < 50 SUV) and study Arm B/C (TLG ≥ 50 SUV) as indicated by ferritin, iron, and transferrin tests. Symptoms of heart failure were evaluated through proBNP where significant difference was observed between study Arm A (TLG < 50 SUV) and study Arm B/C (TLG ≥ 50 SUV) with elevated detection of brain natriuretic peptide (BNP) in study Arm B/C (TLG ≥ 50 SUV) (Table 3.2. and Figure 3.1B.). However, no significant difference was detected in heart muscle damage as indicated by troponin detection. Even though vitamin D was detected at normal levels, significantly low levels of vitamin D (p=0.0192) were observed in study Arm A (TLG ≥ 50 SUV) compared to study Arm B/C (TLG ≥ 50 SUV) (Table 3.2 and Figure 3.1C). Hematological parameters such as CD4 counts (HIV-positive patients only), neutrophil, lymphocyte, platelet, and white blood cell counts were all observed within normal frequencies after completion of anti-TB treatment, and no significant differences were observed between study Arm A (TLG ≥ 50 SUV) and study Arm B/C (TLG ≥ 50 SUV). Evaluation of inflammatory indicators such as C-reactive protein (CRP) and Neutrophil-to-Lymphocyte (NLR) ratio showed significantly elevated CRP levels in study Arm B/C (TLG ≥ 50 SUV) compared to study Arm A (TLG ≥ 50 SUV) (Table 3.2 and Figure 3.1D), whereas no significant difference was observed in NLR between the study groups (Table 3.2.).

Table 3.2. Summary table showing biochemical, hematological, and inflammatory parameters measured from StatinTB clinical trial study participants after completion of anti-TB treatment. Data is represented as mean±SD where minimal lung inflammation is shown by TLG < 50 SUV and persisting lung inflammation is highlighted by TLG ≥ 50 SUV. Data was analysed using Shapiro-Wilk test followed by Mann-Whitney t-test. Neutrophil-to-Lymphocyte Ratio (NLR) was determined through the division of neutrophils into lymphocytes. TLG= Total Lung Glycolysis, SUV= Standardized Uptake Value, U/L= units per litre, µmol/L=micromole per litre, mg/milligrams per litre, and †= HIV positive only.

Classification	Tests	Study Arm A (TLG<50 SUV) (mean±SD)	Study Arm B/C (TLG≥50 SUV) (mean±SD)	p-value
Biochemical	Alkaline Phosphatase (U/L)	94.38 ± 20.29	115.1 ± 30.94	0.0029
	Alanine Transaminase (U/L)	23.48 ± 13.82	23.10 ± 12.92	0.9005
	Aspartate Aminotransferase (U/L)	29.95 ± 8.93	30.69 ± 6.23	0.2516
	Bilirubin (µmol/L)	6.71 ± 4.20	6.44 ± 2.77	0.5236
	Gamma-glutamyl transferase (U/L)	53.19 ± 43.97	58.17 ± 38.28	0.1768
	Creatinine (µmol/L)	68.48 ± 13.92	67. 07 ± 15.04	0.5745
	Creatine kinase (U/L)	174.4 ± 68.85	151.9 ± 74.99	0.1223
	Hemoglobin A1C (%)	5.37 ± 0.37	5.44 ± 0.31	0.7281
	Hemoglobin (g/dL)	14.30 ± 1.92	13.81 ±1.42	0.3066
	Ferritin (µg/L)	108.4 ± 87.31	148.9 ± 125.70	0.1367
	Iron (µmol/L)	17.80 ± 7.31	14.56 ± 6.32	0.0715
	Transferrin (g/L)	2.83 ± 3.13	2.52 ± 0.54	0.2334
	Natriuretic peptide (proBNP) (ng/L)	44.55 ± 39.42	103.6 ± 131.8	0.0113
	Troponin (ng/L)	5.75 ± 2.32	5.86 ±2.94	0.9693
	Vitamin D (nmol/L)	48.96 ± 18.69	63.21 ± 24.95	0.0192
Hematological	†CD4 (cells/µl)	594.80 ± 165.80	534.1 ± 257.90	0.3450
	Neutrophil ($x10^9$/L)	2.56 ± 1.18	2.86 ± 1.20	0.2089
	Lymphocyte ($x10^9$/L)	1.96 ± 0.58	1.98 ± 0.83	0.6991
	Platelets ($x10^9$/L)	280.3 ± 75.71	304.9 ± 79.0	0.3123
	White Blood Cell Count ($x10^9$/L)	5.23 ± 1.45	5.59 ± 1.64	0.3095
Inflammatory	CRP (mg/L)	4.35 ± 5.92	10.83 ± 8.72	<0.0001
	Neutrophil-to-Lymphocyte Ratio (NLR) ($x10^9$/L)	1.39 ± 0.73	1.64 ± 0.83	0.1357

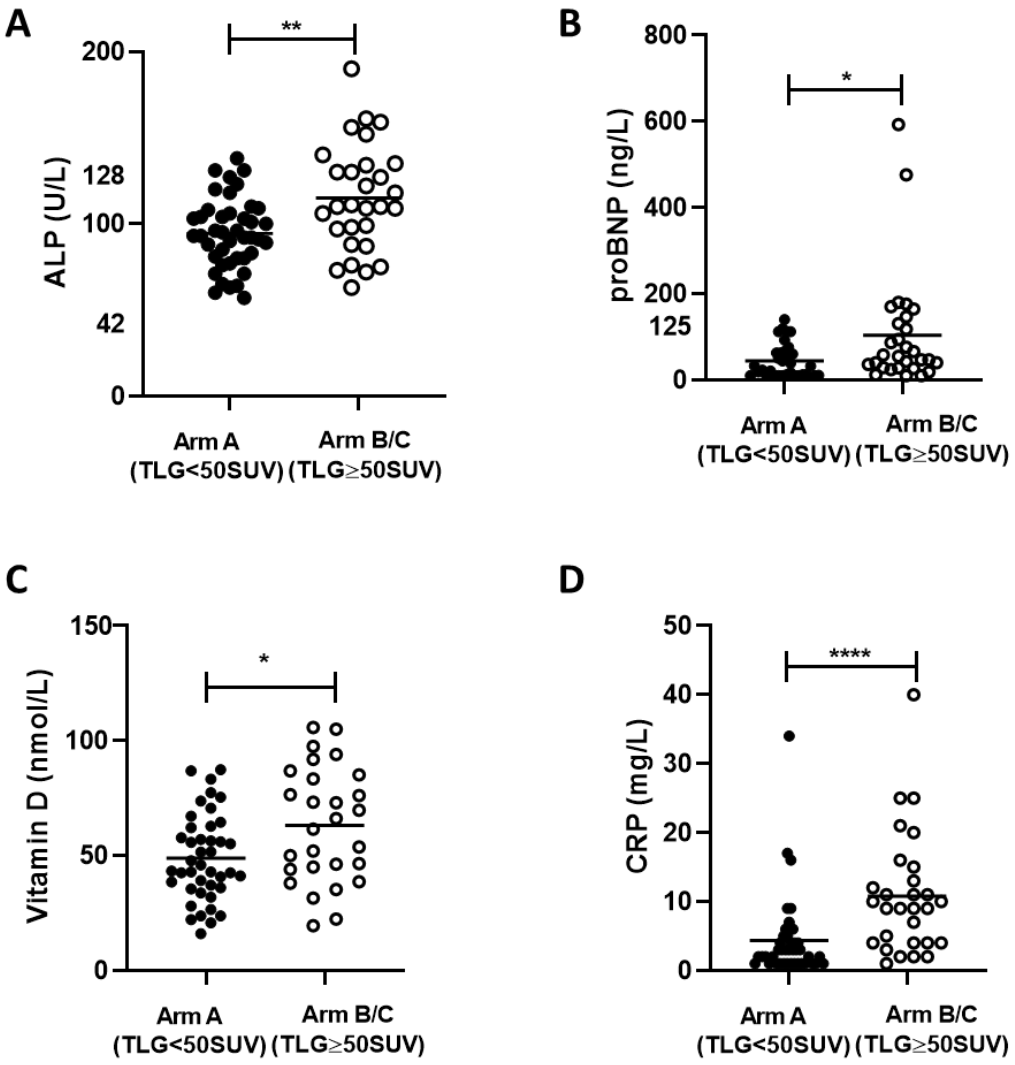

Figure 3.1. Participants with persisting lung inflammation display increased levels in biochemical and inflammatory parameter indicators after completion of anti-TB treatment. Data was evaluated during participant screening and represented as mean where **A.** ALP= Alkaline Phosphatase, **B.** proBNP= Natriuretic peptide, **C.** Vitamin D and **D.** CRP= C-reactive Protein. Participants were stratified based on lung inflammation where minimal lung inflammation is shown by TLG < 50 SUV and persisting lung inflammation is shown by TLG ≥ 50 SUV. Data was analysed using Shapiro-Wilk test followed by Mann-Whitney t-test, *p≤0.05, **p≤0.01 and ****p≤0.0001.

3.1.3. Healthy participants demographic information

A total of 28 healthy participants were included in the study, and they were stratified based on QuantiFERON (QFT)-TB gold analysis. The included study participants showed an overall mean±SD age (years) of 20.89±2.85 with 35.71% being males and 64.29% being females. Among them, 14 participants were QFT- with a mean±SD age (years) of

21.21±2.63, where 6 (42.85%) were males and 8 (57.15%) were females. The other 14 participants were shown to be QFT+ based on IFN-γ response. They showed a mean±SD age (years) of 20.57±3.13, where 4 (28.57%) being males and 10 (71.43%) being females. There was no significant difference (p=0.3964) observed in age (years) between the QFT study arms (Table 3.3.), and all included participants were HIV-negative.

Table 3.3. Healthy participants demographic information stratified by QFT analysis. Data is shown as total numbers (n), percentages (%) and mean±SD (age). QFT= QuantiFERON-TB, n= Total number, SD= standard deviation

	All	**QFT-**	**QFT+**
Participants, n	28	14	14
Age (years), mean±SD	20.89±2.85	21.21±2.63	20.57±3.13
Male, n (%)	10 (35.71)	6 (42.85)	4 (28.57)
Female, n (%)	18 (64.29)	8 (57.15)	10 (71.43)

3.2. Evaluation of atorvastatin effects on soluble biomarker secretion *ex-vivo* using ELISA method

Atorvastatin effects on regulating the secretion profile of soluble biomarkers, were evaluated *ex-vivo* in which different atorvastatin concentrations were used to stimulate PBMCs prior to Mtb infection. The secretion of three pro-inflammatory biomarkers, including IL-1β, IL-6, and IL-8, was evaluated. This study showed significant reduction of IL-1β with 100µM and 200µM atorvastatin after 1-Day Post Infection (1 DPI) regardless of Mtb strain. However, IL-6 and IL-8 were not affected by atorvastatin stimulation or Mtb strain (Figure 3.2A.). Further evaluations were performed at 3 DPI, where a significant reduction in IL-1β was observed with 50µM atorvastatin, regardless of Mtb strain. Additionally, IL-6 and IL-8 were significantly reduced by 50µM atorvastatin stimulation only with H37Rv *ex-vivo* infection. Furthermore, IL-6 was significantly reduced by 100µM only with HN878 *ex-vivo* infection, whereas no significance was observed with IL-8, which showed to be significantly upregulated at 3 DPI with CDC1551 *ex-vivo* infection (Figure 3.2B). At 6 DPI, IL-1β showed significant reduction by all atorvastatin concentrations (50, 100, and 200µM), regardless of Mtb strain. However, IL-6 showed significant upregulation with 100µM atorvastatin stimulation and HN878 *ex-vivo* infection, whereas IL-8 was significantly reduced by 200µM atorvastatin stimulation and H37Rv *ex-vivo* stimulation (Figure 3.2C). Collectively, these results show that atorvastatin regulates secretion of pro-inflammatory biomarkers, with IL-1β being mostly affected.

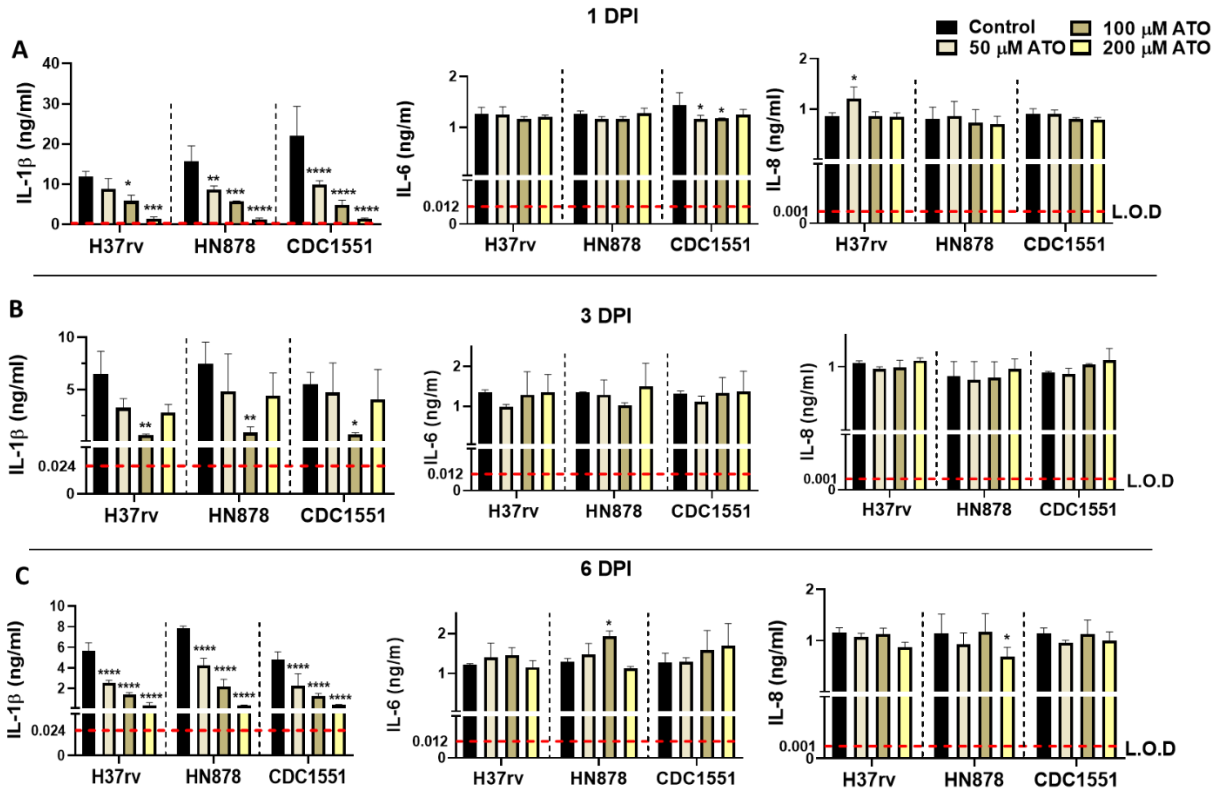

Figure 3.2. *Ex-vivo* evaluation of pro-inflammatory cytokine secretion profiles in H37Rv, HN878, and CDC1551 infected PBMC following 24-hours atorvastatin stimulation with 50µM, 100µM, and 200µM. Cytokines IL-1β, IL-6 and IL-8 were measured using the sandwich ELISA method at **A.** 1 DPI, **B.** 3 DPI, and **C.** 6 DPI where dotted line indicates detection limits. Data is shown as a representative of three replicates and shown as mean±SD. Data was analysed using Shapiro-Wilk test for normality. Data was analysed using two-way ANOVA followed by Dunnett's corrected multiple comparisons against control; *p≤0.05, **p≤0.01, ***p≤0.001, ****p≤0.0001. ATO: atorvastatin, DPI: Days Post Infection, LOD: Limit of Detection.

3.3. Luminex multiplex analysis of host serum biomarkers from StatinTB cohort and healthy individuals

3.3.1. Baseline evaluation of host serum biomarkers from StatinTB cohort at time point 0 (Week 0) using heat map

A panel of 48 soluble biomarkers (Biorad, 48 Human Screening Panel) was evaluated in this study. Among these, a total of 33 soluble biomarkers were detected in the serum samples from recruited study participants. Observed concentrations (pg/ml) were used to evaluate differences in the secretion profiles between study Arm A (TLG < 50 SUV) and study Arm B/C (TLG ≥ 50 SUV). The obtained data was visualized through heat map analysis, where normalization was performed per column; 0% (green) was defined as the small value and 100% (red) was defined as the high value. This analysis revealed an elevated secretion profile

of detected biomarkers in study Arm B/C (TLG ≥ 50 SUV) compared to study Arm A (TLG < 50 SUV), as indicated by intensifying red colour (Figure 3.3.). This inflammatory storm was observed in all biomarker classes which include chemokines, growth factors, pleiotropic mediators, pro-inflammatory, and anti-inflammatory cytokines.

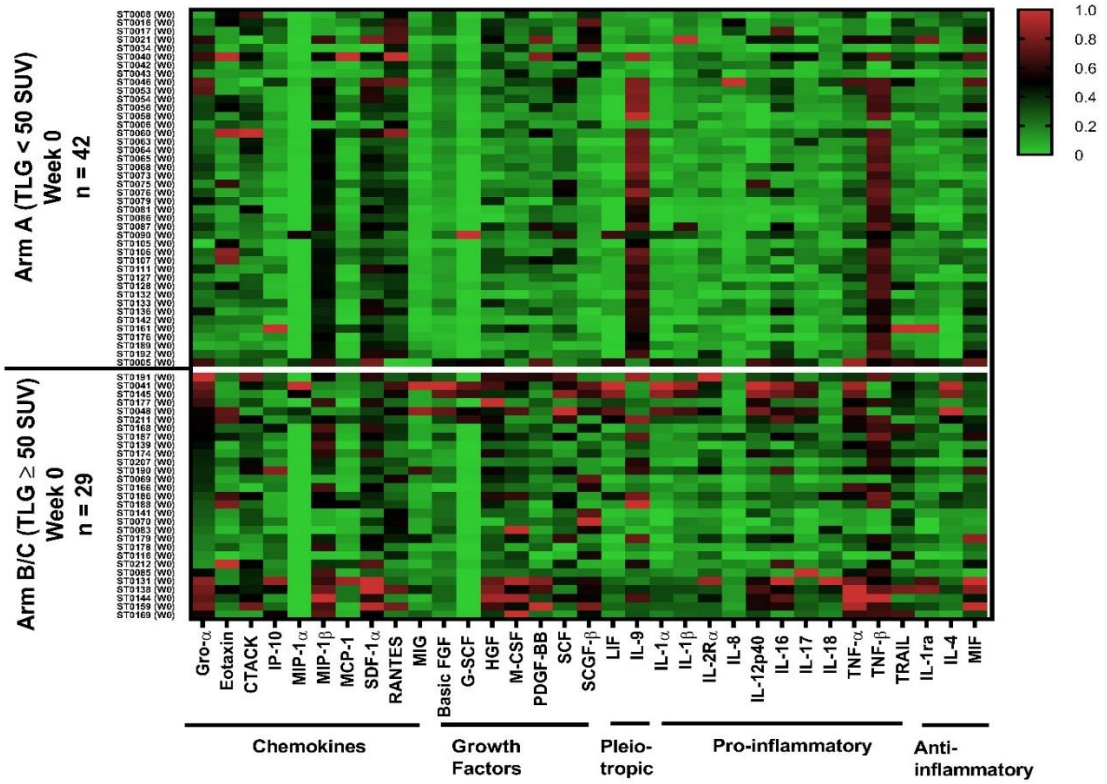

Figure 3.3. Evaluation of host serum biomarkers at week 0 time point after successful completion of anti-TB treatment using Luminex multiplex assay. Study participants stratification was based on persisting lung inflammation as indicated by Total Lung Glycolysis (TLG) cut-off value of 50 Standard Uptake Values (SUV) where TLG < 50 SUV show minimal lung inflammation (Arm A, n=42) and TLG ≥ 50 SUV show persisting lung inflammation (Arm B/C, n=29). Secretion profile of 33 soluble biomarkers classified as chemokines (n=10), growth factors (n=7), pleiotropic mediators (n=2), pro-inflammatory (n=11), and anti-inflammatory cytokines (n=3) was summarized using heatmap analysis. Data is a representative of four Luminex assays. Data was normalized per column where 0% (green colour) and 100% (red colour) detections were represented by the lowest and highest values, respectively.

3.3.2. Host serum biomarker evaluation at week 0 time point after completion of anti-TB treatment in patients with or without persisting lung inflammation

This study identified three chemokines (Gro-α (p=0.0005), IP-10 (p=0.0002), and MIG (p<0.0001)) that were significantly upregulated in study participants presenting with persisting lung inflammation (Arm B/C (TLG ≥ 50 SUV)) compared to those with minimal

lung inflammation (Arm A (TLG < 50 SUV)) at week 0 after anti-TB treatment completion (Figure 3.4. and Table 3.4).

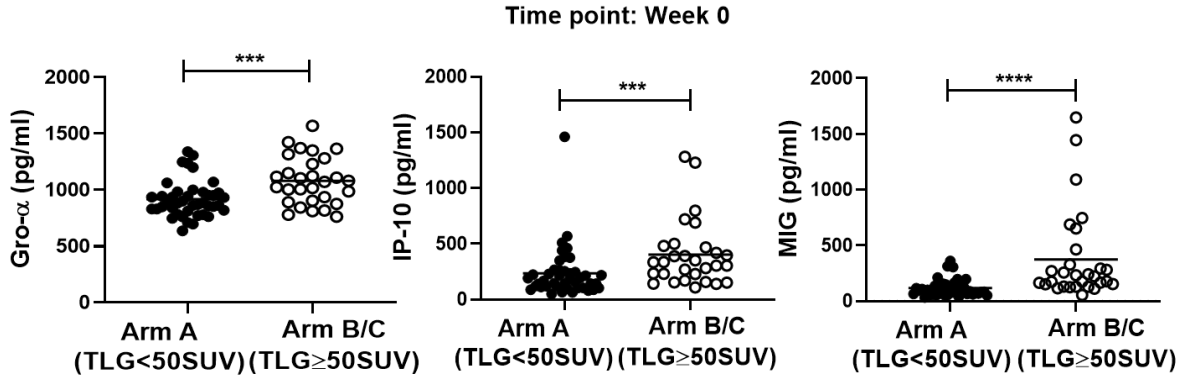

Figure 3.4. Representative plots showing secretion profile of Gro-α, IP-10, and MIG chemokines expressed in pg/ml in serum samples measured using Luminex multiplex assay at week 0 time point after completion of anti-TB treatment in patients presenting with minimal lung inflammation (Arm A TLG < 50 SUV, n=42) or persisting lung inflammation (study Arm B/C TLG ≥ 50 SUV, n=29). Data is a representative of four Luminex assays and shown as mean. Data was analysed using Shapiro-Wilk test followed by Mann-Whitney t-test where significance is shown as ***p≤0.001 and ****p≤0.0001.

A total of five growth factors were significantly upregulated in study Arm B/C (TLG ≥ 50 SUV) compared to Arm A (TLG < 50 SUV) at week 0 post-anti-TB treatment. These included Basic FGF (p=0.0042), G-CSF (p=0.0411), HGF (p<0.0001), M-CSF (p<0.0001), and SCGF-β (p<0.0001) (Figure 3.5. and Table 3.4.).

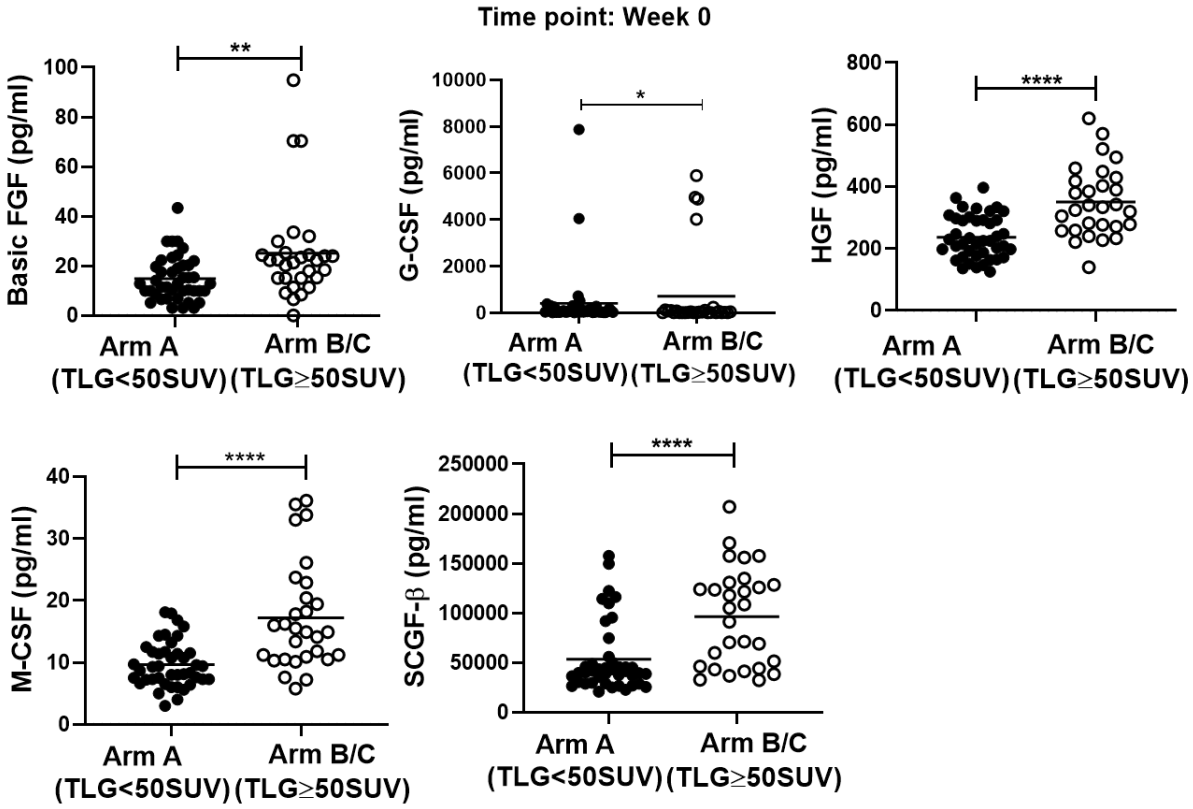

Figure 3.5. Measurement of Basic FGF, G-CSF, HFG, M-CSF, and SCGF-β growth factors expressed in pg/ml in serum samples at week 0 after successful TB treatment using Luminex multiplex platform. Study arms were stratified based on lung inflammation where Arm A (TLG < 50 SUV) (n=42) showed participants with minimal lung inflammation and Arm B/C (TLG ≥ 50 SUV) (n=29) showed participants with persisting lung inflammation. Data is a representative of four Luminex assays and shown as mean. Data was analysed using Shapiro-Wilk test followed by Mann-Whitney t-test where significance is shown as *p≤0.05 **p≤0.01 and ****p≤0.0001.

Two pleiotropic mediators (LIF and IL-9) were evaluated from successfully treated TB patients, and they displayed a different secretion profile between study arms. LIF was significantly upregulated in study Arm B/C (TLG ≥ 50 SUV) compared to Arm A (TLG < 50 SUV) (Figure 3.6.) with p<0.0001. However, IL-9 secretion was significantly downregulated in study Arm B/C (TLG ≥ 50 SUV) compared to study Arm A (TLG < 50 SUV) (Figure 3.6.) with p=0.0324 (Table 3.4.).

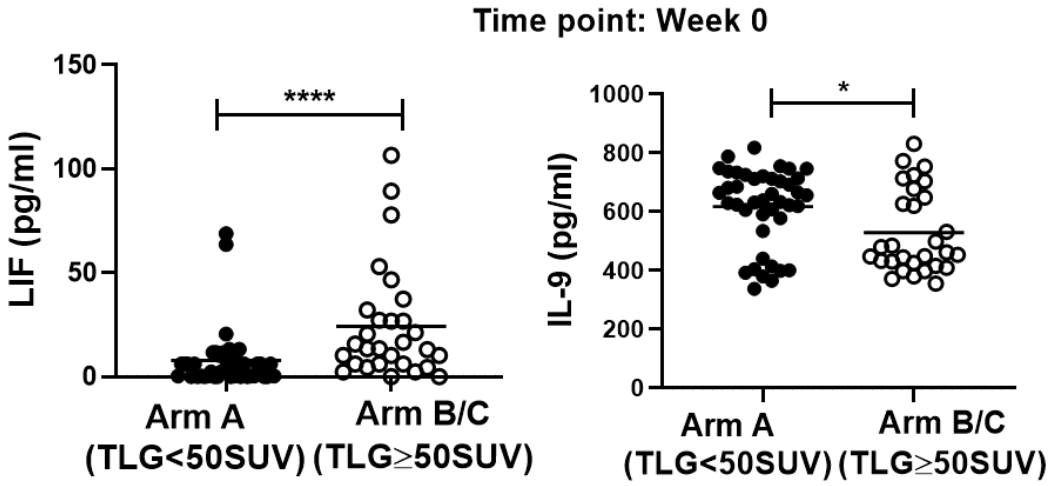

Figure 3.6. Evaluation of pleiotropic mediators (LIF and IL-9) expressed in pg/ml in serum samples at week 0 after completion of anti-TB treatment using Luminex multiplex assay. Stratification of study arms was based on lung inflammation where Arm A (TLG < 50 SUV) (n=42) showed participants with minimal lung inflammation and Arm B/C (TLG ≥ 50 SUV) (n=29) showed participants with persisting lung inflammation. Data is a representative of four Luminex assays and shown as mean. Data was analysed using Shapiro-Wilk test followed by Mann-Whitney t-test where significance is shown as *$p \leq 0.05$ and ****$p \leq 0.0001$.

A total of nine pro-inflammatory cytokines showed significant upregulation in study Arm B/C (TLG ≥ 50 SUV) compared to study Arm A (TLG < 50 SUV) after completion of anti-TB treatment (week 0). These includes IL-1α ($p=0.0007$), IL-1β ($p=0.0018$), IL2Rα ($p<0.0001$), IL-12p40 ($p<0.0001$), IL-16 ($p=0.0409$), IL-17 ($p=0.0041$), IL-18 ($p=0.0024$), TNF-α ($p=0.0036$), and TRAIL ($p=0.0018$) (Figure 3.7. and Table 3.4).

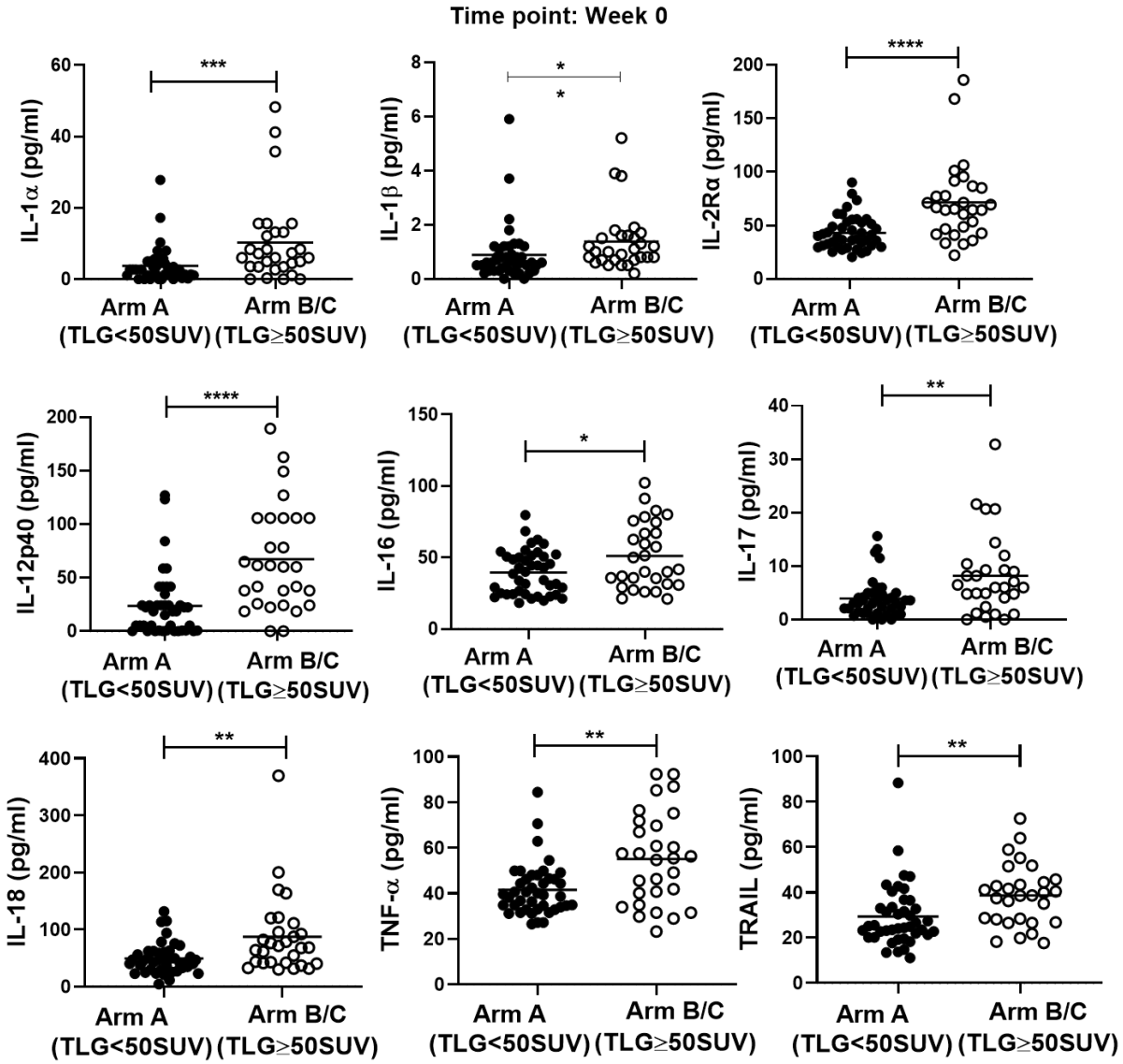

Figure 3.7. Representative plots showing the secretion profile of pro-inflammatory cytokines expressed in pg/ml which includes IL-α, IL-1β, IL-2Rα, IL-12p40, IL-16, IL-17, IL-18, TNF-α, and TRAIL in serum samples obtained at week 0 time point after anti-TB treatment completion. Luminex multiplex assay was used to evaluate the secretion profile between study arms which are stratified based on lung inflammation where Arm A (TLG < 50 SUV) (n=42) shows participants with minimal lung inflammation and Arm B/C (TLG ≥ 50 SUV) (n=29) show participants with persisting lung inflammation. Data is a representative of four Luminex assays and shown as mean. Data was analysed using Shapiro-Wilk test followed by Mann-Whitney t-test where significance is shown as * p≤0.05, ** p≤0.01, *** p≤0.001 ****p≤0.0001.

One anti-inflammatory cytokine (IL-4) showed significant upregulation in study Arm B/C (TLG ≥ 50 SUV) compared to study Arm A (TLG<50 SUV) at week 0 post-anti-TB treatment (Figure 3.8.) with p=0.0105 (Table 3.4.).

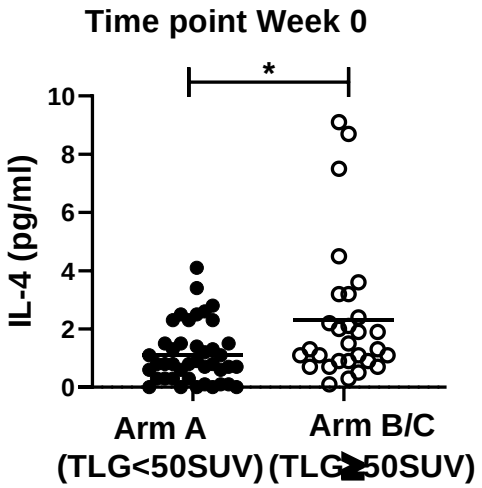

Figure 3.8. Evaluation of anti-inflammatory cytokine, IL-4, expressed in pg/ml in serum samples collected at week 0 after anti-TB treatment completion using Luminex multiplex assay. Study arms were stratified based on lung inflammation where Arm A (TLG < 50 SUV) (n=42) showed participants with minimal lung inflammation and Arm B/C (TLG ≥ 50 SUV) (n=29) showed participants with persisting lung inflammation. Data is a representative of four Luminex assays and shown as mean. Data was analysed using Shapiro-Wilk test followed by Mann-Whitney t-test where significance is shown as * $p \leq 0.05$.

Collectively, this study identified a total of twenty soluble biomarkers that were significantly secreted differently between study Arm A (TLG < 50 SUV) and study Arm B/C (TLG ≥ 50 SUV) (Table 3.4.). These biomarkers were distributed within different classes, including chemokines (n= 3), growth factors (n= 5), pleiotropic mediators (n= 2), pro-inflammatory (n= 9), and anti-inflammatory cytokines (n= 1). Nineteen soluble biomarkers were significantly upregulated in successfully treated TB patients with persisting lung inflammation (Arm B/C (TLG ≥ 50 SUV)). However, one biomarker (pleiotropic mediator (IL-9)), showed significant downregulation in successfully treated TB patients with persisting lung inflammation (Arm B/C (TLG ≥ 50 SUV)) compared to treated TB patients without persisting lung inflammation (Arm A (TLG ≥ 50 SUV)).

Table 3.4. Summary table showing the secretion profile of soluble biomarkers (n=20) which are expressed significantly differently at week 0 time point after completion of anti-TB treatment in participants stratified based on lung inflammation. Study Arm A (TLG < 50 SUV) includes study participants with minimal lung inflammation and study Arm B/C (TLG ≥ 50 SUV) includes study participants with persisting lung inflammation. Data is a representative of four Luminex assays and shown as mean±SD. Data was analysed using Shapiro-Wilk test followed by Mann-Whitney t-test. TLG=Total Lung Glycolysis, SUV=Standardized Uptake Value, SD=Standard Deviation.

Classification	Biomarkers	Arm A (TLG<50 SUV) (mean±SD)	Arm B (TLG≥50 SUV) (mean±SD)	p-value
Pro-inflammatory	IL-1α	3.77±5.03	10.26±11.99	0.0007
	IL-1β	0.88±1.02	1.37±1.12	0.0018
	IL-2Rα	43.04±15.64	71.42±36.42	<0.0001
	IL-12p40	23.71±29.97	67.34±49.02	<0.0001
	IL-16	39.55±15.28	51.04±23.06	0.0409
	IL-17	3.94±3.52	8.20±7.60	0.0041
	IL-18	49.12±27.06	87.08±69.94	0.0024
	TNF-α	41.52±11.48	55.06±20.16	0.0036
	TRAIL	29.35±13.91	38.69±13.67	0.0018
Anti-Inflammatory	IL-4	1.12±1.00	2.29±2.37	0.0105
Growth factors	Basic FGF	14.79±8.83	25.13±20.33	0.0042
	G-CSF	400.1±1334	715.5±1737	0.0411
	HGF	236.5±69.46	350.6±112.6	<0.0001
	M-CSF	9.66±3.67	17.21±8.62	<0.0001
	SCGF-β	53533±35244	96499±49185	<0.0001
Pleiotropic	IL-9	616.8±132.3	528.9±141.8	0.0324
	LIF	7.87±14.22	24.16±27.04	<0.0001
Chemokines	Gro-α	917.3±160.8	1081±212.7	0.0005
	IP-10	233.9±230.8	402.2±294.4	0.0002
	MIG	117.9±74.52	373.3±400.6	<0.0001

3.3.3. Soluble biomarkers correlate with TLG (SUV) values in successfully treated TB patients

In total, thirteen soluble biomarkers measured through the Luminex platform showed significant correlation with TLG (SUV) measured by Fluorodeoxyglucose Positron Emission Tomography/Computed Tomography (FDG PET/CT) scan, where R^2 and p-values were determined. This study identified two chemokines, IP-10 and MIG, which showed a

significant correlation with TLG (SUV) with R^2=0.1421, p=0.0012 and R^2=0.2718, p<0.0001, respectively (Figure 3.9. and Table 3.5.).

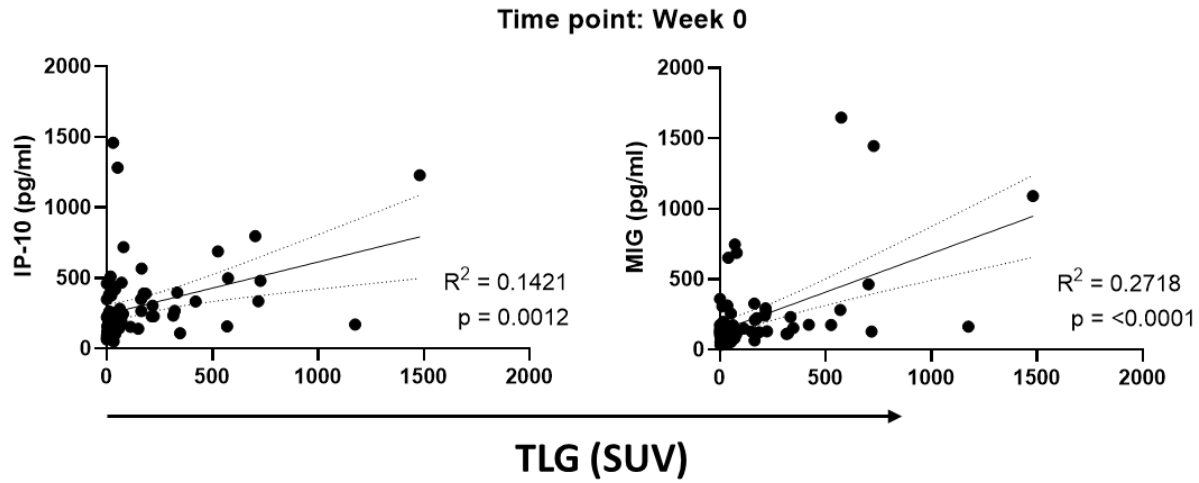

Figure 3.9. Total Lung Glycolysis (TLG) expressed in Standardized Uptake Value (SUV) correlates with chemokines IP-10 and MIG secretion at week 0 time point after completion of anti-TB treatment. FDG PET/CT scan was used to measure TLG (SUV) and the chemokine profile was measured through Luminex multiplex assay. Data was analysed using a two-tailed Pearson correlation coefficient where R^2 and p-values were determined. Dotted line indicates 95% confidence bands of the best-fit line.

Four growth factors showed significant correlation with TLG (SUV), including Basic FGF (R^2=0.0592, p=0.0408), HGF (R^2=0.1569, p=0.0006), M-CSF (R^2=0.0823, p=0.0153), and SCGF-β (R^2=0.1029, p=0.0064) (Figure 3.10. and Table 3.5.).

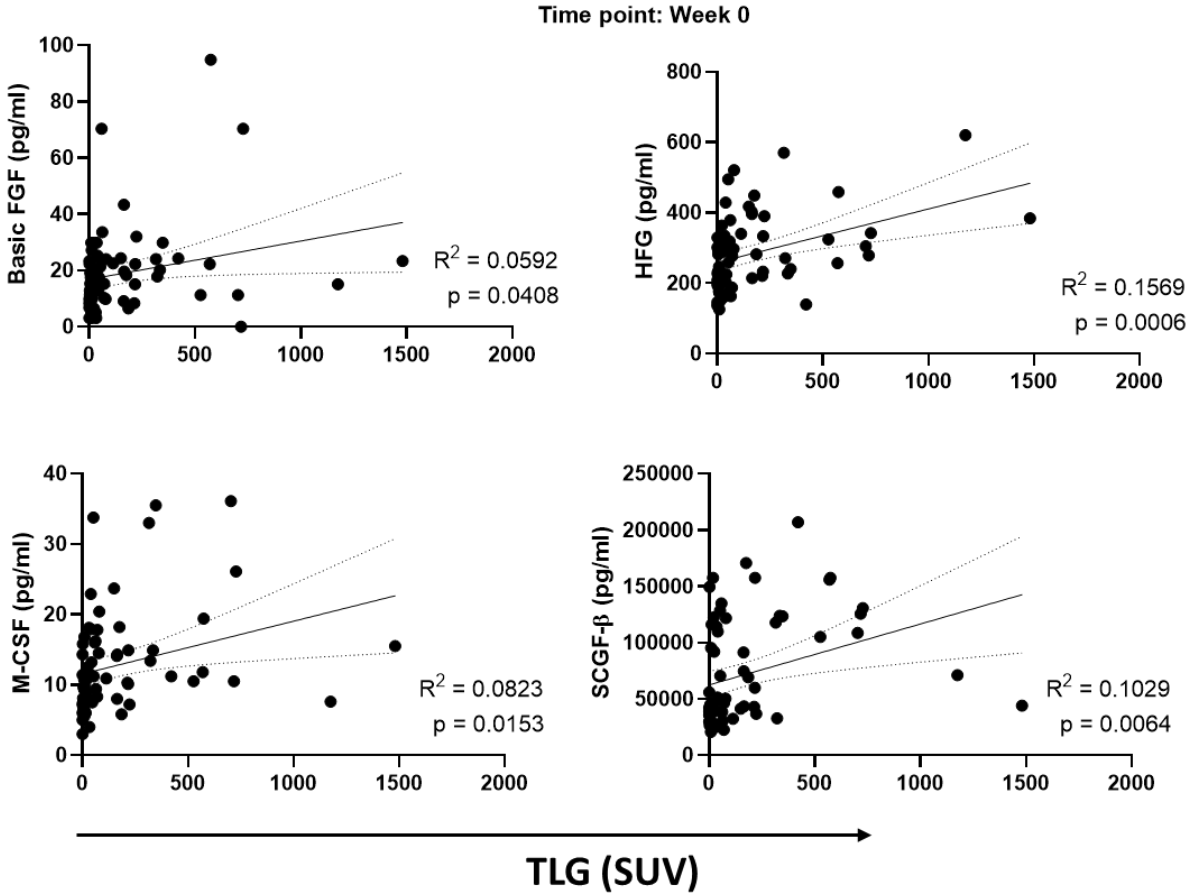

Figure 3.10. Representative plots showing correlation between TLG (SUV) measured by FDG PET/CT scan with growth factors Basic FGF, HFG, M-CSF, and SCGF-β at week 0 time point after anti-TB treatment completion measured through Luminex multiplex assay. Data was analysed using a two-tailed Pearson correlation coefficient where R^2 and p-values were determined. Dotted line indicates 95% confidence bands of the best-fit line.

Two pleiotropic mediators significantly correlated with TLG (SUV): LIF displayed a p-value of 0.0120 and an R^2 value of 0.0879, while IL-9 displayed a p-value of 0.0139 and an R^2 of 0.0844 (Figure 3.11. and Table 3.5.).

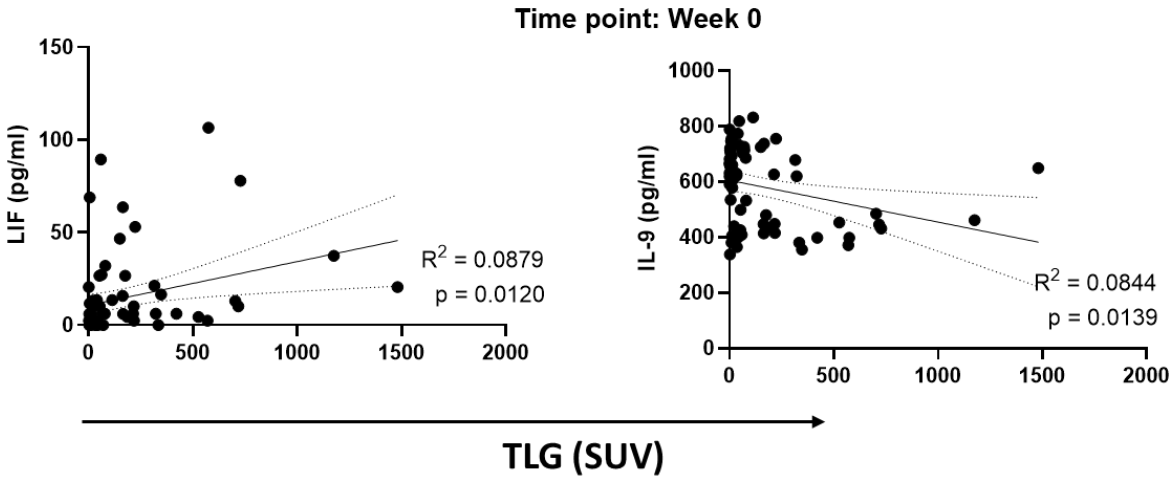

Figure 3.11. Correlation of pleiotropic mediators measured through Luminex multiplex assay, LIF, and IL-9, with TLG (SUV) measured by FDG PET/CT at week 0 time point visit after completion of anti-TB treatment. Data was analysed using a two-tailed Pearson correlation coefficient where R^2 and p-values were determined. Dotted line indicates 95% confidence bands of the best-fit line.

Five pro-inflammatory cytokines were significantly correlated with the TLG (SUV). These included IL-1α (R^2=0.0974, p=0.0080), IL2Rα (R^2=0.0551, p=0.0488), IL12p40 (R^2=0.1090, p=0.0049), TNF-α (R^2=0.0916, p=0.0103), and TRAIL (R^2=0.1158, p=0.0037) (Figure 3.12. and Table 3.5.).

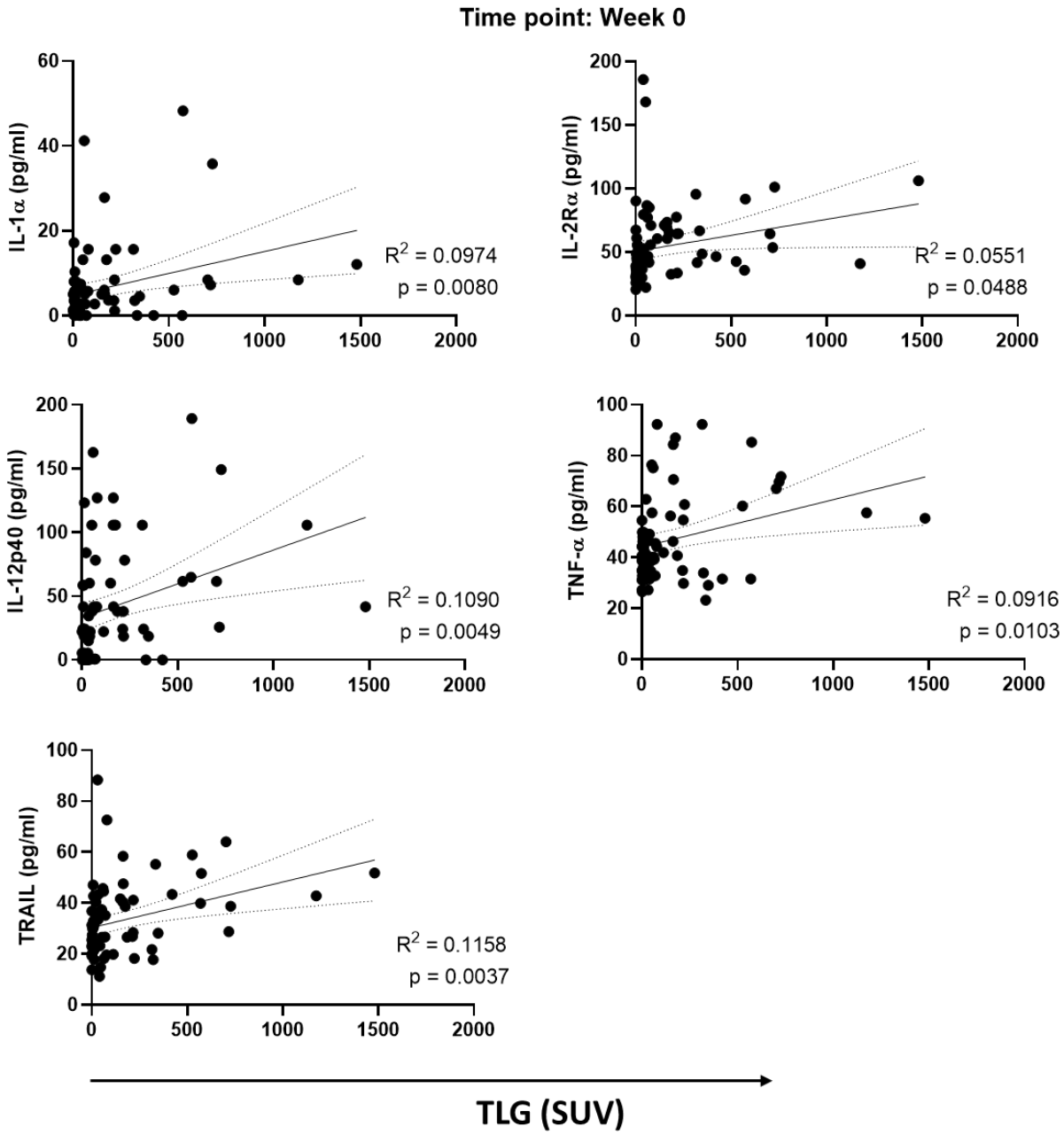

Figure 3.12. Pro-inflammatory cytokines IL-1α, IL-2Rα, IL-12p40, TNF-α, and TRAIL measured through Luminex multiplex assay correlates with TLG (SUV) measured by FDG PET/CT scan at week 0 time point following completion of anti-TB therapy. Data was analysed using a two-tailed Pearson correlation coefficient where R^2 and p-values were determined. Dotted line indicates 95% confidence bands of the best-fit line.

Table 3.5. Summary table showing soluble biomarkers (n=13) which significantly correlated with TLG (SUV) at week 0 after completion of anti-TB treatment. Statistical analysis was achieved through a two-tailed Pearson correlation coefficient, where R^2 values were determined to evaluate the relationship between variables and p-values were determined to show statistical significance. TLG=Total Lung Glycolysis, SUV=Standardized Uptake Value.

Biomarkers	Classification	R^2	p-value
IP-10	Chemokines	0.1421	0.0012
MIG		0.2718	<0.0001
Basic FGF	Growth Factors	0.0592	0.0408
HGF		0.1569	0.0006
M-CSF		0.0823	0.0153
SCGF-β		0.1029	0.0064
LIF	Pleiotropic	0.0879	0.0120
IL-9		0.0844	0.0139
IL-1α	Pro-inflammatory	0.0974	0.0080
IL-2Rα		0.0551	0.0488
IL-12p40		0.1090	0.0049
TNF-α		0.0916	0.0103
TRAIL		0.1158	0.0037

3.3.4. Evaluation of soluble biomarkers as potential diagnostic targets to discriminate between successfully treated TB patients with or without persisting lung inflammation

A total of 20 biomarkers, which were significantly different between study Arm A (TLG < 50 SUV) and study Arm B/C (TLG ≥ 50 SUV), were evaluated for diagnostic potential through Receiver Operating Characteristic (ROC) curves. In this study, a total of fourteen soluble biomarkers were identified as potential diagnostic targets with an Area Under the ROC Curve (AUC) ≥ 0.70, suggesting a 70% chance of discriminating between the two study arms. Seven pro-inflammatory biomarkers displayed an AUC between 0.702 and 0.796. Three chemokines were identified as acceptable diagnostic candidates with AUC ranging from 0.739 to 0.833, where Gro-α had AUC=0.739, IP-10 had an AUC of 0.753, and MIG had an AUC of 0.833 (Figure 3.13A.). Furthermore, three growth factors were identified as acceptable diagnostic candidates with AUC ranging from 0.780 to 0.805, where HGF showed an AUC of 0.805, M-CSF showed an AUC of 0.798, and SCGF-β had an AUC of 0.780 (Figure 3.13B.). Seven pro-inflammatory cytokines, including IL-1α (AUC=0.731), IL-1β (AUC=0.715), IL-2Rα (AUC=0.785), IL-12p40 (AUC=0.796), IL-18 (AUC=0.710), TNF-α

(AUC=0.702), and TRAIL (AUC=0.715), also showed acceptable diagnostic potential (Figure 3.13C.). Additionally, one pleiotropic mediator, LIF, showed an acceptable AUC of 0.770 (Figure 3.13D).

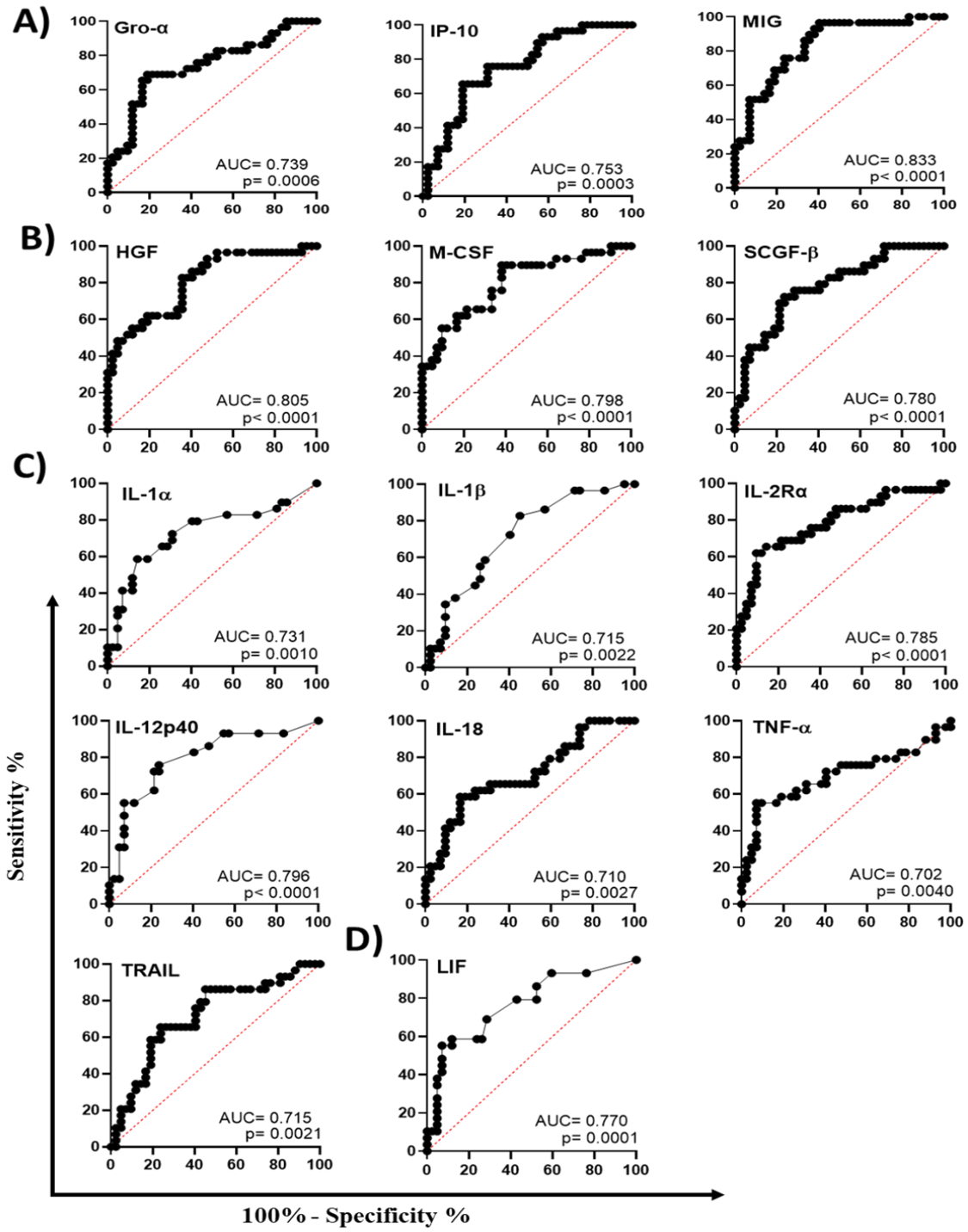

Figure 3.13. Receiver Operating Characteristic (ROC) curves showing diagnostic performances of individual biomarkers to discriminate between participants with minimal or persisting lung inflammation after completion of anti-TB treatment. ROC plots showing diagnostic performances with Area Under Curve (AUC)≥0.70 **A.** three chemokines (Gro-α, IP-10 and MIG), **B.** three growth factors (HGF, M-CF and SCGF-β), **C.** seven pro-inflammatory cytokines (IL-1α, IL-1β, IL-2Rα, IL-12p40, IL-18, TNF-α, and TRAIL), and **D.** one pleiotropic mediator (LIF). Data is a representative of four Luminex assays measured against Total Lung Glycolysis and analysed as ROC curves using Wilson/Brown method where AUC and p-values are shown.

Fourteen soluble biomarkers, which were identified as potential diagnostic targets to discriminate between study Arm A (TLG < 50 SUV) and study Arm B/C (TLG ≥ 50 SUV), were further evaluated for specific cut-off points using Youden's J statistic, which may provide a sensitivity ≥60% and sensitivity ≥70%. This study identified thirteen soluble biomarkers with sensitivity ranging between 62.07 and 75.86%, with MIG showing the highest sensitivity of 75.86%. One biomarker, IL-1β, which was identified as an acceptable diagnostic candidate showed a poor sensitivity of 58.52%. Evaluated biomarkers showed a specificity range between 71.43% and 80.95%, with IL-2Rα, HGF, and IP-10 displaying the highest specificity of 80.95%. IL-1β and LIF displayed the lowest specificity of 71.43% (Table 3.6.).

Table 3.6. Summary table highlighting diagnostic performances of individual biomarkers to discriminate between participants with or without persisting lung inflammation after completion of anti-TB treatment. Study participants were stratified based on lung inflammation where Arm A shows participants with minimal lung inflammation (TLG < 50 SUV) and Arm B/C shows participants with persisting lung inflammation (TLG ≥ 50 SUV). Data is a representative of four Luminex assays and shown as mean±SD, area (95%CI) and % (95%CI). Statistical significance between study arms was analysed using Shapiro-Wilk test followed by Mann-Whitney t-test. Area Under the ROC Curve (AUC) was determined through Wilson/Brown method and Youden's J statistics was used to determine cut-off values at respective sensitivity and specificity. CI=confidence interval, SD=standard deviation.

Biomarkers	**Arm A mean±SD**	**Arm B/C mean±SD**	**p-value**	**AUC (95% CI)**	**Cut-off value**	**Sensitivity% (95% CI)**	**Specificity% (95% CI)**
IL-1α	3.77±5.03	10.26±11.99	0.0010	0.731 (0.604-0.859)	>4.8	65.52 (47.35-80.06)	73.81 (58.93-84.70)
IL-1β	0.883±1.02	1.37±1.12	0.0022	0.715 (0.595-0.834)	>0.8	58.62 (40.74-74.49)	71.43 (56.43-82.83)
IL-2Rα	43.04±15.64	71.42±36.42	<0.0001	0.785 (0.673-0.897)	>55.6	65.52 (47.35-80.06)	80.95 (66.70-90.02)
IL-12p40	23.71±29.97	67.34±49.02	<0.0001	0.796 (0.686-0.906)	>36.3	72.41 (54.28-85.30)	78.57 (64.06-88.29)
IL-18	49.12±27.06	87.08±69.94	0.0027	0.710 (0.586-0.834)	>60.7	62.07 (44.00-77.31)	76.19 (61.47-86.52)
TNF-α	41.52±11.48	55.06±20.16	0.0040	0.702 (0.566-0.837)	>46.2	62.07 (44.00-77.31)	73.81 (58.93-84.70)
TRAIL	29.35±13.91	38.69±13.67	0.0021	0.715 (0.592-0.839)	>34.3	65.52 (47.35-80.06)	76.19 (61.47-86.52)
HGF	236.5±69.46	350.6±112.6	<0.0001	0.805 (0.702-0.908)	>303.3	62.07 (44.00-77.31)	80.95 (66.70-90.02)
M-CSF	9.66±3.67	17.21±8.61	<0.0001	0.798 (0.691-0.904)	>11.75	65.52 (47.35-80.06)	78.57 (64.06-88.29)
SCGF-β	53533±35244	96499±49185	<0.0001	0.780 (0.671-0.888)	>50833	72.41 (54.28-85.30)	76.9 (61.47-86.52)
LIF	7.87±14.22	24.16±27.04	0.0001	0.770 (0.655-0.884)	>8.20	68.97 (50.77-82.72)	71.43 (56.43-82.83)
Gro-α	917.3±160.8	1081±212.7	0.0006	0.739 (0.618-0.861)	>986.4	68.97 (50.77-82.72)	80.95 (66.7-90.02)
IP-10	233.9±230.8	402.2±294.4	0.0003	0.753 (0.640-0.866)	>266.9	65.52 (47.35-80.06)	80.95 (66.7-90.02
MIG	117.9±74.52	373.3±400.6	<0.0001	0.833 (0.739-0.927)	>149.2	75.86 (57.89-87.78)	76.19 (61.47-86.52)

3.3.5. Evaluation of host serum biomarkers after completion of standard anti-TB treatment in HIV-negative and HIV-positive adults

Host serum biomarkers were evaluated based of HIV stratification after completion of anti-TB treatment. Out of the total 71 study participants, 14 (19.71%) were HIV-positive. Among the 42 study participants with minimal lung inflammation (Arm A (TLG < 50 SUV)), 6 (14.28%) were HIV-positive, while 36 (85.72%) were HIV-negative. HIV stratification of study participants with persisting lung inflammation (Arm B/C (TLG ≥ 50 SUV)) (n =29) revealed 8 (27.58%) participants who were HIV-positive, while 21 (72.42%) participants were HIV-negative. A panel of 48 soluble biomarkers (Bio-Rad, 48 Human Screening Panel) were evaluated using Luminex multiplex assay, detecting 33 biomarkers from serum samples. These were classified based on function and included chemokines (n=10), growth factors (n=7), pleiotropic mediators (n=2), pro-inflammatory (n=11), and anti-inflammatory cytokines (n=3). A heat-map analysis was performed to visualise the secretion profile of soluble biomarkers between study groups. Data normalization was performed per column, where 0% (green colour) and 100% (red colour) values were defined by the lowest and highest values, respectively. As indicated by intensive red colour, this analysis showed high detection of serum biomarkers in both HIV-negative and HIV-positive participants from study Arm B/C (TLG ≥ 50 SUV) compared to study Arm A (TLG < 50 SUV) participants stratified by HIV status (Figure 3.14).

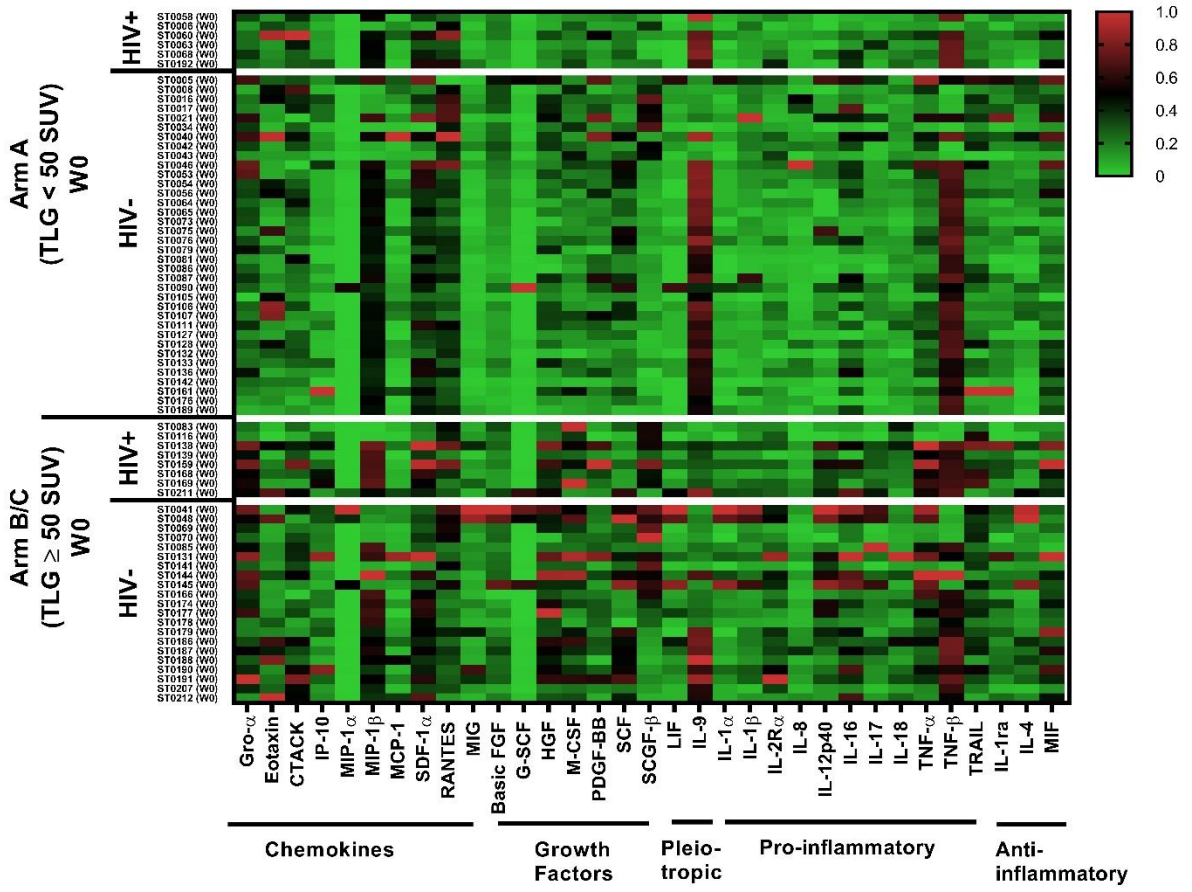

Figure 3.14. Heat-map analysis of host serum biomarkers measured by Luminex multiplex assay after completion of anti-TB treatment in study participants with minimal lung inflammation (Arm A (TLG < 50 SUV)) or persisting lung inflammation (Arm B/C (TLG ≥ 50 SUV)) stratified by HIV status. Study participants were stratified based on HIV status within each study arm where study Arm A (TLG < 50 SUV) had 6 HIV-positive and study Arm B/C (TLG ≥ 50 SUV) had 8 HIV-positive participants. Serum biomarkers (n=33) were classified into chemokines (n=10), growth factors (n=7), pleiotropic mediators (n=2), pro-inflammatory (n=11), and anti-inflammatory cytokines (n=3) and summarized using heatmap analysis. Data is a representative of four Luminex assays. Data was normalized per column where 0% (green colour) and 100% (red colour) detections were represented by the lowest and highest values, respectively.

Evaluation of host serum biomarkers in HIV-stratified participants with minimal or persisting lung inflammation showed significant upregulation of 2 growth factors (HGF and SCGF-β) in both HIV-negative and HIV-positive participants with persisting lung inflammation (Arm B/C (TLG ≥ 50 SUV)) compared to HIV-positive participants with minimal lung inflammation (Arm A (TLG < 50 SUV)) (Figure 3.15A.). LIF showed significant upregulation in both HIV-negative and HIV-positive participants with persisting lung

inflammation compared to participants with minimal lung inflammation after completion of anti-TB treatment (Figure 3.15B.). Pro-inflammatory cytokines including IL-1α, IL-12p40 and TRAIL, were significantly upregulated in both HIV-negative and HIV-positive participants with persisting lung inflammation compared to participant with minimal lung inflammation (Figure 3.15C.). This data shows that the elevated levels of soluble biomarkers in participants with persisting lung inflammation after completion of anti-TB treatment are not affected by HIV co-infection.

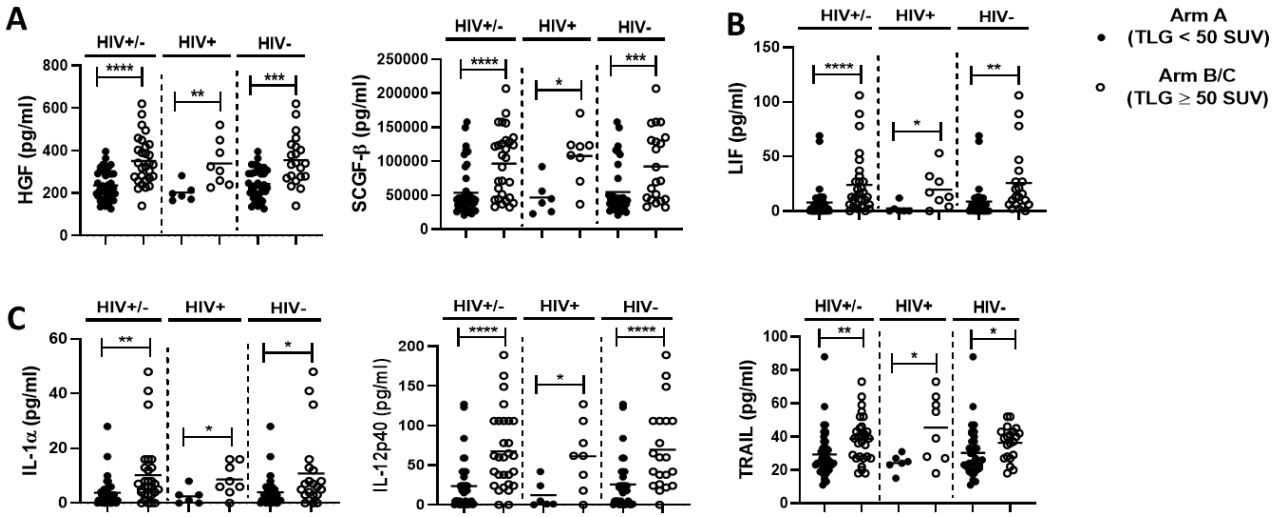

Figure 3.15. Elevated levels of soluble biomarkers in participants presenting with persisting lung inflammation (Arm B/C (TLG ≥ 50 SUV)) after completion of anti-TB treatment are not affected by HIV co-infection. Biomarkers were measured using Luminex multiplex assay and study participants were stratified based on HIV status within each arm where Arm A (TLG < 50 SUV) (n=6 HIV+) and Arm B/C (TLG ≥ 50 SUV) (n=8 HIV+). **A.** growth factors, **B.** pleiotropic mediator, and **C.** pro-inflammatory cytokines. Data is expressed in pg/ml and shown as mean. Data is a representative of four Luminex assays. Data was analysed using Shapiro-Wilk test followed by Mann-Whitney test where significance is shown as *p≤0.05, **p≤0.01, ***p≤0.001 and ****p≤0.0001.

A total of 13 serum biomarkers, evaluated through Luminex multiplex assay, were significantly upregulated in HIV-negative participants with persisting lung inflammation (Arm B/C TLG ≥ 50 SUV) compared to HIV-negative participants with minimal lung inflammation (Arm A (TLG < 50 SUV)) after completion of anti-TB treatment. These include 3 chemokines (Gro-α, IP-10 and MIG) (Figure 3.16A.); 3 growth factors (Basic FGF, M-CSF and SCF) (Figure 3.16B.); 6 pro-inflammatory cytokines (IL-1β, IL-2Rα, IL-16, IL-17, IL-18 and TNF-α) (Figure 3.15C); and 1 anti-inflammatory cytokines (IL-4) (Figure

3.16D.). There were no significant differences observed on the secretion profile of these biomarkers between HIV-positive participants with or without persisting lung inflammation. This data shows that HIV co-infection does not affect the secretion profile of these biomarkers in patients who have completed anti-TB treatment.

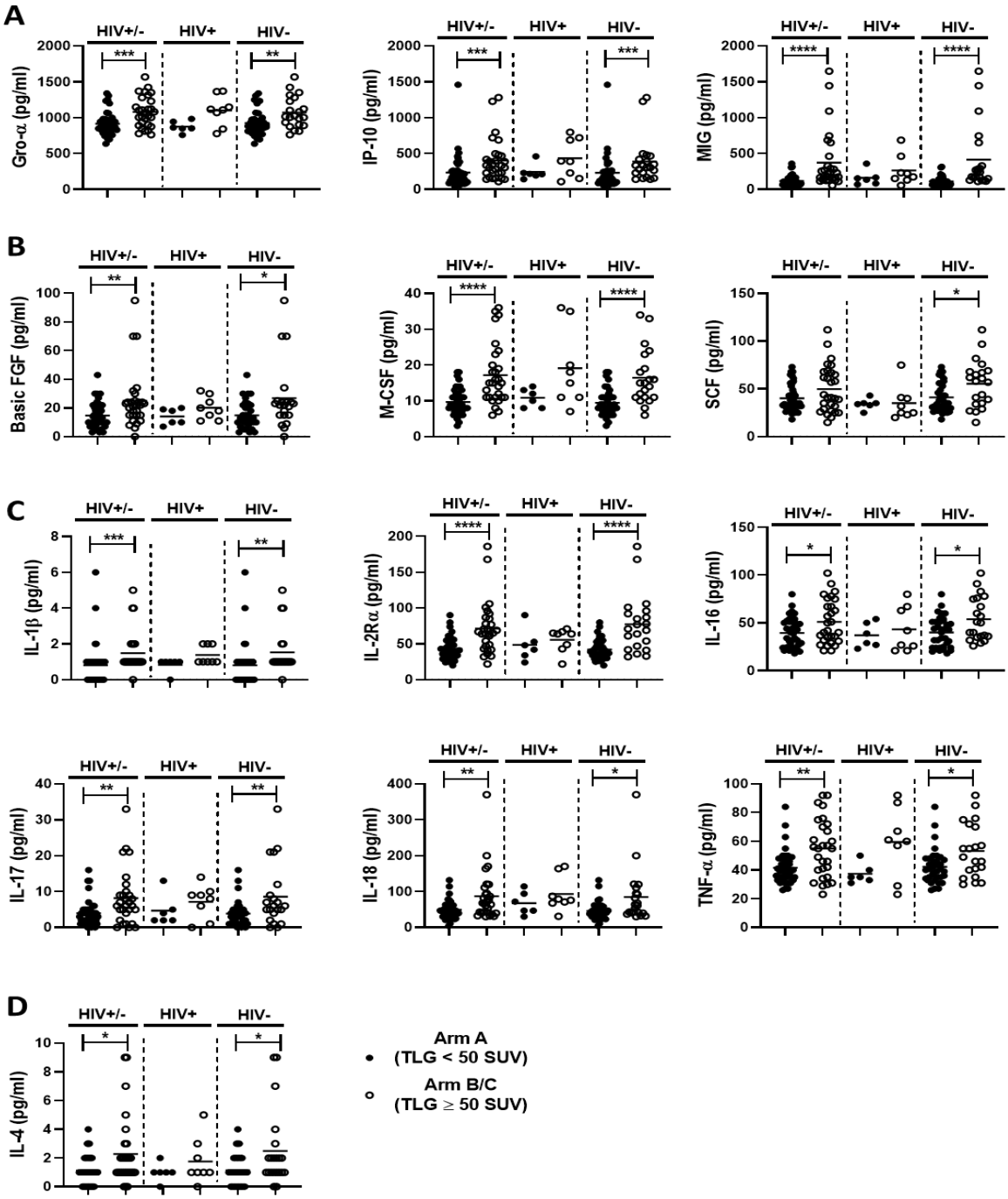

Figure 3.16. Host serum biomarkers measured using Luminex multiplex assay show significant upregulation in HIV-negative and not in HIV-positive participants presenting with persisting lung inflammation (Arm B/C (TLG ≥ 50 SUV)). Study participants were stratified based on HIV status within each arm where Arm A (TLG < 50 SUV) (n=6 HIV+) and Arm B/C (TLG ≥ 50 SUV) (n=8 HIV+). **A.** chemokines B. growth factors, **C.** pro-inflammatory cytokines, and **D.** anti-inflammatory cytokines. Data is expressed in pg/ml and shown as mean. Data is a representative of four Luminex assays. Data was analysed using Shapiro-Wilk test followed by Mann-Whitney test where significance is shown as *p≤0.05, **p≤0.01, ***p≤0.001 and ****p≤0.0001.

3.3.6. Heat map analysis of host serum biomarkers at Week 12 of StatinTB clinical trial

Soluble biomarkers were further evaluated at week 12 of the StatinTB clinical trial, where participant stratification was based on TLG (SUV). This data is part of an ongoing double-blind clinical trial (StatinTB), where study Arm B/C (TLG ≥ 50 SUV) serves as the experimental group; these participants had been given either atorvastatin 40mg/day or placebo for 12 weeks from recruitment. However, for the purpose of this thesis and due to continued clinical trial blinding, this data is collectively analysed relative to lung inflammation after the completion of anti-TB treatment. A total of 39 participants were analysed from study Arm A (TLG < 50 SUV), and 28 participants in study Arm B/C (TLG ≥ 50 SUV). Three participants had missed time point visits in study Arm A (TLG < 50 SUV), and one participant from study Arm B/C (TLG ≥ 50 SUV) was withdrawn from the study. In a panel of 48 soluble biomarkers, 33 biomarkers were detected from the serum samples. Heat map analysis showed that participants in study Arm B/C (TLG ≥ 50 SUV) remained with increased secretion of soluble mediators at week 12 compared to study Arm A (TLG < 50 SUV). These biomarkers are classified into chemokines, growth factors, pleiotropic mediators, pro-inflammatory, and anti-inflammatory cytokines (Figure 3.17.).

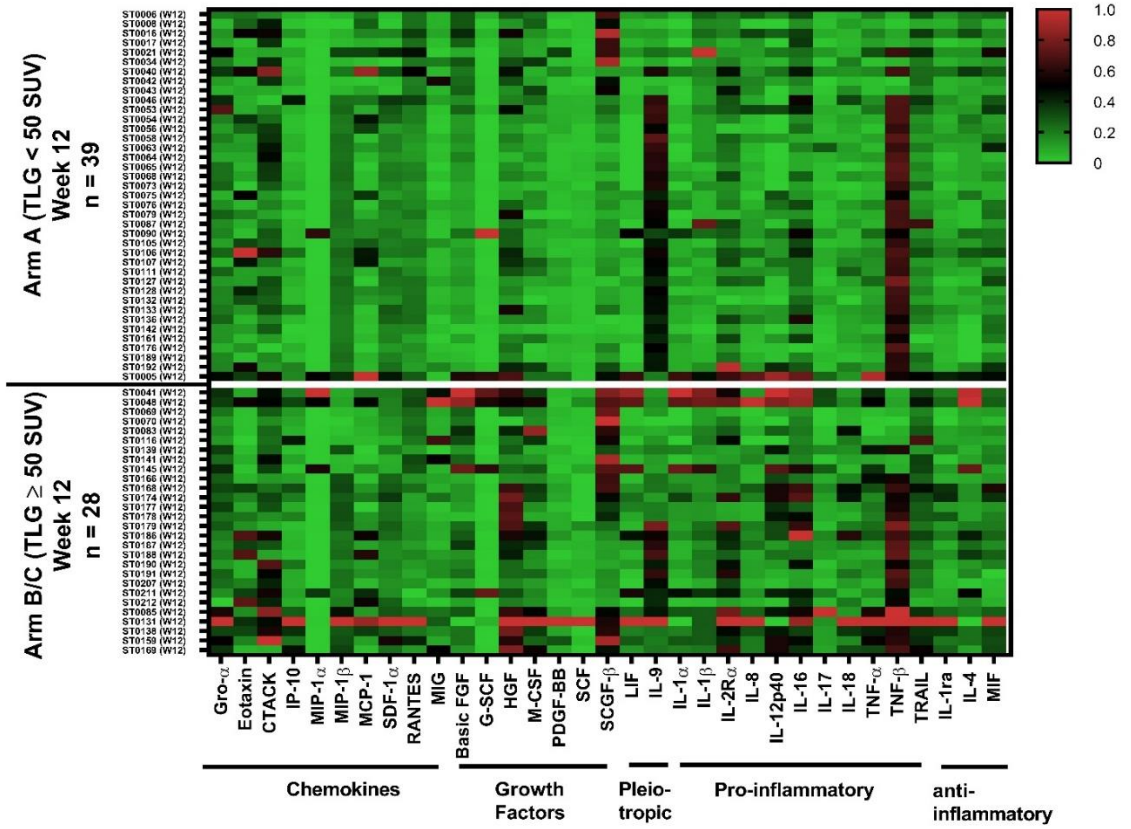

Figure 3.17. Heat map analysis showing secretion profile of host serum biomarkers evaluated using Luminex multiplex assay at week 12 time point after successful completion of anti-TB treatment. Study participants were stratified based on persisting lung inflammation indicated by TLG (SUV) where study Arm A (TLG < 50 SUV) (n=39) showed participants without persisting lung inflammation and study Arm B/C (TLG ≥ 50 SUV) (n=28) showed participants with persisting lung inflammation. Study participants in Arm B/C (TLG ≥ 50 SUV) are randomized to atorvastatin or identical placebo and due to ongoing blinding this data is collectively analysed. Secretion profile of 33 soluble biomarkers classified as chemokines (n=10), growth factors (n=7), pleiotropic mediators (n=2), pro-inflammatory (n=11), and anti-inflammatory cytokines (n=3) was summarized using heatmap analysis. Data is a representative of four Luminex assays. Data was normalized per column where 0% (green colour) and 100% (red colour) detections were represented by the lowest and highest values, respectively**.**

3.3.7. Evaluation of host serum biomarkers at week 12 of StatinTB clinical trial

This study identified three chemokines (Gro-α, IP-10, and MIG) that remained significantly upregulated in study Arm B/C (TLG ≥ 50 SUV) at week 12 when compared to study Arm A (TLG < 50 SUV) (Figure 3.18. and Table 3.7).

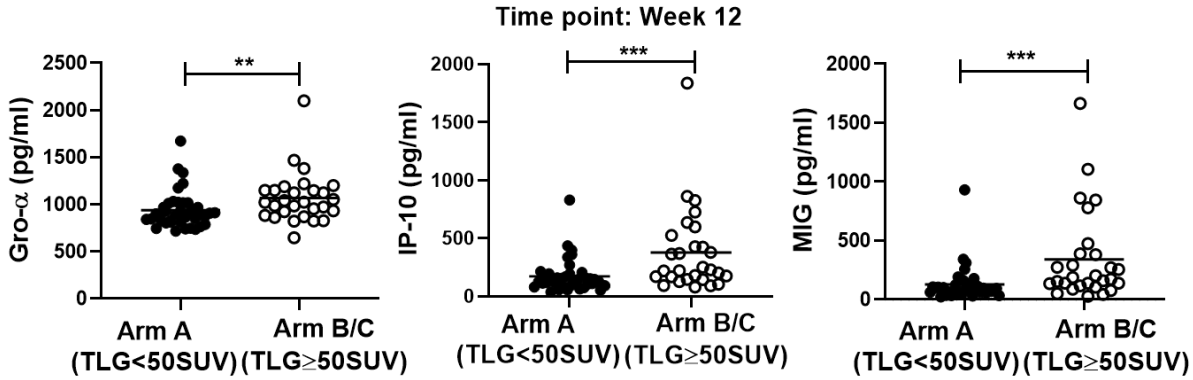

Figure 3.18. Secretion profile of Gro-α, IP-10, and MIG chemokines evaluated using Luminex multiplex assay between study Arm A (TLG < 50 SUV) (n=39) and study Arm B/C (TLG ≥ 50 SUV) (n=28) at week 12 after completion of anti-TB treatment. Study participants in Arm B/C (TLG ≥ 50 SUV) are randomized to atorvastatin or identical placebo and due to ongoing blinding this data is collectively analysed. Data is a representative of four Luminex assays and shown as mean. Data was analysed using Shapiro-Wilk test followed by Mann-Whitney t-test where significance is shown as **p≤0.01 and ***p≤0.001.

A total of four growth factors remained significantly upregulated in study Arm B/C (TLG ≥ 50 SUV) at week 12 when compared to Arm A (TLG < 50 SUV). These include Basic FGF (p=0.0153), HGF (p=0.0004), M-CSF (p<0.0001), and SCGF-β (p=0.0008) (Figure 3.19. and Table 3.7.).

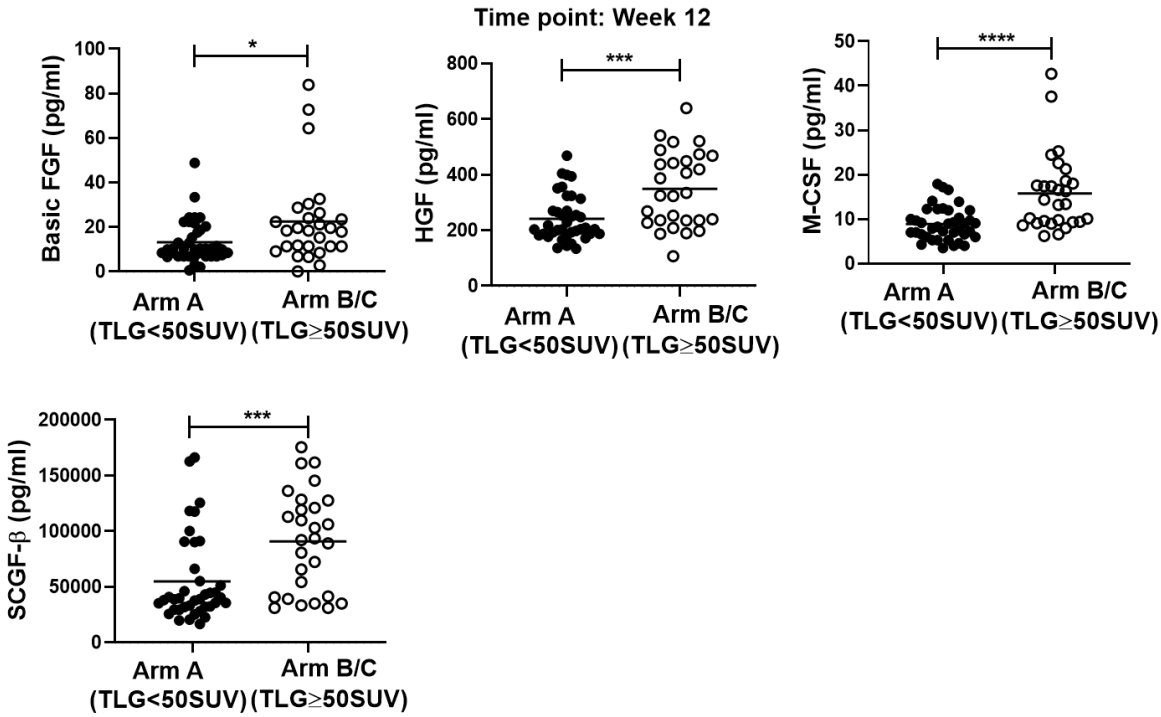

Figure 3.19. Evaluation of Basic-FGF, HGF, M-CSF, and SCGF-β growth factors in serum samples measured using Luminex multiplex assay at week 12 after completion of anti-TB therapy. Study participants were stratified based on lung inflammation where Arm A (TLG < 50 SUV) (n=39) showed participants with minimal lung inflammation and Arm B/C (TLG ≥ 50 SUV) (n=28) showed participants with persisting lung inflammation. Study participants in Arm B/C (TLG ≥ 50 SUV) are randomized to atorvastatin or identical placebo and due to ongoing blinding this data is collectively analysed. Data is a representative of four Luminex assays and shown as mean. Data was analysed using Shapiro-Wilk test followed by Mann-Whitney t-test where significance is shown as *p≤0.05 and ***p≤0.001.

Evaluation of pleiotropic mediators at week 12 post-anti-TB treatment showed significant upregulation of LIF (p=0.0005) in study Arm B/C (TLG ≥ 50 SUV) whereas IL-9 (p=0.0465) was significantly downregulated when compared to Arm A (TLG < 50 SUV) (Figure 3.20. and Table 3.7).

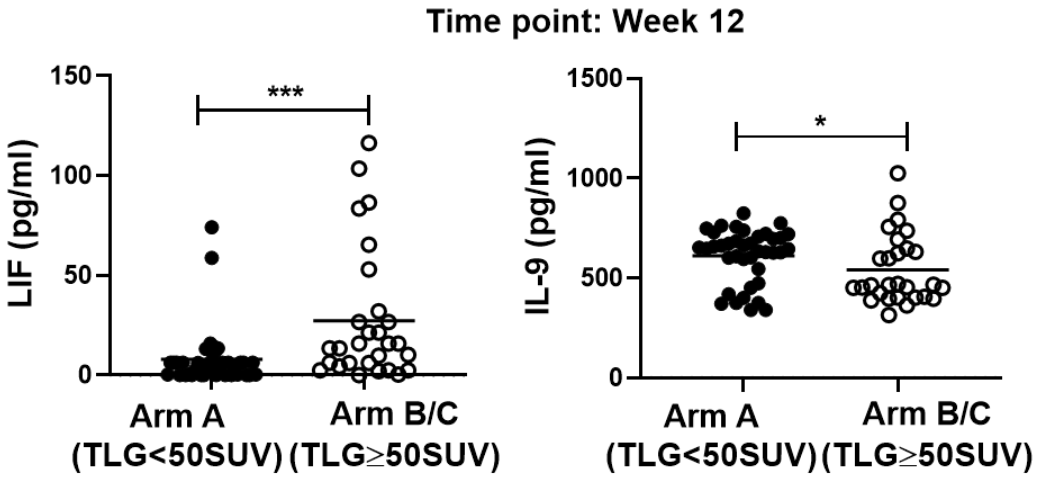

Figure 3.20. Representative plots showing secretion profile of pleiotropic mediators (LIF and IL-9) in serum samples at week 12 after completion of anti-TB treatment. Biomarkers were measured using Luminex multiplex assay where study arms were stratified based on lung inflammation. Study Arm A (TLG < 50 SUV) (n=39) shows participants with minimal lung inflammation and Arm B/C (TLG ≥ 50 SUV) (n=28) shows participants with persisting lung inflammation. Study participants in Arm B/C (TLG ≥ 50 SUV) are randomized to atorvastatin or identical placebo and due to ongoing blinding this data is collectively analysed. Data is a representative of four Luminex assays and shown as mean. Data was analysed using Shapiro-Wilk test followed by Mann-Whitney t-test where significance is shown as *p≤0.05 and ***p≤0.001.

A total of nine pro-inflammatory cytokines remained significantly upregulated in study Arm B/C (TLG ≥ 50 SUV) at week 12 of the StatinTB clinical trial when compared to Arm A (TLG < 50 SUV). Figure 3.21. and Table 3.7. highlights significantly upregulated pro-inflammatory which includes IL-1α (p=0.0193), IL-1β (p=0.0007), IL2Rα (p=0.0163), IL-12p40 (p=0.0004), IL-16 (p=0.0154), IL-17 (p=0.0112), IL-18 (p= 0.0004), TNF-α (p=0.0079), and TRAIL (p=0.0007).

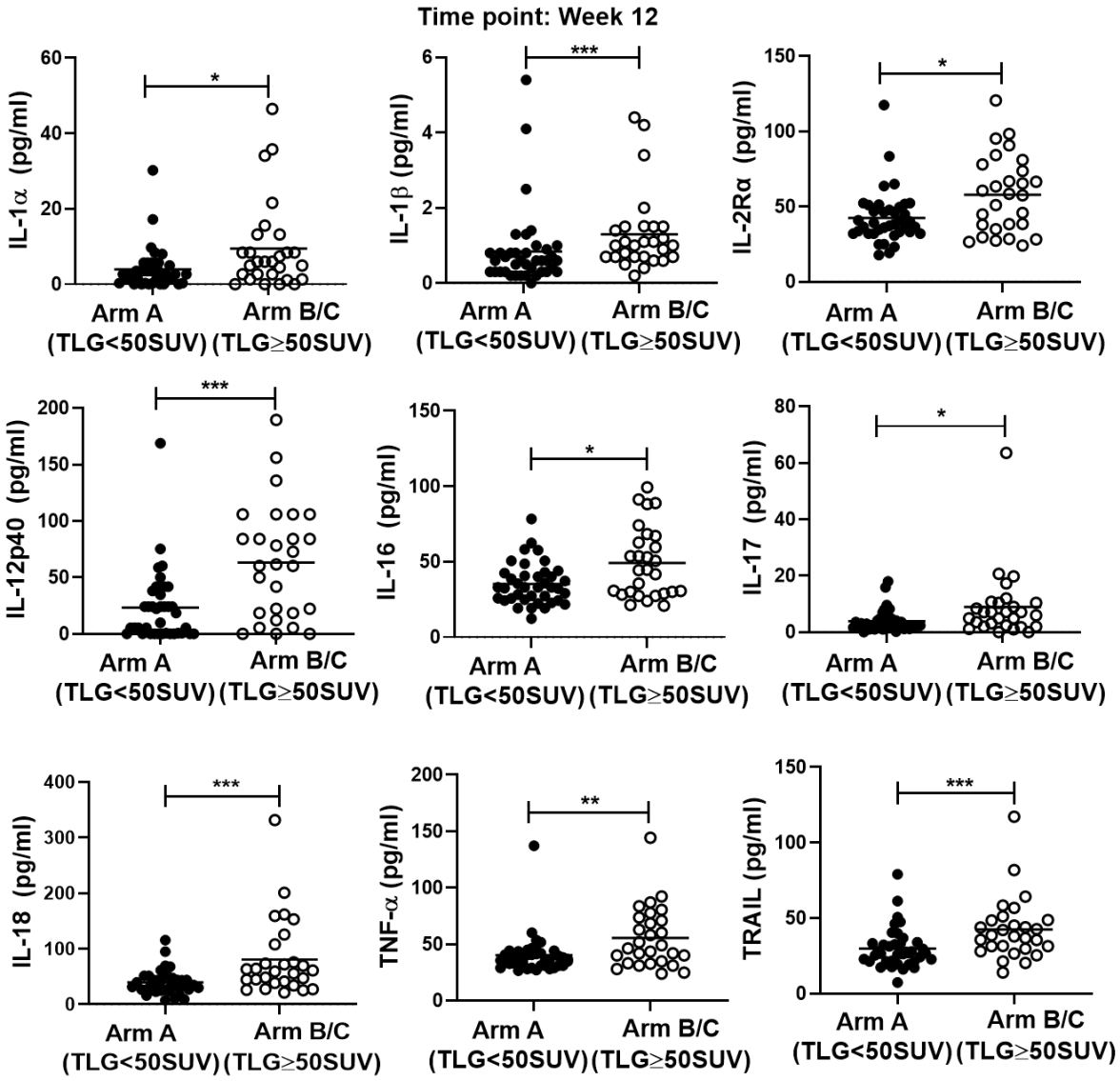

Figure 3.21. Secretion profile of pro-inflammatory cytokines (IL-1α, IL-1β, IL-2Rα, IL12p40, IL-16, IL-17, IL-18, TNFα, and TRAIL) measured using Luminex multiplex assay from serum samples at week 12 after completion of anti-TB treatment therapy. Study participants were stratified based on lung inflammation where Arm A (TLG < 50 SUV) (n=39) showed participants with minimal lung inflammation and Arm B/C (TLG ≥ 50 SUV) (n=28) showed participants with persisting lung inflammation. Study participants in Arm B/C (TLG ≥ 50 SUV) are randomized to atorvastatin or identical placebo and due to ongoing blinding this data is collectively analysed. Data is a representative of four Luminex assays and shown as mean. Data was analysed using Shapiro-Wilk test followed by Mann-Whitney t-test where significance is shown as *p≤0.05, **p≤0.01 and ***p≤0.001.

Anti-inflammatory cytokine, IL-4 (p=0.0199) remained significantly upregulated in study Arm B/C (TLG ≥ 50 SUV) at week 12 compared to study Arm A (TLG < 50 SUV) (Figure 3.22. and Table 3.7.).

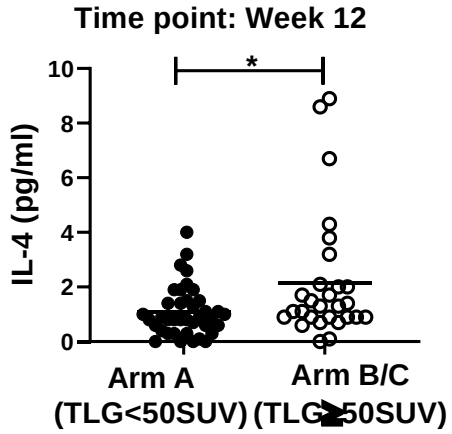

Figure 3.22. Evaluation of anti-inflammatory biomarker (IL-4) secretion using Luminex multiplex assay in serum samples at week 12 after successful completion of anti-TB treatment therapy. Study participants were stratified based on lung inflammation where Arm A (TLG < 50 SUV) (n=39) showed participants with minimal lung inflammation and Arm B/C (TLG ≥ 50 SUV) (n=28) showed participants with persisting lung inflammation. Study participants in Arm B/C (TLG ≥ 50 SUV) are randomized to atorvastatin or identical placebo and due to ongoing blinding this data is collectively analysed. Data is a representative of four Luminex assays and shown as mean. Data was analysed using Shapiro-Wilk test followed by Mann-Whitney t-test where significance is shown as *p≤0.05.

Soluble biomarker analysis at week 12 of the StatinTB clinical trial showed a total of 19 biomarkers, which were significantly expressed differently between study Arm A (TLG < 50 SUV) and study Arm B/C (TLG ≥ 50 SUV) (Table 3.7.). These biomarkers were classified as chemokines (n=3), growth factors (n=4), pleiotropic mediators (n=2), pro-inflammatory cytokines (n=9), and anti-inflammatory cytokines (n=1). In relation to baseline (week 0) analysis, no significant difference was observed in G-CSF secretion at week 12 between the study arms. Thus, a total of eighteen soluble biomarkers were significantly upregulated in successfully treated TB patients with persisting lung inflammation (Arm B/C (TLG ≥ 50 SUV)). Additionally, one soluble biomarker (IL-9), remained significantly downregulated in these successfully treated TB patients.

Table 3.7. Summary table showing host serum biomarker expression measured by Luminex multiplex assay at week 12 after completion of anti-TB treatment. Study participants were stratified based on lung inflammation where Arm A (TLG < 50 SUV) showed participants with minimal lung inflammation and Arm B/C (TLG ≥ 50 SUV) showed participants with persisting lung inflammation. Study participants in Arm B/C (TLG ≥ 50 SUV) are randomized to atorvastatin or identical placebo and due to ongoing blinding this data is collectively analysed. Data is a representative of four Luminex assays and shown as mean±SD. Data was analysed using Shapiro-Wilk test followed by Mann-Whitney t-test. TLG=Total Lung Glycolysis, SUV=Standardized Uptake Value, SD=Standard Deviation.

Classification	**Biomarkers**	**Arm A (TLG<50 SUV) (mean±SD)**	**Arm B (TLG≥50 SUV) (mean±SD)**	**p-value**
Pro-inflammatory	IL-1α	3.98±5.48	9.47±11.70	0.0193
	IL-1β	0.84±1.03	1.30±1.04	0.0007
	IL-2Ra	42.49±17.81	57.76±25.69	0.0163
	IL-12p40	23.11±31.47	63.18±50.30	0.0004
	IL-16	35.25±13.72	49.18±23.39	0.0154
	IL-17	3.83±3.78	8.88±12.08	0.0112
	IL-18	39.44±21.63	80.70±68.29	0.0004
	TNF-α	40.24±17.72	55.50±26.81	0.0079
	TRAIL	29.74±13.30	42.51±20.56	0.0007
Anti-Inflammatory	IL-4	1.09±0.91	2.15±2.32	0.0199
Growth factors	Basic FGF	13.13±9.32	22.48±19.99	0.0153
	HGF	241.20±82.66	348.70±136.10	0.0004
	M-CSF	8.89±3.71	15.81±8.77	<0.0001
	SCGF-β	54903.00±38736.00	90824.00±44951.00	0.0008
Pleiotropic	IL-9	612.1±134.6	541.2±174.7	0.0465
	LIF	8.01±14.69	27.26±33.25	0.0005
Chemokines	Gro-α	937.30±194.40	1067.00±268.80	0.0049
	IP-10	171.80±142.30	377.40±365.60	0.0003
	MIG	127.00±150.10	339.40±380.50	0.0002

3.3.8. Heat map analysis of serum biomarkers at week 24 after completion of anti-TB treatment

Further evaluation of soluble biomarkers was performed at week 24 of the StatinTB clinical trial which is the end of the observation period in the experimental group (Arm B/C (TLG ≥ 50 SUV)) and final samples collection time point for both study arms. A total of 42 participants were analysed from study Arm A (TLG < 50 SUV) and 27 participants from

study Arm B/C (TLG ≥ 50 SUV). Compared to the baseline analysis (week 0) two participants from study Arm B/C (TLG ≥ 50 SUV) were withdrawn from the study. This data forms part of a double-blind clinical trial (StatinTB clinical trial), which is still ongoing where participants in study Arm B/C (TLG ≥ 50 SUV) which is an experimental group are randomly given atorvastatin (40mg/day) or matching placebo. However, for the purpose of this thesis work and to prevent involuntary unblinding of the data; study Arm B/C has been analysed as a collective study arm. A total of 33 soluble biomarkers were detected from the serum samples. Heat map analysis showed that participants in study Arm B/C (TLG ≥ 50 SUV) remained with increased secretion of inflammatory mediators at week 24 compared to study Arm A. These biomarkers are classified into chemokines, growth factors, pleiotropic mediators, pro-inflammatory, and anti-inflammatory cytokines (Figure 3.23.).

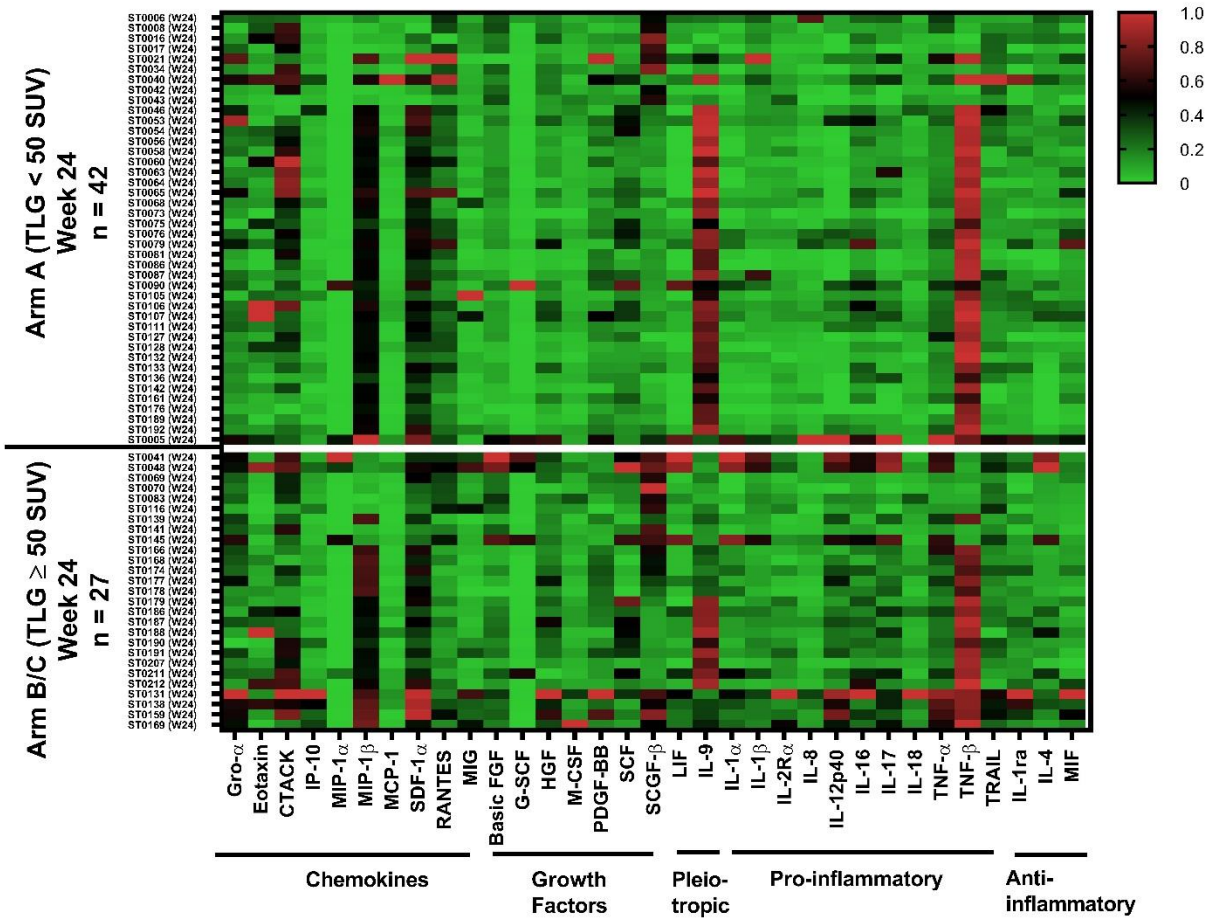

Figure 3.23. Heat map analysis showing secretion profile of host serum biomarkers evaluated using Luminex multiplex assay at week 24 time point after successful completion of anti-TB treatment. Study participants were stratified based on persisting lung inflammation indicated by TLG (SUV) where study Arm A (TLG < 50 SUV) (n=42) showed participants without persisting lung inflammation and study Arm B/C (TLG ≥ 50 SUV) (n=27) showed participants with persisting lung inflammation. Secretion profile of 33 soluble biomarkers classified as chemokines (n=10), growth factors (n=7), pleiotropic mediators (n=2), pro-inflammatory (n=11), and anti-inflammatory cytokines (n=3) was summarized using heatmap analysis. Study participants in Arm B/C (TLG ≥ 50 SUV) are randomized to atorvastatin or identical placebo and due to ongoing blinding this data is collectively analysed. Data is a representative of four Luminex assays. Data was normalized per column where 0% (green colour) and 100% (red colour) detections were represented by the lowest and highest values, respectively.

3.3.9. Host serum biomarker analysis at week 24 of StatinTB clinical trial

Two chemokines remained significantly upregulated in study Arm B/C (TLG ≥ 50 SUV) compared to study Arm A (TLG < 50 SUV) at week 24 of the StatinTB clinical trial. These included Gro-α (p=0.0180) and IP-10 (p=0.0404) (Figure3.24. and Table 3.8.).

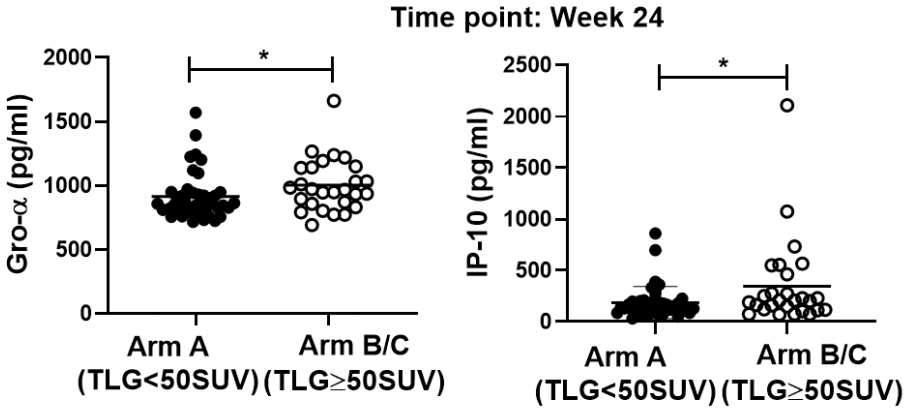

Figure 3.24. Secretion profile of Gro-α and IP-10 chemokines evaluated using Luminex multiplex assay between study Arm A (TLG < 50 SUV) (n=42) and study Arm B/C (TLG ≥ 50 SUV) (n=27) at week 24 after successful completion of anti-TB treatment. Study participants were stratified based on lung inflammation where TLG < 50 SUV showed participants with minimal lung inflammation and TLG ≥ 50 SUV showed participants with persisting lung inflammation. Study participants in Arm B/C (TLG ≥ 50 SUV) are randomized to atorvastatin or identical placebo and due to ongoing blinding this data is collectively analysed. Data is a representative of four Luminex assays and shown as mean. Data was analysed using Shapiro-Wilk test followed by Mann-Whitney t-test where significance is shown as *p≤0.05.

A total of four growth factors (Basic FGF (p=0.0037), HFG (p=0.0008), M-CSF (p=0.0048), and SCGF-β (p=0.0016) were observed to remain significantly upregulated in study Arm B/C (TLG ≥ 50 SUV) at week 24 of StatinTB clinical trial when compared to Arm A (TLG < 50 SUV) (Figure 3.25. and Table 3.8.).

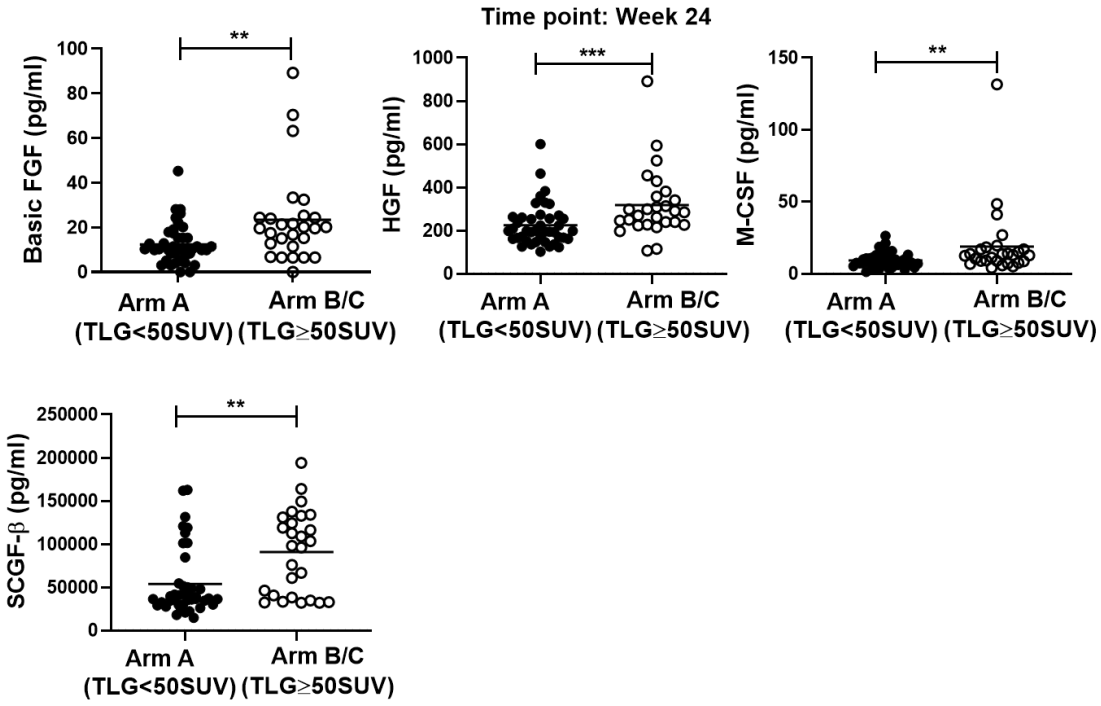

Figure 3.25. Measurement of Basic FGF, HFG, M-CSF, and SCGF-β growth factors expressed in pg/ml in serum samples at week 24 after successful TB treatment using Luminex multiplex platform. Study arms were stratified based on lung inflammation where Arm A (TLG < 50 SUV) (n=42) showed participants with minimal lung inflammation and Arm B/C (TLG ≥ 50 SUV) (n=27) showed participants with persisting lung inflammation. Study participants in Arm B/C (TLG ≥ 50 SUV) are randomized to atorvastatin or identical placebo and due to ongoing blinding this data is collectively analysed. Data is a representative of four Luminex assays and shown as mean. Data was analysed using Shapiro-Wilk test followed by Mann-Whitney t-test where significance is shown as **p≤0.01 and ***p≤0.001.

At week 24 after completion of anti-TB treatment, the secretion profile of pleiotropic mediators showed significant upregulation of LIF (p=0.0016) and significant downregulation of IL-9 (p=0.0094) in participants with persisting lung inflammation (Arm B/C (TLG ≥ 50 SUV)) compared to participants with minimal lung inflammation (Arm A (TLG < 50 SUV)) (Figure 3.26. and Table 3.8.)

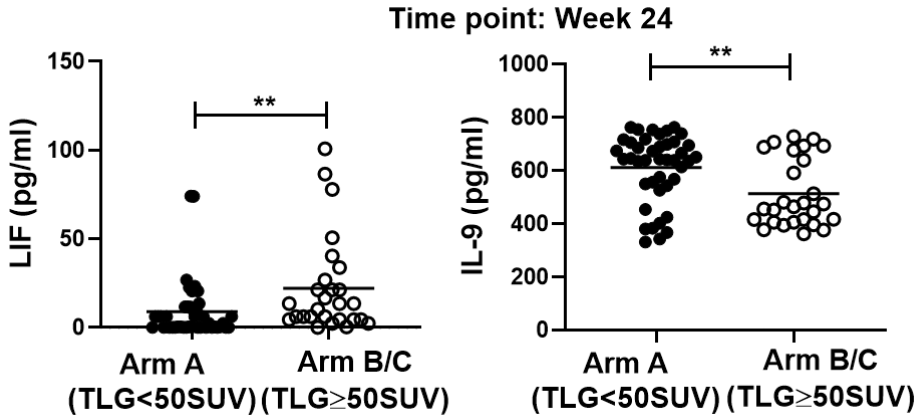

Figure 3.26. Representative plots showing secretion profile of pleiotropic mediators (LIF and IL-9) in serum samples at week 24 after completion of anti-TB treatment. Biomarkers were measured using Luminex multiplex assay where study arms were stratified based on lung inflammation. Study Arm A (TLG < 50 SUV) (n=42) shows participants with minimal lung inflammation and Arm B/C (TLG ≥ 50 SUV) (n=27) shows participants with persisting lung inflammation. Study participants in Arm B/C (TLG ≥ 50 SUV) are randomized to atorvastatin or identical placebo and due to ongoing blinding this data is collectively analysed. Data is a representative of four Luminex assays and shown as mean. Data was analysed using Shapiro-Wilk test followed by Mann-Whitney t-test where significance is shown as **p≤0.01 and ***p≤0.001.

The secretion profile of pro-inflammatory cytokines at week 24 showed a total of eight pro-inflammatory cytokines which remained significantly elevated in study Arm B/C (TLG ≥ 50 SUV) when compared to study Arm A (TLG < 50 SUV). These included IL-1α (p=0.0029), IL-1β (p=0.0049), IL2Rα (p=0.0206), IL-12p40 (p<0.0001), IL-17 (p=0.0027), IL-18 (p=0.0120), TNF-α (p=0.0105), and TRAIL (p=0.0213) (Figure 3.2. and Table 3.8.).

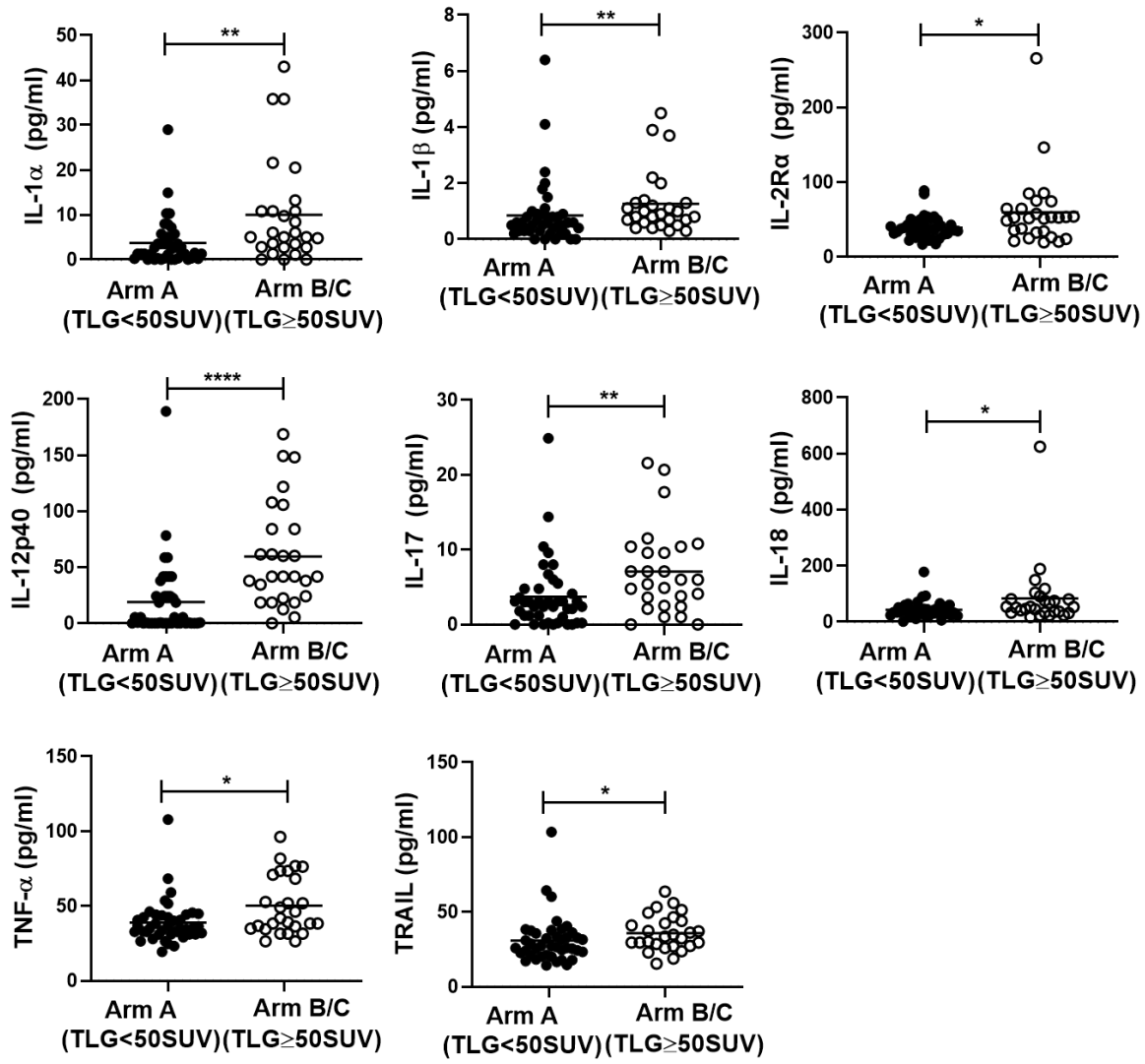

Figure 3.27. Secretion profile of pro-inflammatory cytokines (IL-1α, IL-1β, IL-2Rα, IL12p40, IL-17, IL-18, TNFα, and TRAIL) measured using Luminex multiplex assay from serum samples at week 24 after completion of anti-TB treatment therapy. Study participants were stratified based on lung inflammation where Arm A (TLG < 50 SUV) (n=42) showed participants with minimal lung inflammation and Arm B/C (TLG ≥ 50 SUV) (n=27) showed participants with persisting lung inflammation. Study participants in Arm B/C (TLG ≥ 50 SUV) are randomized to atorvastatin or identical placebo and due to ongoing blinding this data is collectively analysed. Data is a representative of four Luminex assays and shown as mean. Data was analysed using Shapiro-Wilk test followed by Mann-Whitney t-test where significance is shown as *p≤0.05, **p≤0.01 and ****p≤0.0001.

At week 24 of the StatinTB clinical trial, study Arm B/C (TLG ≥ 50 SUV) remained with the significantly upregulated secretion of IL-4 (p=0.0078) when compared to study Arm A (TLG < 50 SUV) (Figure 3.28. and Table 3.8.).

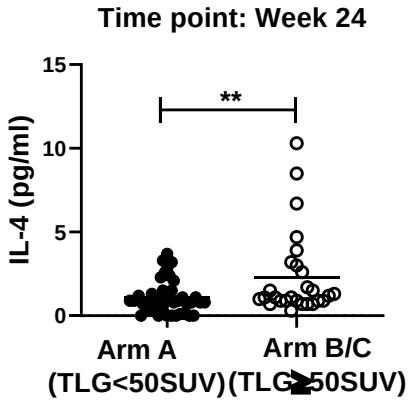

Figure 3.28. Evaluation of anti-inflammatory biomarker (IL-4) secretion using Luminex multiplex assay in serum samples at week 24 after successful completion of anti-TB treatment therapy. Study participants were stratified based on lung inflammation where Arm A (TLG < 50 SUV) (n=42) showed participants with minimal lung inflammation and Arm B/C (TLG ≥ 50 SUV) (n=27) showed participants with persisting lung inflammation. Study participants in Arm B/C (TLG ≥ 50 SUV) are randomized to atorvastatin or identical placebo and due to ongoing blinding this data is collectively analysed. Data is a representative of four Luminex assays and shown as mean. Data was analysed using Shapiro-Wilk test followed by Mann-Whitney t-test where significance is shown as **$p \leq 0.01$.

A total of seventeen soluble biomarkers were shown to be significantly expressed differently between study Arm A (TLG < 50 SUV) and study Arm B/C (TLG ≥ 50 SUV) at week 24 of the StatinTB clinical trial (Table 3.8.). These are classified into chemokines (n=2), growth factors (n=4), pleiotropic mediators (n=2), pro-inflammatory (n=8) and anti-inflammatory cytokines (n=1). Among these, sixteen were significantly upregulated in study Arm B/C (TLG ≥ 50 SUV) whereas one (IL-9) was significantly downregulated in these patients compared to study Arm A (TLG < 50 SUV).

Table 3.8. Summary table showing the secretion profile of soluble biomarkers (n=20) at week 24 time point after completion of anti-TB treatment. Study participants were stratified based on lung inflammation where Arm A (TLG < 50 SUV) and Arm B/C (TLG ≥ 50 SUV) show participants with minimal or persisting lung inflammation, respectively. Study participants in Arm B/C (TLG ≥ 50 SUV) are randomized to atorvastatin or identical placebo and due to ongoing blinding this data is collectively analysed. Data is a representative of four Luminex assays and shown as mean±SD. Data was analysed using Shapiro-Wilk test followed by Mann-Whitney t-test. TLG=Total Lung Glycolysis, SUV=Standardized Uptake Value, SD=Standard Deviation.

Classification	**Biomarkers**	**Arm A (TLG<50SUV) (mean±SD)**	**Arm B (TLG≥50SUV) (mean±SD)**	**p-value**
Pro-inflammatory	IL-1α	3.69±5.23	9.99±11.62	0.0029
	IL-1β	0.84±1.15	1.26±1.10	0.0049
	IL-2Rα	39.26±14.75	59.80±49.20	0.0206
	IL-12p40	18.87±33.60	59.64±6.64	<0.0001
	IL-17	3.72±4.62	7.08±5.77	0.0027
	IL-18	42.59±29.03	83.61±115.50	0.0120
	TNF-α	38.93±14.47	50.20±19.62	0.0105
	TRAIL	30.80±15.66	35.86±11.85	0.0213
Anti-Inflammatory	IL-4	1.06±0.98	2.29±2.52	0.0078
Growth factors	Basic FGF	12.38±8.82	23.36±20.38	0.0037
	HGF	224.70±97.68	318.00±158.20	0.0008
	M-CSF	9.22±5.09	18.88±24.70	0.0048
	SCGF-β	53805.00±38712.00	90642±47869.00	0.0018
Pleiotropic	IL-9	611.00±127.30	513.00±128.00	0.0094
	LIF	9.03±16.52	22.05±27.15	0.0016
Chemokines	Gro-α	914.60±182.20	1002.00±204.40	0.0180
	IP-10	185.20±156.70	345.70±425.00	0.0404

3.3.10. Evaluation of host serum biomarker changes at different time points of the StatinTB clinical trial

Changes in host serum biomarkers were evaluated at 3-time point visits (week 0, 12, and 24) in study participants with minimal lung inflammation (Arm A (TLG < 50 SUV)) after completion of anti-TB treatment. These participants are not given any intervention after completion of anti-TB treatment and they are considered as a control population for the StatinTB clinical trial which is an ongoing proof of concept, double-blind, randomized clinical trial. There were no significant changes observed between the time point visits on the secretion profile of 33 detected biomarkers measured using Luminex multiplex assay. These biomarkers included 10 chemokines (Gro-α, Eotaxin, CTACK, IP-10, MIP-1α, MIP-1β, MCP-1, SDF-1α, RANTES, and MIG) (Figure 3.29A); 7 Growth Factors (Basic FGF, G-CSF, HGF, M-CSF, PDGF-BB, SCF, and SCGF-β) (Figure 3.29B); 2 pleiotropic mediators (LIF and IL-9) (Figure 3.29C); 11 pro-inflammatory cytokines (IL-1α, IL-1β, IL-2Rα, IL-8, IL-12p40, IL-16, IL-17, IL-18, TNF-α, TNF-β, and TRAIL) (Figure 3.29D); and 3 anti-inflammatory cytokines (IL-1ra, IL-4, and MIF) (Figure 3.29E).

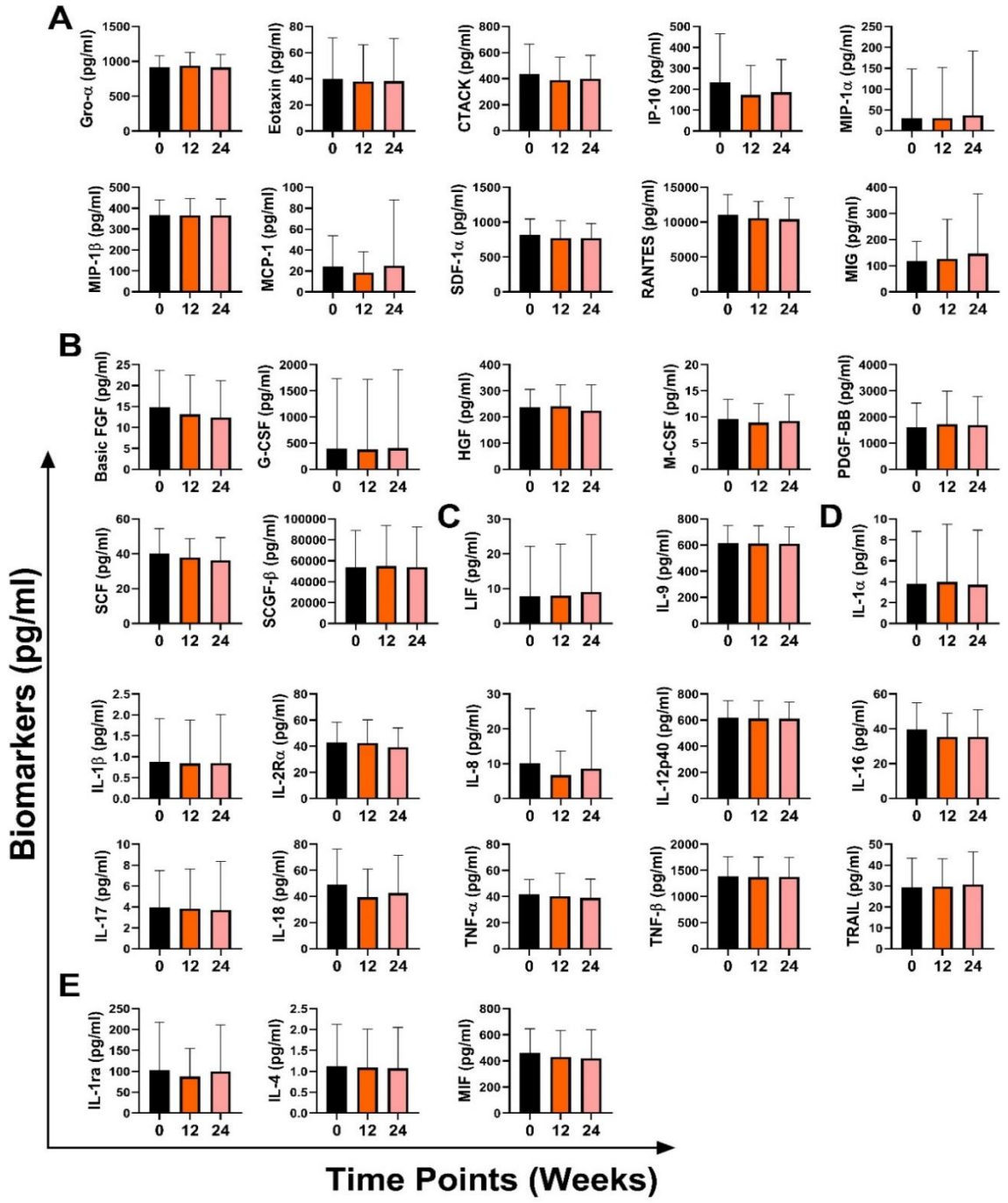

Figure 3.29. Host serum biomarkers measured using Luminex multiplex assay remain unchanged at different time points after completion of anti-TB treatment in participants with minimal lung inflammation (Arm A (TLG < 50 SUV)). Data is a representative of four Luminex assays and shown as mean±SD. **A.** chemokines; **B.** growth factors; **C.** pleiotropic mediators; **D.** pro-inflammatory cytokines; **E.** anti-inflammatory cytokines. Data was analysed using Kruskal-Wallis test followed by Dunn's multiple comparison test against each time point.

Similarly, host serum biomarkers were evaluated at 6-time point visits (week 0, 2, 4, 8, 12, and 24) for study participants who remained with persisting lung inflammation (Arm B/C (TLG ≥ 50 SUV) after completion of anti-TB treatment. Study participants with persisting lung inflammation represent an experimental group for the StatinTB clinical trial where they are randomly given atorvastatin (40mg/day) or a matching placebo. As observed with study Arm A, no significant changes were observed in study Arm B/C (TLG ≥ 50 SUV) between the time point visits on the secretion profile of 33 detected biomarkers measured using Luminex multiplex assay. These biomarkers included 10 chemokines (Gro-α, Eotaxin. CTACK, IP-10, MIP-1α, MIP-1β, MCP-1, SDF-1α, RANTES, and MIG) (Figure 3.30A); 7 Growth Factors (Basic FGF, G-CSF, HGF, M-CSF, PDGF-BB, SCF and SCGF-β) (Figure 3.30B); 2 pleiotropic mediators (LIF and IL-9) (Figure 3.30C); 11 pro-inflammatory cytokines (IL-1α, IL-1β, IL-2Rα, IL-8, IL-12p40, IL-16, IL-17, IL-18, TNF-α, TNF-β, and TRAIL) (Figure 3.30D); and 3 anti-inflammatory cytokines (IL-1ra, IL-4, and MIF) (Figure 3.30E). Evaluation of host serum biomarker changes between the atorvastatin and placebo group is not possible yet due to the blinded status of the clinical trial since the StatinTB clinical trial is still ongoing, and this data remains blinded. However, for the purpose of this thesis work and to prevent involuntary unblinding of the data; study Arm B/C has been analysed as a collective study arm.

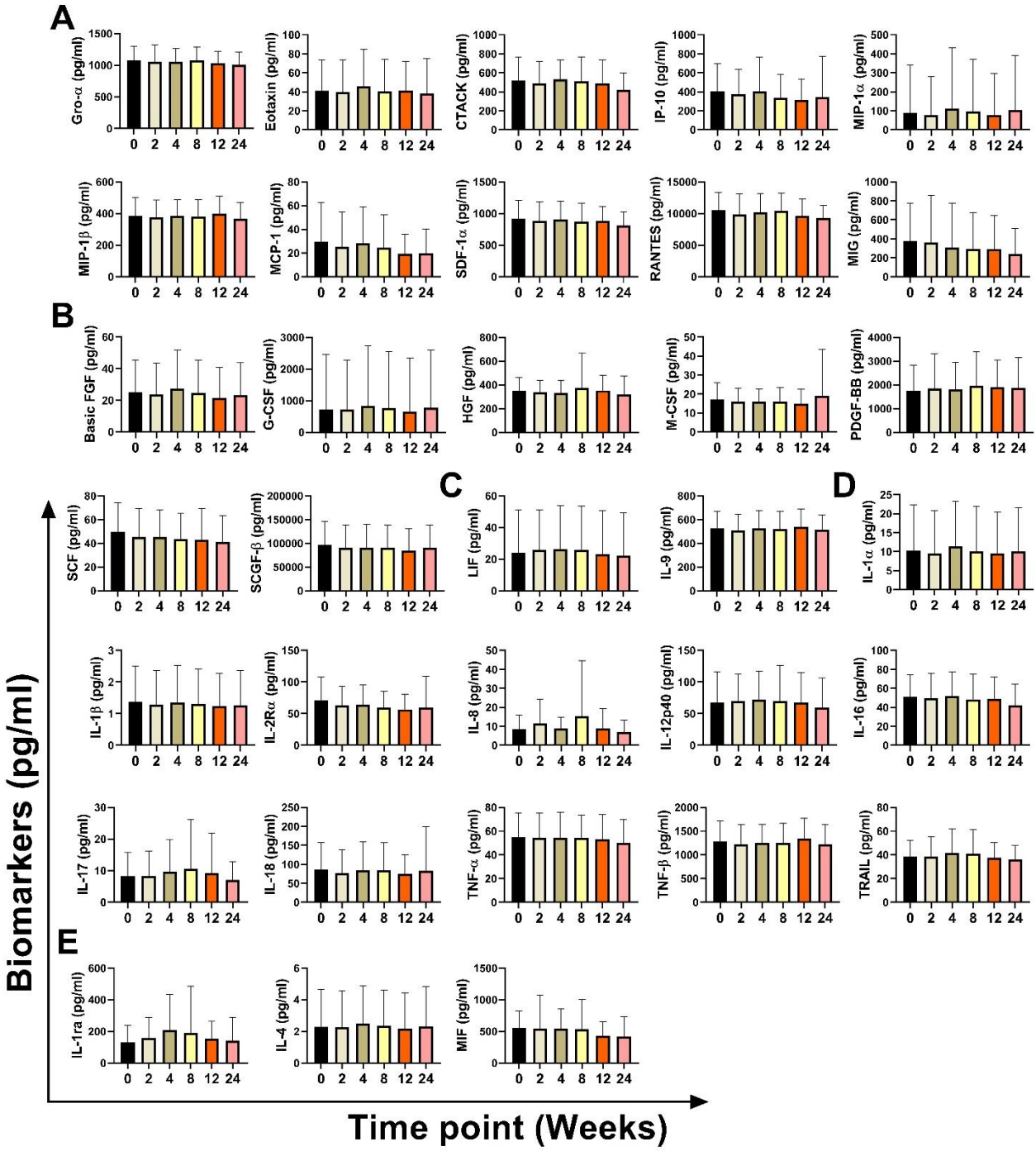

Figure 3.30. Measurement of host serum biomarkers using Luminex multiplex assay at different time point visits after completion of anti-TB treatment in patients presenting with persisting lung inflammation (Arm B/C (TLG ≥ 50 SUV)). Data is a representative of four Luminex assays and shown as mean±SD. **A.** chemokines; **B.** growth factors; **C.** pleiotropic mediators; **D.** pro-inflammatory cytokines; E. anti-inflammatory cytokines. Data was analysed using Kruskal-Wallis test followed by Dunn's multiple comparison test against each time point.

Serum biomarkers were evaluated at three-time point visits for study Arm A (TLG < 50 SUV) (week 0, 12, and 24) and six-time point visits for study Arm B/C (TLG ≥ 50 SUV) (week 0, 2, 4, 8, 12, and 24). Using the Kruskal-Wallis test with Dunn's multiple comparison showed no significant changes in the secretion profile of detected serum biomarkers in both study Arm A (TLG < 50 SUV) (Figure 3.29) and study Arm B/C (TLG ≥ 50 SUV) (Figure 3.30 and Figure 3.31A-B) at different time points visits compared against each other. However, analysis through the Mann-Whitney t-test comparing baseline (week 0) with week 24 showed a significant decrease in three soluble biomarkers in study Arm B/C (TLG ≥ 50 SUV). These include two chemokines (MIG (p=0.0103) and IP-10 (p=0.0453)) (Figure 3.31C and Table 3.9.) and one anti-inflammatory cytokine (MIF (p=0.0061)) (Figure 3.31D and Table 3.9.).

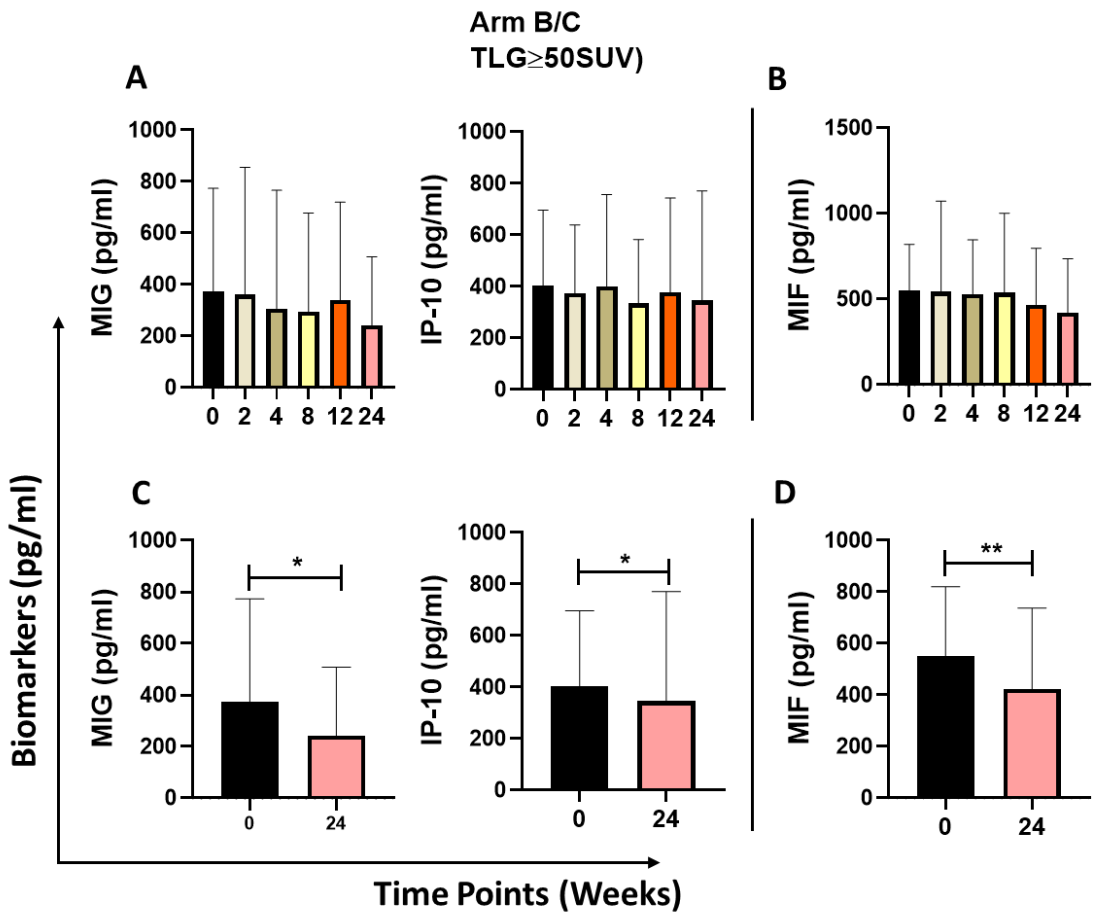

Figure 3.31. Representative plots showing secretion profile of host serum biomarkers evaluated using Luminex multiplex assay at different time point visits after completion of anti-TB treatment in participants presenting with persisting lung inflammation (Arm B/C (TLG ≥ 50 SUV)). Data is a representative of four Luminex assays and shown as mean±SD. **A.** MIG and IP-10 chemokines evaluation at week 0, 2, 4, 8, 12, and 24; **B.** Evaluation of MIF growth factor at week 0, 2, 4, 8, 12, and 24; **C.** Evaluation of chemokines (MIG and IP-10) at week 0 and 24; and D. Evaluation of growth factor (MIF) at week 0 and 24. Data was analysed using Kruskal-Wallis test followed by Dunn's multiple comparison test against each time point (A-B) and Shapiro-Wilk test followed by Mann-Whitney t-test (C-D) where, *p≤0.05, **p≤0.01.

Table 3.9. Changes in host serum biomarker secretion levels in study participants with persisting lung inflammation (Arm BC (TLG ≥ 50 SUV)) after completion of anti-TB treatment between week 0 (n=29) and week 24 (n=27). Data is a representative of four Luminex experiments and shown as mean±SD. Statistical analysis was performed using Shapiro-Wilk test followed by Mann-Whitney t-test. TLG= Total Lesion Glycolysis, SUV= Standardized Uptake Value, SD=Standard Deviation.

Biomarkers	**Arm B/C (TLG≥50 SUV) (mean±SD)**		**p-value**
	Week 0	**Week 24**	
MIG	373.30±400.60	241.80±266.60	0.0103
IP-10	402.20±294.40	345.70±425.00	0.0453
MIF	550.10±270.00	422.30±314.40	0.0061

3.3.11. Treated TB patients (StatinTB cohort) display different secretion profiles of soluble biomarkers compared to healthy individuals stratified based on QFT response

There were no significant differences observed on the expression of most soluble biomarkers between QFT- and QFT+ individuals. However, IP-10 showed significant upregulation ($p=0.0265$) in QFT+ individuals compared to QFT- individuals (Figure 3.32A). Evaluation of secretion profile between healthy individuals (QFT- and QFT+) and successfully treated TB patients showed that treated TB patients remain with elevated levels of soluble inflammatory mediators. This study identified a total of five soluble biomarkers that were elevated in study Arm A (TLG < 50 SUV) at the end of anti-TB treatment (week 0) compared to QFT- participants (Figure 3.32.). These include Basic FGF ($p<0.0001$), G-CSF ($p=0.0002$), IL-4 ($p<0.0001$), IL-1α ($p<0.0001$), and IL-12p40 ($p<0.0001$). Furthermore, four biomarkers including Basic FGF ($p<0.0001$), IL-4 ($p<0.0001$), IL-1α ($p<0.0001$), and IL-12p40 ($p=0.0002$) were elevated in study Arm A (TLG<50 SUV) at the end of anti-TB treatment (week 0) compared to QFT+. However, MIP-1α showed a significant reduction ($p=0.0061$) in study Arm A (TLG < 50 SUV) compared to QFT+ individuals (Figure 3.32A-D and Table 3.10.).

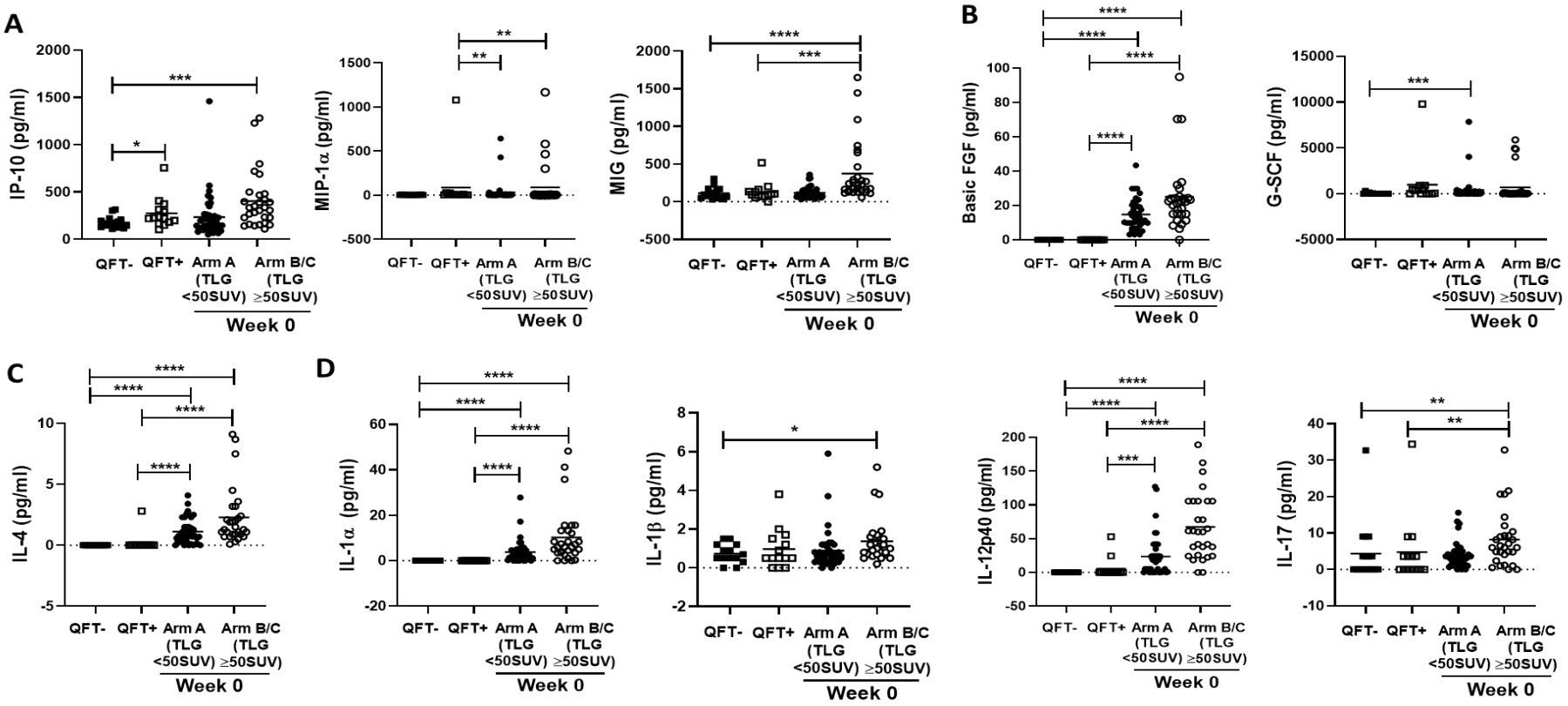

Figure 3.32. Representative plots showing the secretion profile of serum biomarkers measured using Luminex multiplex assay between healthy individuals and successfully treated TB patients at week 0 time point following anti-TB treatment. Healthy individuals were stratified into QFT- (n=14) or QFT+ (n=14) using QFT assay. Study participants who have completed anti-TB treatment were stratified based on lung inflammation where Arm A (TLG < 50 SUV) (n=42) shows participants with minimal lung inflammation and Arm B/C (TLG ≥ 50 SUV) (n=29) shows participants with persisting lung inflammation. Data is a representation of four Luminex assays and shown as mean. **A.** chemokines (IP-10, MIP-1α and MIG), **B.** growth factors (Basic FGF and G-CSF), **C.** anti-inflammatory cytokine (IL-4), and **D.** pro-inflammatory cytokines (IL-1α, IL-1β, IL-12p40, and IL-17). Data was analysed using Kruskal-Wallis followed by Dunn's multiple comparison; *p≤0.05, **p≤0.01, ***p≤0.001, **** p≤0.0001. QFT= QuantiFERON, TLG= Total Lung Glycolysis, SUV= Standardized Uptake Value

Table 3.10. Evaluation of host serum biomarkers between study participants with minimal lung inflammation (Arm A (TLG < 50 SUV)) (n=42) after anti-TB treatment completion and healthy individuals stratified into QFT- (n=14) and QFT+ (n=14) based on QFT assay. Data is a representative of five Luminex assays and shown as mean±SD. Data was analysed using Shapiro-Wilk test followed by Mann-Whitney t-test. QFT= QuantiFERON, TLG= Total Lung Glycolysis, SUV= Standardized Uptake Value, SD= Standard Deviation, ns= not significant.

Biomarkers	**QFT-, n=14 (mean±SD)**	**Arm A (TLG<50 SUV), n=42 (mean±SD)**	**p-value**	**QFT+, n=14 (mean±SD)**	**Arm A (TLG<50 SUV), n=42 (mean±SD)**	**p-value**
MIP-1α	3.7±1.2	31.1±117.0	**ns**	85.5±286.0	31.1±117.0	0.0061
Basic FGF	0.0±0.0	14.7±8.8	<0.0001	0.0±0.0	14.7±8.8	<0.0001
G-CSF	37.5±85.44	400.1±1334.0	0.0002	993.2±2552.0	400.1±1334.0	**ns**
IL-4	0.0±0.0	1.1±1.0	<0.0001	0.2±0.7	1.1±1.0	<0.0001
IL-1α	0.0±0.0	3.7±5.0	<0.0001	0.0±0.0	3.7±5.0	<0.0001
IL-12p40	0.0±0.0	23.7±29.9	<0.0001	5.5±15.1	23.7±29.9	0.0002

Results further showed evidence of eight elevated soluble biomarkers in study Arm B/C (TLG ≥ 50SUV) at the end of anti-TB treatment (week 0) compared to QFT- individuals (Figure 3.32A-D). These include IP-10 (p=0.0005), MIG (p=0.0002), Basic FGF (p<0.0001), IL-4 (p<0.0001), IL-1α (p<0.0001), IL-1β (p=0.0235), IL-12p40 (p<0.0001), and IL-17 (p=0.0035) (Table 3.11). Additionally, seven soluble biomarkers were significantly elevated in study Arm B/C (TLG ≥ 50SUV) at the end of anti-TB treatment (week 0) compared to QFT+ individuals (Figure 3.32A-D). These include MIP-1α (p=0.0051), MIG (p=0.0002), Basic FGF (p<0.0001), IL-4 (p<0.0001), IL-1α (p<0.0001), IL-12p40 (p<0.0001), and IL-17 (p=0.0082) (Table 3.11).

Table 3.11. Evaluation of host serum biomarkers between participants with persisting lung inflammation (Arm B/C (TLG < 50 SUV)) (n=29) after completion of anti-TB treatment and healthy individuals stratified into QFT- (n=14) and QFT+ (n=14) based on QFT assay. Data is a representative of five Luminex assays and shown as mean±SD. Data was analysed using Shapiro-Wilk test followed by Mann-Whitney t-test. QFT= QuantiFERON, TLG= Total Lung Glycolysis, SUV= Standardized Uptake Value, SD= Standard Deviation, ns= not significant.

Biomarkers	QFT-, n=14 (mean±SD)	Arm B/C (TLG≥50 SUV), n=29 (mean±SD)	p-value	QFT+, n=14 (mean±SD)	Arm B/C (TLG≥50 SUV), n=29 (mean±SD)	p-value
IP-10	179.9±64.61	402.2±294.4	0.0005	273.8±162.5	402.2±294.4	**ns**
MIP-1α	3.7±1.2	89.42±251.9	**ns**	85.5±286.0	89.42±251.9	0.0051
MIG	119.9±78.45	373.3±400.6	0.0002	130.3±74.52	373.3±400.6	0.0002
Basic FGF	0.0±0.0	25.1±20.3	<0.0001	0.0±0.0	25.1±20.3	<0.0001
G-SCF	37.53±85.44	715.5±1737.0	**ns**	993.2±2552.0	715.5±1737.0	**ns**
IL-4	0.0±0.0	2.2±2.3	<0.0001	0.2±0.7	2.2±2.3	<0.0001
IL-1α	0.0±0.0	10.2±11.9	<0.0001	0.0±0.0	10.2±11.9	<0.0001
IL-1β	0.7±0.4	1.3±1.1	0.0235	0.9±1.0	1.3±1.1	**ns**
IL-12p40	0.0±0.0	67.3±49.0	<0.0001	5.5±15.1	67.3±49.0	<0.0001
IL-17	2.9±3.6	8.2±7.6	0.0035	4.7±9.1	8.2±7.6	0.0082

3.4. Cell phenotype analysis in successfully treated TB patients presenting with or without lung inflammation using flow cytometer

Flow cytometric analysis was performed to evaluate cell phenotype differences from study participants who were stratified into two study arms based on lung inflammation after completion of anti-TB treatment. In this analysis, six participants from both study Arm A (TLG < 50 SUV) and Arm B/C (TLG ≥ 50 SUV) were evaluated at three different time points classified as week 0, week 12, and week 24. Study Arm A (TLG < 50 SUV) includes participant with minimal lung inflammation. Study Arm B/C (TLG ≥ 50 SUV) includes participants with persisting lung inflammation, and these are given to atorvastatin (40mg/day) or matching placebo during the StatinTB clinical trial. However, due to continued clinical trial blinding and prevention of involuntary unblinding of the data, this study collectively analysed study Arm B/C (TLG ≥ 50 SUV) participants. Cell phenotypes were analysed from thawed PBMC samples where trypan blue exclusion method showed good cell viability of above 90%. Furthermore, cell recovery percentage ranged from 50-90% of previously stored cell numbers.

3.5. Evaluation of lymphocyte-derived cell populations at different blood collection time points after successful anti-TB treatment therapy

3.5.1. Treated TB patients with persisting lung inflammation have reduced frequency of T-cell population

Total T-cell population was gated from the lymphocyte population and evaluated based on CD3 expression where CD19 was used to exclude the B-cell population (Figure 3.33A.). T-cell population showed no significant difference between study Arm A (TLG < 50 SUV) and study Arm B/C (TLG ≥ 50 SUV) at time point 0 (Week 0) following successful anti-TB treatment. Significant reduction in T-cell population was observed in study Arm B/C (TLG ≥ 50 SUV) at week 12 of the StatinTB clinical trial compared to study Arm A (TLG < 50 SUV). However, at week 24 no significant difference was observed between the study arms (Figure 3.33B.). Using Kruskal-Wallis with Dunn's multiple comparison test, no significant different changes were observed within each study arm between the different time points of blood collection (Figure 3.33C.).

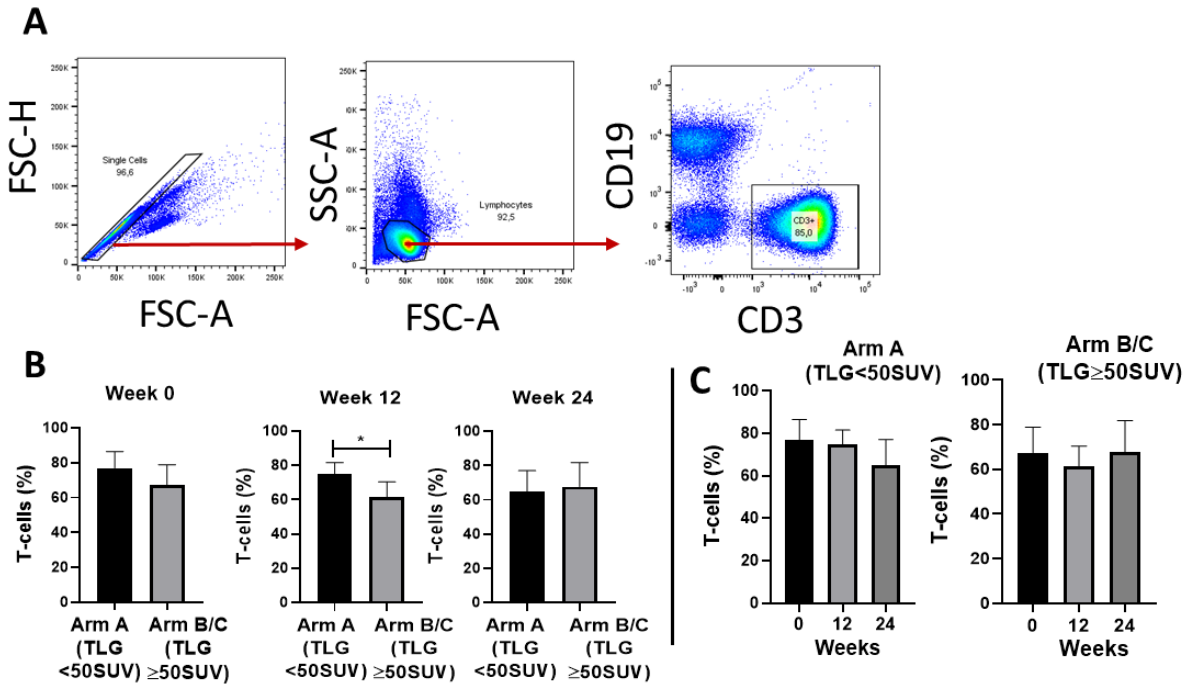

Figure 3.33. Comparison of CD3+ T-cell population frequencies analysed using flow cytometry between study Arm A (TLG < 50 SUV) (n=6) and study Arm B/C (TLG ≥ 50 SUV) (n=6) at different time points (week 0, 12, and 24) after completion of anti-TB treatment. **A.** Representative flow cytometry analysis of CD3+ T-cell population in PBMC where CD19 was used to exclude B-cells; **B.** frequency percentage analysis of CD3+ T-cells at week 0, week 12, and week 24 between study arms; **C.** Evaluation of frequency change in CD3+ T-cell population at different time points within study arms. Data is a representative of three independent experiments and shown as mean±SD. Data was analysed by Shapiro-Wilk test followed by Mann-Whitney t-test **(B)** or Kruskal-Wallis test followed by Dunn's multiple comparison test against week 0 time point **(C)**. Statistical significance is summarized as *p≤0.05. TLG= Total Lung Glycolysis, SUV= Standardized Uptake Value, FSC-H= Forward Scatter-Hight, FSC-A= Forward Scatter-Area, SSC-A= Side Scatter-Area**.**

3.5.2. PD1 expression in cytotoxic T-cells (CD8+) remained elevated in successfully treated TB patients with persisting lung inflammation

PD1 (CD279) expression was evaluated in the cytotoxic T-cell population (CD8+) (Figure 3.34A.). Results showed significant upregulation of PD1 expression within cytotoxic T-cells (CD3+CD8+) at week 24 of the StatinTB clinical trial in study Arm B/C (TLG ≥ 50 SUV) compared to study Arm A (TLG < 50SUV). However, there was no significant difference observed at week 0 and week 12 between study arms (Figure 3.34B.). Evaluation of PD1 expressing cytotoxic T-cells showed no significant difference within study Arm B/C (TLG ≥ 50 SUV) at different time points. However, PD1 expression within study Arm A showed

significant reduction at week 24 compared to both week 0 and week 12 time points (Figure 3.34C.).

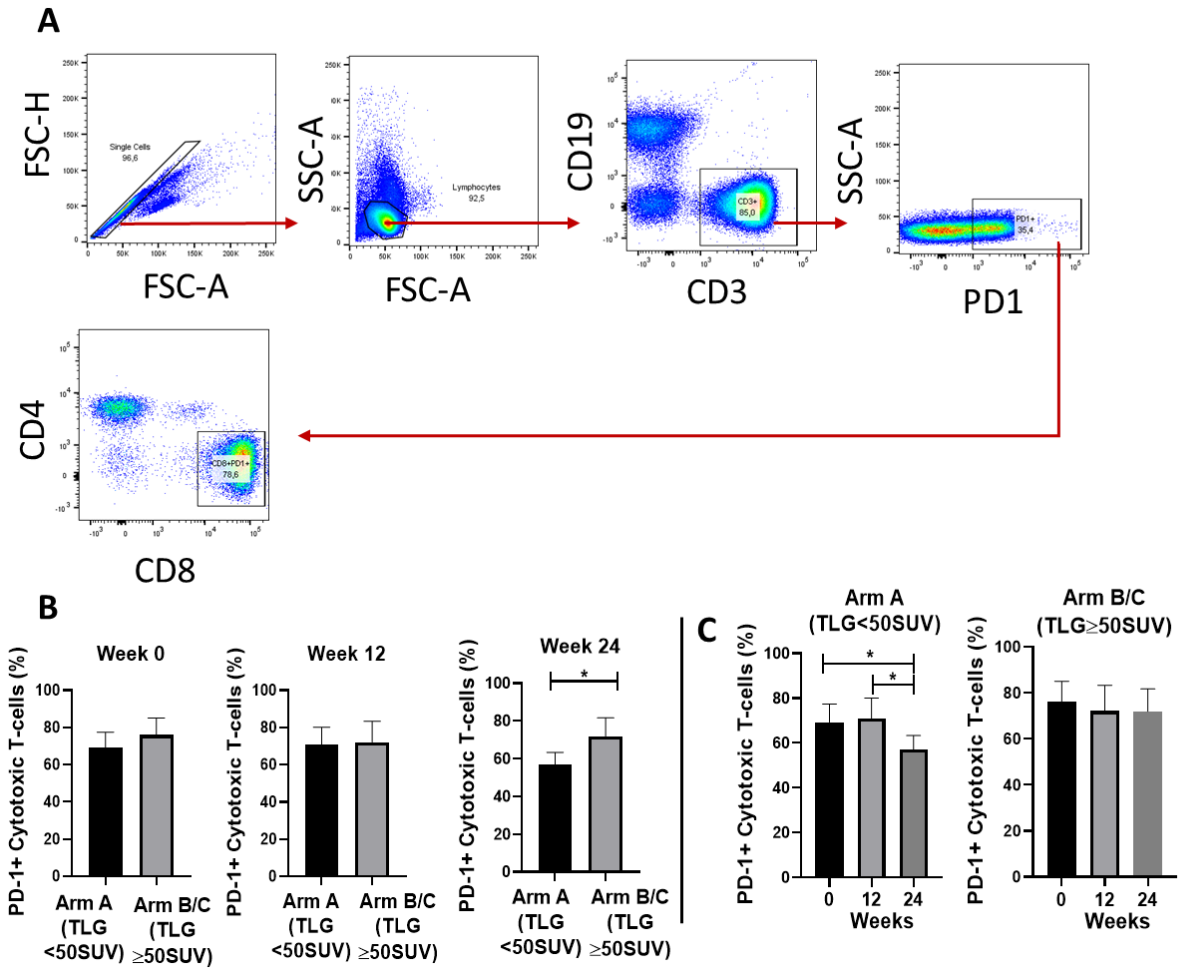

Figure 3.34. Evaluation of PD1 expression in cytotoxic T-cells (CD3+CD8+) between study Arm A (TLG < 50 SUV) (n=6) and study Arm B/C (TLG ≥ 50 SUV) (n=6) using flow cytometry. A. Representative flow cytometry plots showing gated PD-1+ cytotoxic T-cells from PBMC where CD19 and CD4 were used to exclude B-cells and helper T-cells, respectively; **B.** Comparison of frequency percentage between study Arm A (TLG < 50 SUV) and study Arm B/C (TLG ≥ 50 SUV) at week 0, 12, and 24; **C.** Evaluation of frequency percentage changes at different time points within each study arm. Data is a representative of three independent experiments and shown as mean±SD. Data was analysed by Shapiro-Wilk test followed by Mann-Whitney t-test **(B)** or Kruskal-Wallis test followed by Dunn's multiple comparison test against week 0 time point **(C)**. Statistical significance is summarized as *p≤0.05. TLG= Total Lung Glycolysis, SUV= Standard Uptake Value, FSC-H= Forward Scatter-Hight, FSC-A= Forward Scatter-Area, SSC-A= Side Scatter-Area.

3.5.3. Evaluation of B-cell memory phenotype in successfully treated TB patients stratified based on lung inflammation

3.5.3.1. Successfully treated TB patients with persisting lung inflammation have increased frequency of naïve B-cells

Memory B-cells were evaluated from CD19+ cell population based on CD21 and CD27 expression where CD21+CD27- were characterised as naïve B-cells (Figure 3.35A.) in accordance with Oliviero et al. (2020) [98]. This study showed that there are no significant differences in the frequency percentage of CD19+CD21+CD27- naïve B-cells between successfully treated TB patients presenting with different lung inflammation (Arm A (TLG<50 SUV and Arm B/C (TLG≥50 SUV)) at week 0 and week 12 time points. However, significant upregulation of CD19+CD21+CD27- naïve B-cell population was observed in study Arm B/C at week 24 compared to study Arm A (TLG<50 SUV) (Figure 3.35B.). There were no significant changes observed within each study arm at different time points (Figure 3.35C.).

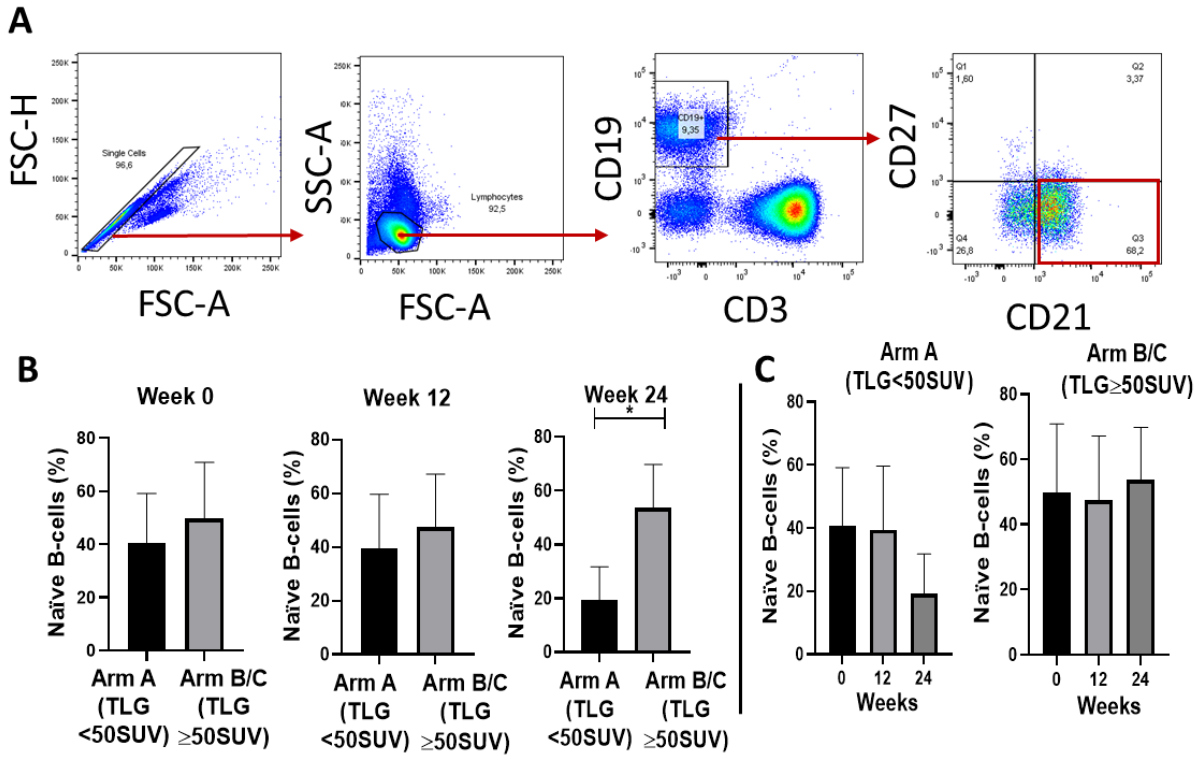

Figure 3.35. Frequency percentage (%) of naïve B-cell population evaluated using flow cytometry between study Arm A (TLG < 50 SUV) (n=6) and study Arm B/C (TLG ≥ 50 SUV) (n=6) at different time points (week 0, 12, and 24) after completion of anti-TB treatment. A. Representative flow cytometry analysis of CD19+CD21+CD27- naïve B-cells from PBMC where CD3 was used to exclude T-cells; **B.** Naïve B-cells frequency (%) comparison between study Arm A (TLG < 50 SUV) and study Arm B/C (TLG ≥ 50 SUV) at week 0, 12 and 24; **C.** Evaluation of frequency percentage changes within each study arm at different time points. Data is a representative of three independent experiments and shown as mean±SD. Data was analysed by Shapiro-Wilk test followed by Mann-Whitney t-test **(B)** or Kruskal-Wallis test followed by Dunn's multiple comparison test against week 0 time point **(C)**. Statistical significance is summarized as *p≤0.05. TLG= Total Lung Glycolysis, SUV= Standardized Uptake Value, FSC-H= Forward Scatter-Hight, FSC-A= Forward Scatter-Area, SSC-A= Side Scatter-Area.

3.5.3.2. Classical memory B-cell frequency is reduced in successfully treated TB patients with persisting lung inflammation

Further evaluation of memory phenotype within B-cells (Figure 3.36A.) showed significant downregulation of classical memory B-cell population (CD19+CD21+CD27+) in study Arm B/C (TLG ≥ 50 SUV) at week 0 compared to study Arm A (TLG < 50 SUV). However, there were no significant differences observed between study arms at week 12 and week 24 time points (Figure 3.36B.). Furthermore, there was significant upregulation of classical memory B-cells observed in study Arm B/C (TLG ≥ 50 SUV) at week 24 compared to week 12 time

point whereas no significant changes were observed within study Arm A (TLG < 50 SUV) at different time points (Figure 3.36C.).

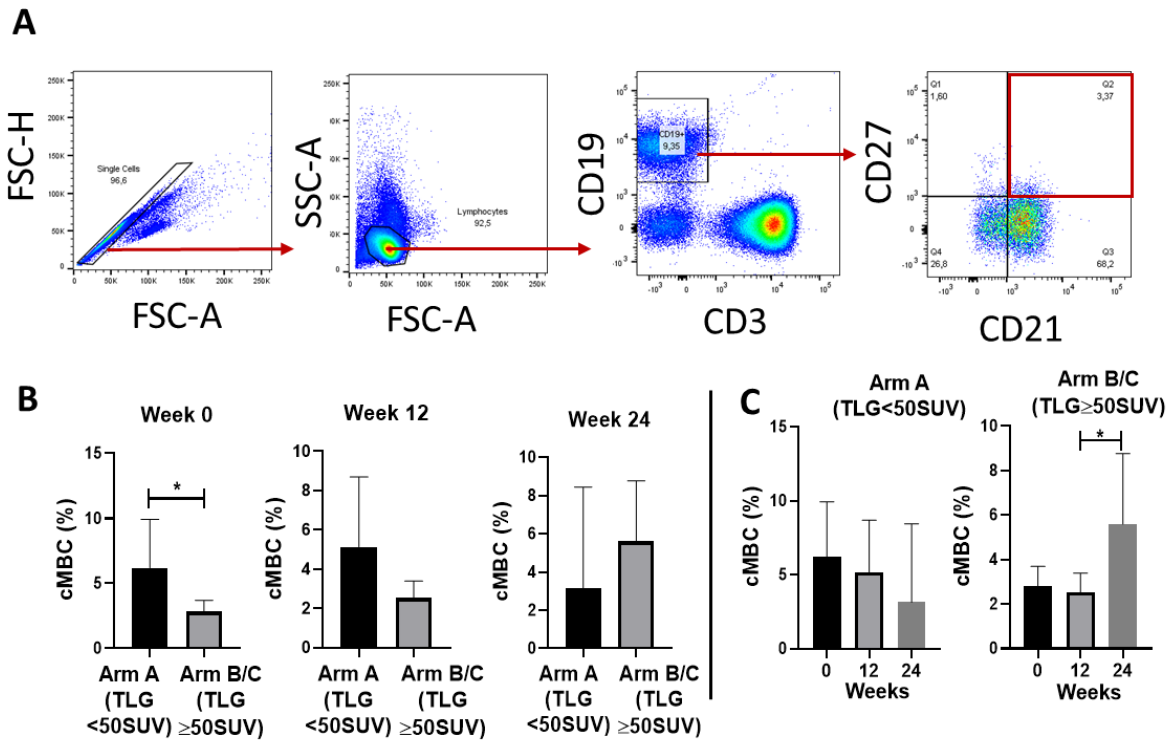

Figure 3.36. Evaluation of classical memory B-cells (cMBC) between study Arm A (TLG < 50 SUV) and study Arm B/C (TLG ≥ 50 SUV) at different time points (week 0, 12 and 24) after completion of anti-TB treatment using flow cytometry. A. Representative flow cytometry gating strategy for identifying CD19+CD21+CD27+ classical memory B-cells from PBMC where CD3 was used to exclude T-cells; **B.** Comparison of classical memory B-cells frequency (%) between study Arm A (TLG < 50 SUV) and study Arm B/C (TLG ≥ 50 SUV) at week 0, 12 and 24; **C.** Evaluation of frequency percentage changes within each study arm at different time points. Data is a representative of three independent experiments and shown as mean±SD. Data was analysed by Shapiro-Wilk test followed by Mann-Whitney t-test **(B)** or Kruskal-Wallis test followed by Dunn's multiple comparison test against week 0 time point **(C)**. Statistical significance is summarized as *p≤0.05. TLG= Total Lung Glycolysis, SUV= Standardized Uptake Value, FSC-H= Forward Scatter-Hight, FSC-A= Forward Scatter-Area, SSC-A= Side Scatter-Area.

3.5.3.3. Successfully treated TB patients have reduced frequency of activated memory B-cells

Activated memory B-cells were gated from the CD19+ cell population and defined based on CD21-CD27+ (Figure 3.37A.) [99]. No significant differences were observed between study Arm A (TLG < 50 SUV) and study Arm B/C (TLG ≥ 50 SUV) at week 0 and week 24 time points. However, a significant reduction of activated memory B-cells (CD19+CD21-CD27+)

was observed at week 12 in study Arm B/C (TLG ≥ 50 SUV) compared to study Arm A (TLG < 50 SUV) (Figure 3.37B.). Evaluation of activated memory B-cells within each study arm showed no significant changes at different time points (Figure 3.37C.).

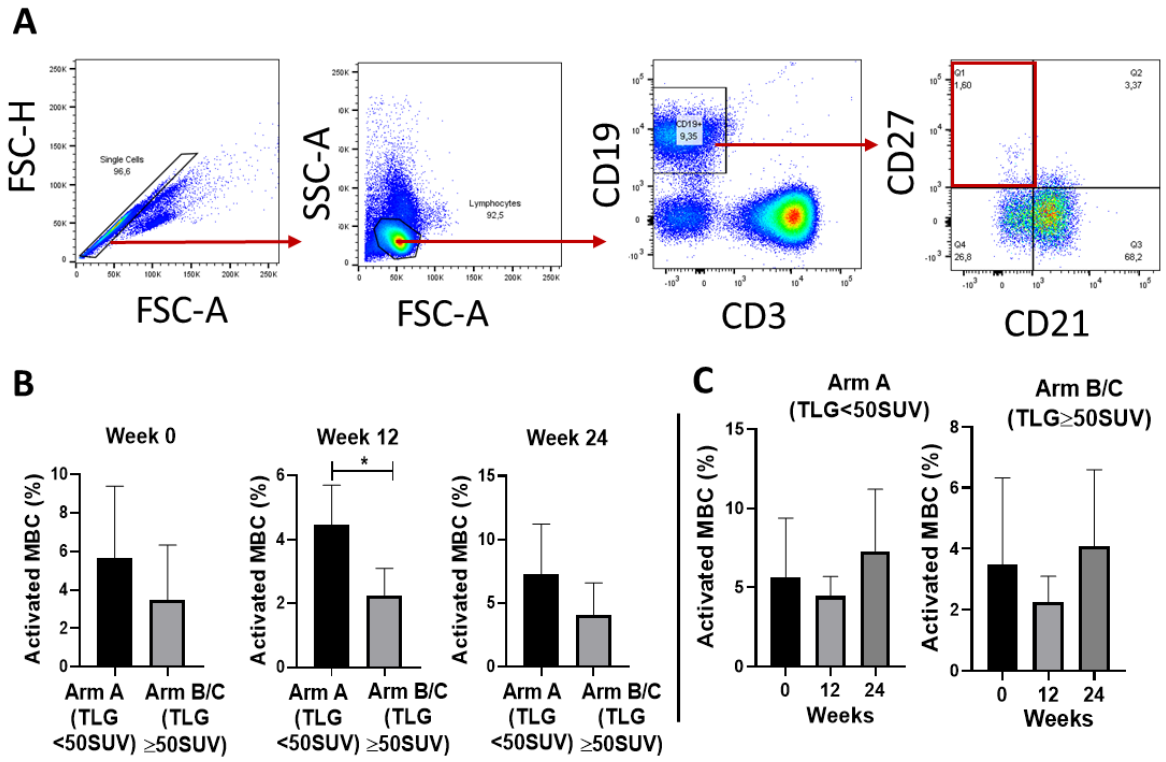

Figure 3.37. Evaluation of activated memory B-cells between study Arm A (TLG < 50 SUV) and study Arm B/C (TLG ≥ 50 SUV) at different time points (week 0, 12 and 24) after completion of anti-TB treatment using flow cytometry. A. Gating strategy for identification of CD19+CD27+CD21- activated memory B-cells from PBMC where CD3 was used to exclude T-cells; **B.** Comparison of activated memory B-cells frequency (%) between study Arm A (TLG < 50 SUV) and study Arm B/C (TLG ≥ 50 SUV) at week 0, 12 and 24; **C.** Evaluation of frequency percentage changes within each study arm at different time points. Data is a representative of three independent experiments and shown as mean±SD. Data was analysed by Shapiro-Wilk test followed by Mann-Whitney t-test **(B)** or Kruskal-Wallis test followed by Dunn's multiple comparison test against week 0 time point **(C)**. Statistical significance is summarized as *p≤0.05. TLG= Total Lung Glycolysis, SUV= Standardized Uptake Value, FSC-H= Forward Scatter-Hight, FSC-A= Forward Scatter-Area, SSC-A= Side Scatter-Area.

3.5.4. Frequency of CD1c+ dendritic cells remains elevated in treated TB patients with persisting lung inflammation

Dendritic cells (DC) were gated from the CD3- lymphocyte population where different subsets were defined based on CD1c and CD11c expression (Figure 3.38A.). This study showed significant upregulation of conventional DC (CD1c+) [100] in study Arm B/C (TLG

≥ 50 SUV) at week 24 compared to study Arm A (TLG < 50 SUV) (Figure 3.38B.). Furthermore, these DC subsets showed a significant reduction within study Arm A (TLG < 50 SUV) by week 24 compared to week 0 and week 12 time points (Figure 3.38C.).

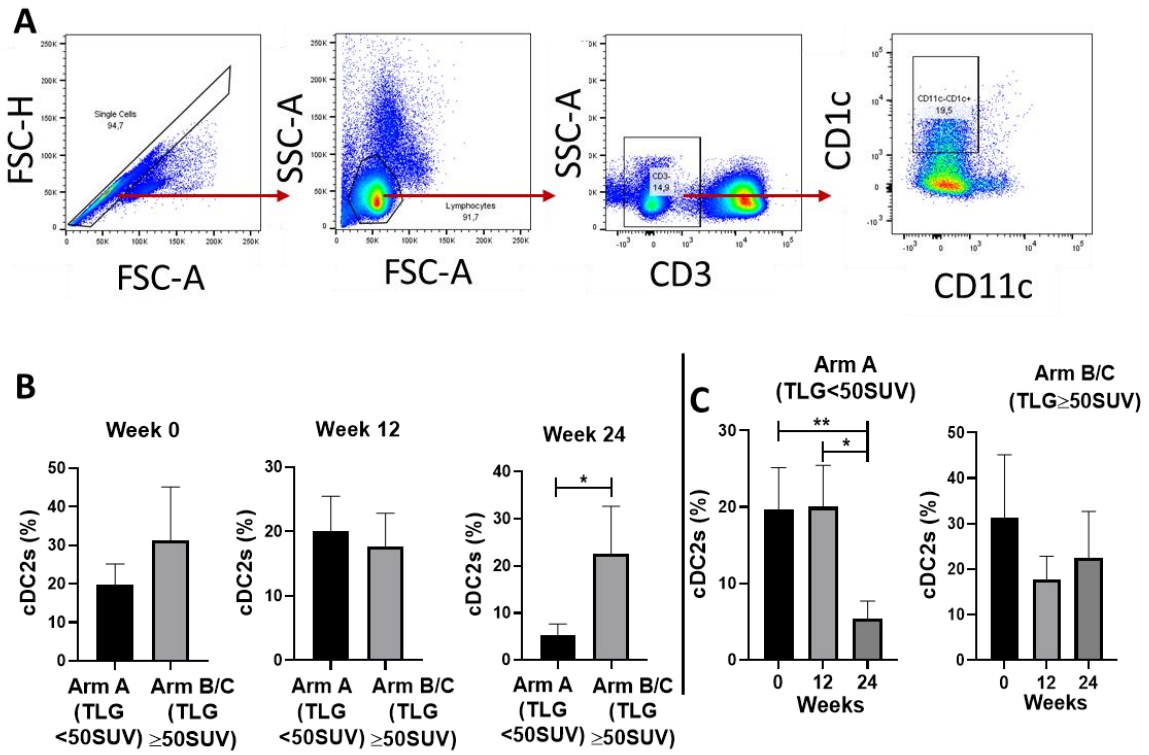

Figure 3.38. Representative plots showing the frequency (%) of conventional type 2 Dendritic Cells (cDC2s) between study Arm A (TLG < 50 SUV) (n=6) and study Arm B/C (TLG ≥ 50 SUV) (n=6) at different time points (week 0, 12 and 24) after completion of anti-TB treatment measured using flow cytometry. A. Representative flow cytometry gating of CD3-CD11c-CD1c+ conventional type 2 DC from PBMC; **B.** frequency percentage comparison between study Arm A (TLG < 50 SUV) and study Arm B/C (TLG ≥ 50 SUV) at week 0, 12 and 24; **C.** Evaluation of frequency percentage changes within each study arm at different time points. Data is a representative of three independent experiments and shown as mean±SD. Data was analysed by Shapiro-Wilk test followed by Mann-Whitney t-test **(B)** or Kruskal-Wallis test followed by Dunn's multiple comparison test against week 0 time point **(C)**. Statistical significance is summarized as *p≤0.05, ** p≤0.01. TLG= Total Lung Glycolysis, SUV= Standardized Uptake Value, FSC-H= Forward Scatter-Hight, FSC-A= Forward Scatter-Area, SSC-A= Side Scatter-Area.

3.5.5. Activated dysfunctional NK cells (CD16+CD56-) frequency remains elevated in successfully treated TB patients with persisting lung inflammation

NK cells were gated from the CD3- lymphocyte population and classified into two subsets based on CD16 and CD56 expression where activation was defined based on NKp46 expression (Figure 3.39A.). CD56-CD16+ NK cells are classified as dysfunctional NK cell

subset [101, 102], even though there were no significant differences observed between study Arm A and study Arm B/C at week 0 and week 12 time points. This study showed significant upregulation of activated dysfunctional DC (CD3-CD16+CD56-NKp46+) in study Arm B/C at week 24 compared to study Arm A (Figure 3.39B.). Additionally, a significant reduction in these activated DC subsets was observed at week 24 of study Arm A compared to both week 0 and week 12 time points; whereas no significant changes were observed within study Arm B/C (Figure 3.39C.).

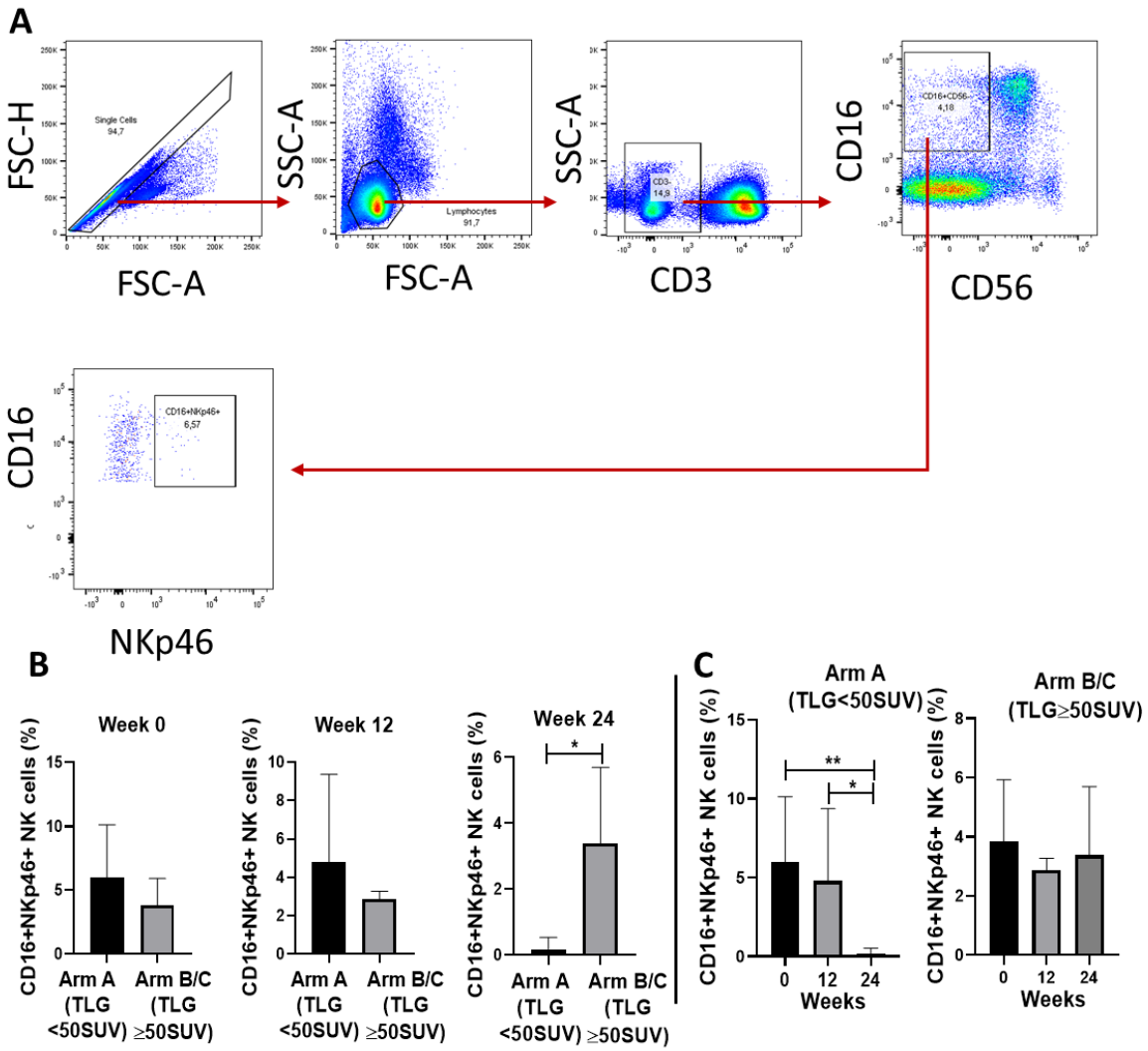

Figure 3.39. Frequency (%) of activated dysfunctional Natural Killer (NK) cell subset evaluated between study Arm A (TLG < 50 SUV) (n=6) and study Arm B/C (TLG ≥ 50 SUV) (n=6) at different time points (week 0, 12 and 24) after completion of anti-TB treatment measured using flow cytometry. A. Representative gating strategy for identification of CD3-CD56-CD16+NKp46+ activated dysfunctional NK cells from PBMC; **B.** frequency percentage comparison of activated dysfunctional NK cells between study Arm A (TLG < 50 SUV) and study Arm B/C (TLG ≥ 50 SUV) at week 0, 12, and 24; **C.** Evaluation of frequency percentage changes within each study arm at different time points. Data is a representative of three independent experiments and shown as mean±SD. Data was analysed by Shapiro-Wilk test followed by Mann-Whitney t-test **(B)** or Kruskal-Wallis test followed by Dunn's multiple comparison test against week 0 time point **(C)**. Statistical significance is summarized as *p≤0.05, ** p≤0.01. TLG= Total Lung Glycolysis, SUV= Standardized Uptake Value, FSC-H= Forward Scatter-Hight, FSC-A= Forward Scatter-Area, SSC-A= Side Scatter-Area.

3.5.6. Activated CD56+CD16- NK cell population significantly decreases after successful anti-TB treatment regardless of lung inflammation

Additionally, this study evaluated CD56+CD16- NK cell subsets where activation was identified based on NKp46 expression (Figure 3.40A.). There were no significant differences observed between study Arm A (TLG < 50 SUV) and study Arm B/C (TLG ≥ 50 SUV) at week 0, week 12, and week 24 time points (Figure 3.40B.). However, there was a significant reduction of CD56+CD16-NKp46+ within both study Arm A (TLG < 50 SUV) and study Arm B/C (TLG ≥ 50 SUV) at week 24 compared to week 0. (Figure 3.40C.).

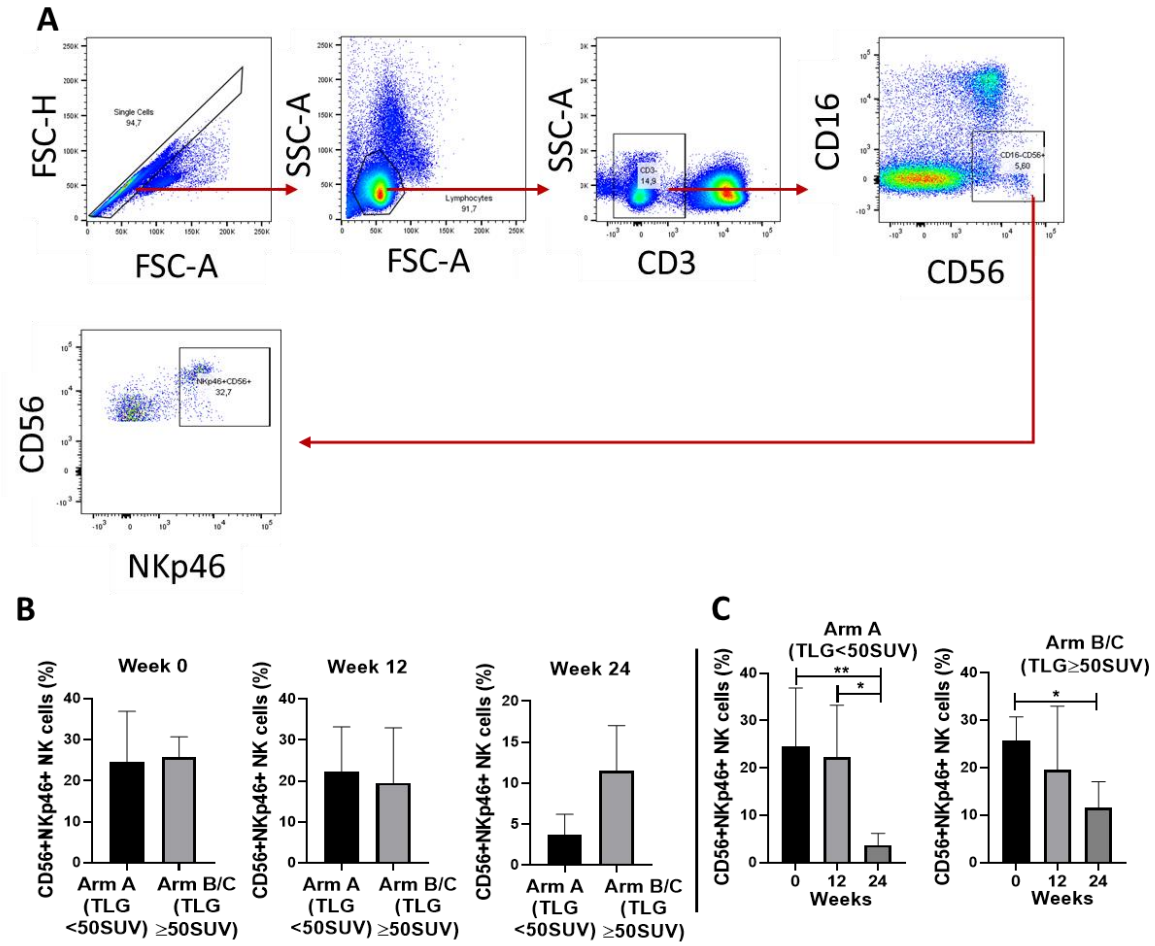

Figure 3.40. Evaluation of CD56+NKp46+ Natural Killer (NK) cell subset between study Arm A (TLG < 50 SUV) (n=6) and study Arm B/C (TLG ≥ 50 SUV) (n=6) at different time points (week 0, 12, and 24) after completion of anti-TB treatment measured using flow cytometry. A. Representative flow cytometry analysis of CD56+NKp46+ NK cells from PBMC; **B.** Comparison of CD56+NKp46+ NK cells frequency (%) between study Arm A (TLG < 50 SUV) and study Arm B/C (TLG ≥ 50 SUV) at week 0, 12, and 24; **C.** Evaluation of frequency percentage changes within each study arm at different time points. Data is a representative of three independent experiments and shown as mean±SD. Data was analysed by Shapiro-Wilk test followed by Mann-Whitney t-test **(B)** or Kruskal-Wallis test followed by Dunn's multiple comparison test against week 0 time point **(C)**. Statistical significance is summarized as *p≤0.05, ** p≤0.01. TLG= Total Lung Glycolysis, SUV= Standardized Uptake Value, FSC-H= Forward Scatter-Hight, FSC-A= Forward Scatter-Area, SSC-A= Side Scatter-Area.

3.6. Evaluation of monocyte cell subsets after completion of anti-TB treatment in patients stratified based on lung inflammation

3.6.1. Monocyte cell population shows reduced frequency at week 0 post-anti-TB treatment in patients with persisting lung inflammation

Monocyte cell populations were defined based on CD14 expression (Figure 3.41A.) [103]. This study showed a significantly reduced frequency of CD14+ monocyte cells after completion of anti-TB treatment in patients with persisting lung inflammation (study Arm B/C (TLG $\geq$ 50 SUV)) at week 0 time point. However, no significant differences were observed at week 12 and week 24 time points between the study arms (Figure 3.41B.). Furthermore, no significant changes were observed in the expression of CD14 within each study arm at different time points (Figure 3.41C.).

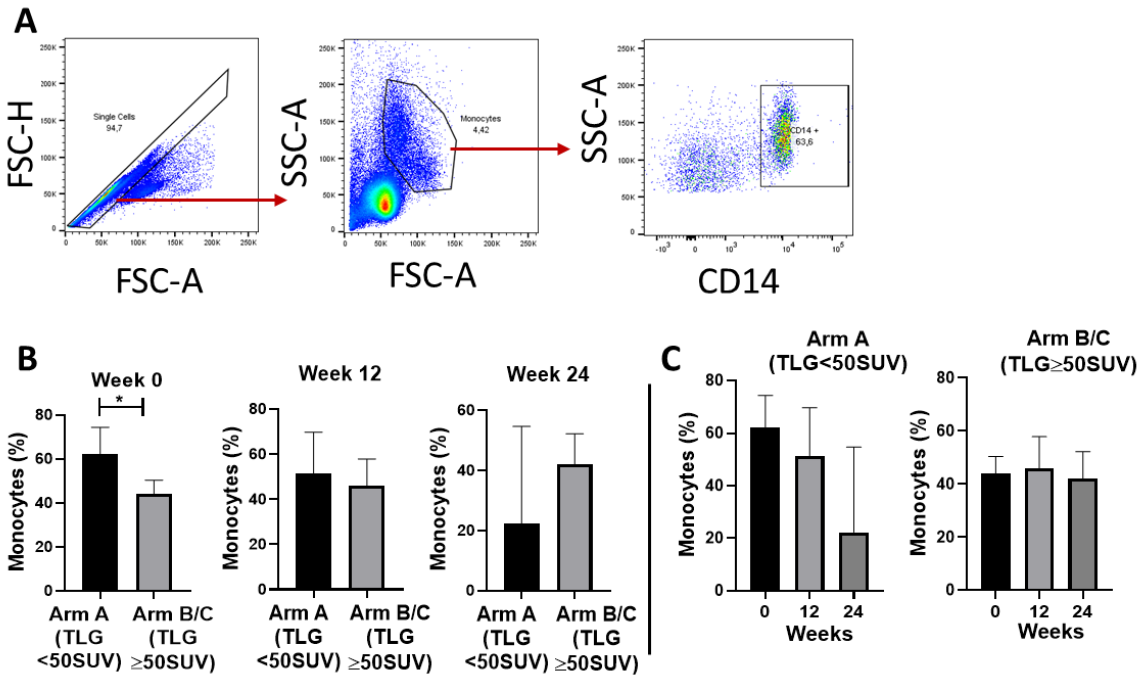

Figure 3.41. Measurement of frequency (%) of monocyte cells using flow cytometry between study Arm A (TLG < 50 SUV) (n=6) and study Arm B/C (TLG ≥ 50 SUV) (n=6) after completion of anti-TB treatment. A. Flow cytometry gating strategy for identifying CD14+ monocyte cells population from PBMC; **B.** Comparison of CD14+ monocyte cell frequency (%) between study Arm A (TLG < 50 SUV) and study Arm B/C (TLG ≥ 50 SUV) at week 0, 12 and 24; **C.** Evaluation of frequency percentage changes within each study arm at different time points. Data is a representative of three independent experiments and shown as mean±SD. Data was analysed by Shapiro-Wilk test followed by Mann-Whitney t-test **(B)** or Kruskal-Wallis test followed by Dunn's multiple comparison test against week 0 time point **(C)**. Statistical significance is summarized as *p≤0.05. TLG= Total Lung Glycolysis, SUV= Standardized Uptake Value, FSC-H= Forward Scatter-Hight, FSC-A= Forward Scatter-Area, SSC-A= Side Scatter-Area.

3.6.2. Classical monocyte cell population shows reduced frequency in participants with persisting lung inflammation at week 0 post-anti-TB treatment

Furthermore, the monocyte cell subset was characterised into classical monocyte and defined by CD14+CD16- (Figure 3.42A.). Successfully treated TB patients with persisting lung inflammation (study Arm B/C (TLG ≥ 50 SUV)) showed significantly reduced frequency of classical monocyte at week 0 compared to treated TB patients with no persisting lung inflammation (Arm A (TLG < 50 SUV)) (Figure 3.42B.). Additionally, there were no significant differences observed within each study arm at different time points (Figure 3.42C.).

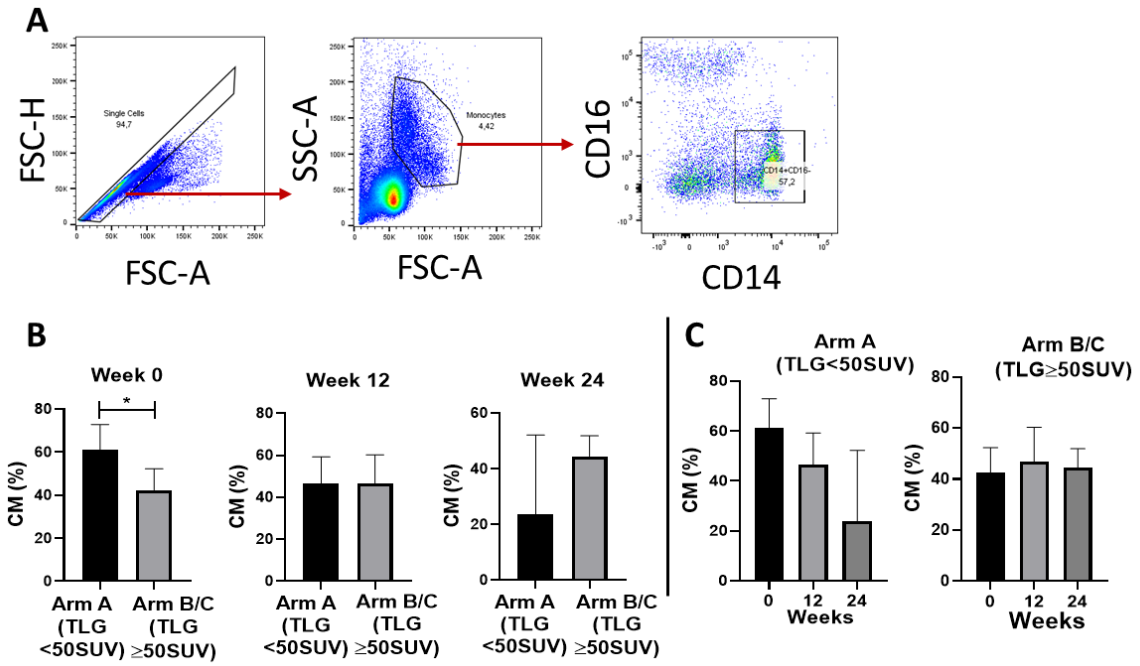

Figure 3.42. Evaluation of classical monocytes (CM) measured using flow cytometry between study Arm A (TLG < 50 SUV) (n=6) and study Arm B/C (TLG≥50 SUV) (n=6) at week 0, 12 and 24 after completion of anti-TB treatment. A. Representative flow cytometry analysis of CD14+CD16- classical monocytes; **B.** Comparison of classical monocyte cell frequency (%) between study Arm A (TLG < 50 SUV) and study Arm B/C (TLG ≥ 50 SUV) at week 0, 12 and 24; **C.** Evaluation of frequency percentage changes within each study arm at different time points. Data is a representative of three independent experiments and shown as mean±SD. Data was analysed by Shapiro-Wilk test followed by Mann-Whitney t-test **(B)** or Kruskal-Wallis test followed by Dunn's multiple comparison test against week 0 time point **(C)**. Statistical significance is summarized as *p≤0.05. TLG= Total Lung Glycolysis, SUV= Standardized Uptake Value, FSC-H= Forward Scatter-Hight, FSC-A= Forward Scatter-Area, SSC-A= Side Scatter-Area.

3.6.3. Expression of co-stimulatory molecule (CD86) in classical monocyte remains elevated at week 24 after post-anti-TB treatment in patients with persisting lung inflammation

Expression of co-stimulatory molecules CD80 and CD86 was evaluated from gated classical monocytes (C14+CD16-) (Figure 3.43A.). Results showed no significant differences in CD14+CD16-CD86+ classical monocytes between study Arm A (TLG < 50 SUV) and Arm B/C (TLG ≥ 50 SUV) at week 0 and week 12 time points. However, there was a significant downregulation of these cell subsets in study Arm A (TLG < 50 SUV) at week 12 compared to study Arm B/C (TLG ≥ 50 SUV) (Figure 3.43B.). Furthermore, a comparison of CD86+ cells within each study arm at different time points showed no significant changes in both study arms (Figure 3.43C.).

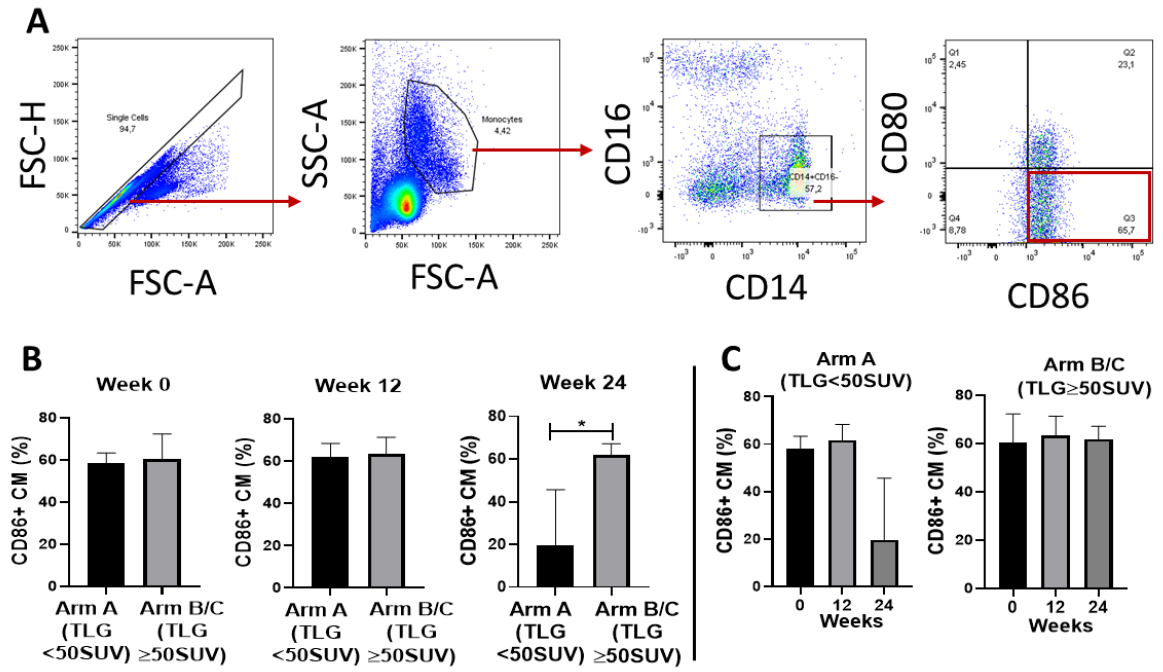

Figure 3.43. Frequency (%) of CD86+ classical monocytes (CM) cell population evaluated using flow cytometry between study Arm A (TLG < 50 SUV) (n=6) and study Arm B/C (TLG ≥ 50 SUV) (n=6) at week 0, 12 and 24 after completion of anti-TB treatment. A. Flow cytometry gating strategy for identifying CD14+CD16-CD80-CD86+ classical monocytes from PBM; **B.** Comparison of CD86+ classical monocyte cell frequency (%) between study Arm A (TLG < 50 SUV) and study Arm B/C (TLG ≥ 50 SUV) at week 0, 12, 24; **C.** Evaluation of frequency percentage changes within each study arm at different time points. Data is a representative of three independent experiments and shown as mean±SD. Data was analysed by Shapiro-Wilk test followed by Mann-Whitney t-test **(B)** or Kruskal-Wallis test followed by Dunn's multiple comparison test against week 0 time point **(C)**. Statistical significance is summarized as *p≤0.05. TLG= Total Lung Glycolysis, SUV= Standardized Uptake Value, FSC-H= Forward Scatter-Hight, FSC-A= Forward Scatter-Area, SSC-A= Side Scatter-Area.

3.6.4. Successfully treated TB patients with persisting lung inflammation present with increased frequency of non-classical monocytes

Non-classical monocytes were defined as CD14-CD16+ cells (Figure 3.44A.). This study showed that successfully treated TB patients with persisting lung inflammation (Arm B/C (TLG ≥ 50 SUV)) have significantly increased population of non-classical monocyte (CD14-CD16+) compared to treated TB patients with no persisting lung inflammation (Arm A (TLG < 50 SUV)). However, this cell population showed to decrease by week 12 time point where there was no significant difference was observed between the study arms. Furthermore, results showed that this cell population remain significantly upregulated at week 24 time point in study Arm B/C (TLG ≥ 50 SUV) (Figure 3.44B.). Evaluation of cell population

changes within each study arm at different time point visits showed significant increase of non-classical monocyte in study Arm A (TLG < 50 SUV) between week 0 and week 12. However, there was significant decrease of these cell at week 24 compared to week 0 and week 12. There were no significant changes observed within study Arm B/C (TLG ≥ 50 SUV) at different time points (Figure 3.44C.).

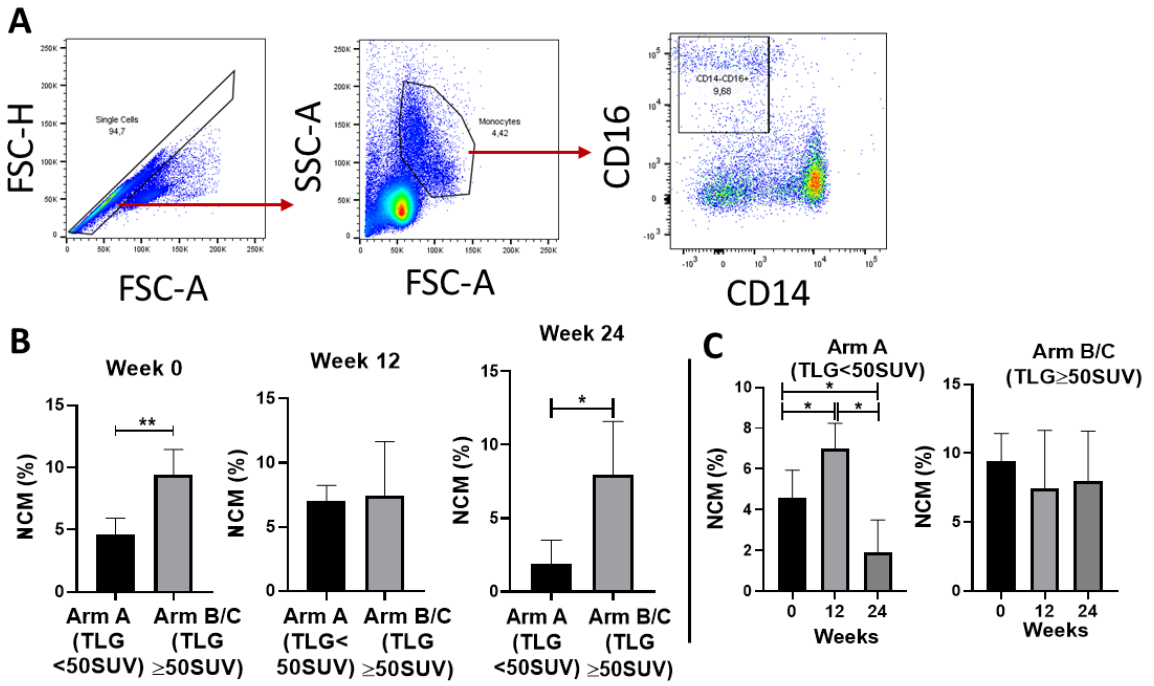

Figure 3.44. Evaluation of non-classical monocytes (NCM) cell frequency (%) between study Arm A (TLG < 50 SUV) (n=6) and study Arm B/C (TLG ≥ 50 SUV) (n=6) measured using flow cytometry after completion of anti-TB treatment. A. Representative flow cytometry analysis of CD14-CD16+ non-classical monocytes from PBMC; **B.** Comparison of non-classical monocytes frequency (%) between study Arm A (TLG < 50 SUV) and study Arm B/C (TLG ≥ 50 SUV) at week 0, 12 and 24; **C.** Evaluation of frequency percentage changes within each study arm at different time points. Data is a representative of three independent experiments and shown as mean±SD. Data was analysed by Shapiro-Wilk test followed by Mann-Whitney t-test **(B)** or Kruskal-Wallis test followed by Dunn's multiple comparison test against week 0 time point **(C)**. Statistical significance is summarized as *p≤0.05, **p≤0.01. TLG= Total Lung Glycolysis, SUV= Standardized Uptake Value, FSC-H= Forward Scatter-Hight, FSC-A= Forward Scatter-Area, SSC-A= Side Scatter-Area.

3.6.5. Expression of co-stimulatory CD86 molecule post-anti-TB treatment in non-classical monocytes is reduced only in participants with minimal lung inflammation

Non-classical monocytes were evaluated for the expression of co-stimulatory molecule CD86 (Figure 3.45A.). There was no significant difference observed in CD86+ non-classical

monocytes between study Arm A (TLG < 50 SUV) and study Arm B/C (TLG ≥ 50 SUV) at week 0. However, study Arm B/C (TLG ≥ 50 SUV) showed a significantly reduced frequency of C14-CD16+CD86+ non-classical monocyte at week 12 compared to study Arm A (TLG < 50 SUV), where there were no significant differences observed at week 24 (Figure 3.45B.). Study Arm A (TLG < 50 SUV) showed significant reduction of CD86+ non-classical monocytes at week 24 compared to week 0 and week 12. However, there were no significant changes observed in study Arm B/C (TLG ≥ 50 SUV) at different time points (Figure 3.45C.).

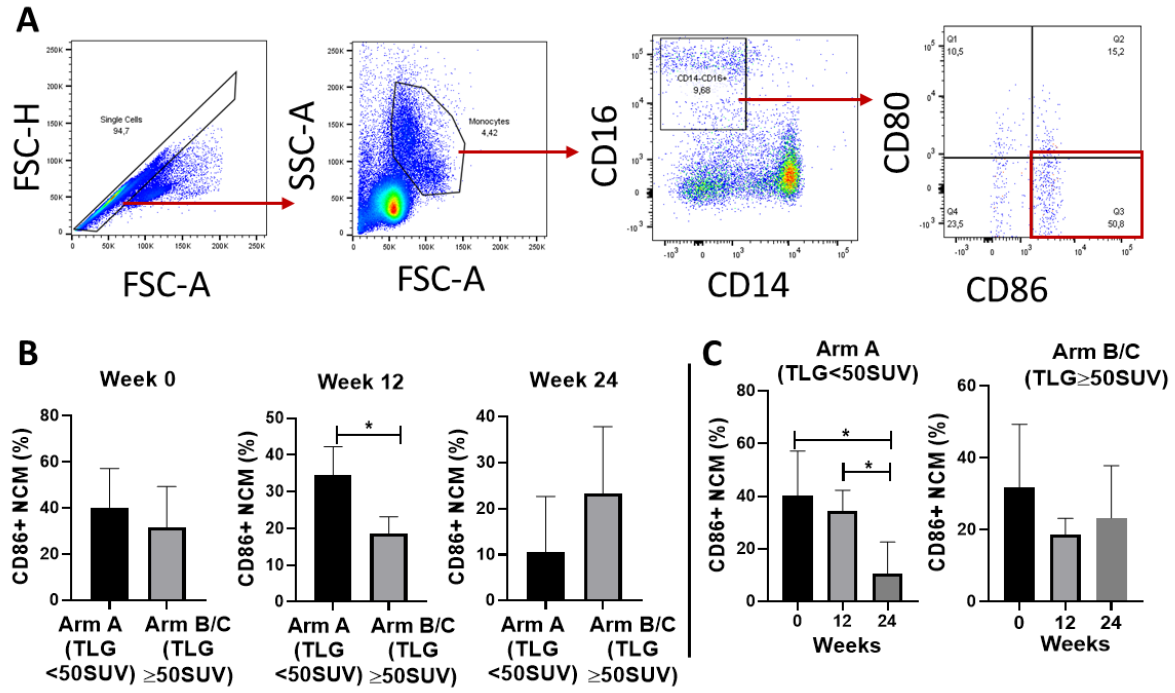

Figure 3.45. Frequency (%) of CD86+ non-classical monocytes (NCM) measured using flow cytometry between study Arm A (TLG < 50 SUV) (n=6) and study Arm B/C (TLG ≥ 50 SUV) (n=6) at week 0, 12 and 24 after completion of anti-TB treatment. A. Flow cytometry gating strategy to identify CD14-CD16+CD80-CD86+ non-classical monocytes from PBMC; **B.** Comparison of CD86+ non-classical monocytes frequency percentage between study Arm A (TLG < 50 SUV) and study Arm B/C (TLG ≥ 50 SUV) at week 0, 12 and 24; **C.** Evaluation of frequency percentage changes within each study arm at different time points. Data is a representative of three independent experiments and shown as mean±SD. Data was analysed by Shapiro-Wilk test followed by Mann-Whitney t-test **(B)** or Kruskal-Wallis test followed by Dunn's multiple comparison test against week 0 time point **(C)**. Statistical significance is summarized as *p≤0.05. TLG= Total Lung Glycolysis, SUV= Standardized Uptake Value, FSC-H= Forward Scatter-Hight, FSC-A= Forward Scatter-Area, SSC-A= Side Scatter-Area.

3.6.6. Non-classical monocytes expressing both CD80 and CD86 co-stimulatory molecules remain unchanged in patients with persisting lung inflammation following anti-TB treatment

Non-classical monocytes expressing both CD80 and CD86 were evaluated between study Arm A (TLG < 50 SUV) and study Arm B/C (TLG ≥ 50 SUV) (Figure 3.46A.). Results showed no significant differences in the frequency of CD80+CD86+ non-classical monocytes between study Arm A (TLG < 50 SUV) and study Arm B/C (TLG ≥ 50 SUV) at week 0 and week 24. However, at week 12, study Arm B/C (TLG ≥ 50 SUV) showed a significantly reduced frequency of double-positive non-classical monocytes (Figure 3.46B.). Additionally, no significant changes were observed within each study arm at different time points (Figure 3.46C.).

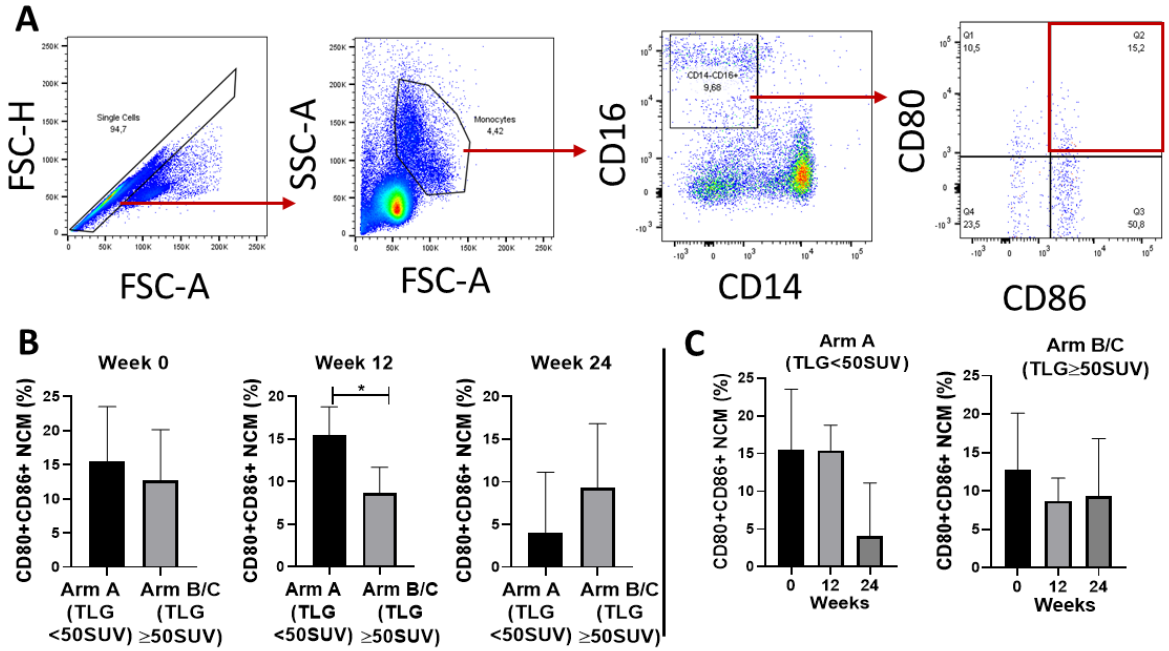

Figure 3.46. Frequency percentage of CD80+CD86+ non-classical monocytes (NCM) between study Arm A (TLG < 50 SUV) (n=6) and study Arm B/C (TLG ≥ 50 SUV) (n=6) measured using flow cytometry at different time points after completion of anti-TB treatment. A. Gated CD14-CD16+CD80+CD86+ non-classical monocytes from PBMC; **B.** frequency (%) of CD14-CD16+CD80+CD86+ non-classical monocytes compared between study Arm A (TLG < 50 SUV) and study Arm B/C (TLG ≥ 50 SUV) at week 0, 12 and 24; **C.** Evaluation of frequency percentage changes within each study arm at different time points. Data is a representative of three independent experiments and shown as mean±SD. Data was analysed by Shapiro-Wilk test followed by Mann-Whitney t-test **(B)** or Kruskal-Wallis test followed by Dunn's multiple comparison test against week 0 time point **(C)**. Statistical significance is summarized as *p≤0.05. TLG= Total Lung Glycolysis, SUV= Standardized Uptake Value, FSC-H= Forward Scatter-Hight, FSC-A= Forward Scatter-Area, SSC-A= Side Scatter-Area.

3.6.7. CD80 expression remains elevated in successfully treated TB patients with persisting lung inflammation

Non-classical monocyte cell population expressing CD80 was evaluated between study Arm A (TLG < 50 SUV) and study Arm B/C (TLG ≥ 50 SUV) (Figure 3.47A). There were no significant differences observed in the frequency of CD14-CD16+CD80+ cell population at week 0 and week 24 between study Arm A (TLG < 50 SUV) and study Arm B/C (TLG ≥ 50 SUV). However, these cell populations showed significant upregulation in study Arm B/C (TLG ≥ 50 SUV) at week 12 compared to study Arm A (TLG ≥ 50 SUV) (Figure 3.47B). Additionally, there were no significant changes observed within each study arm at different time points (Figure 3.47C).

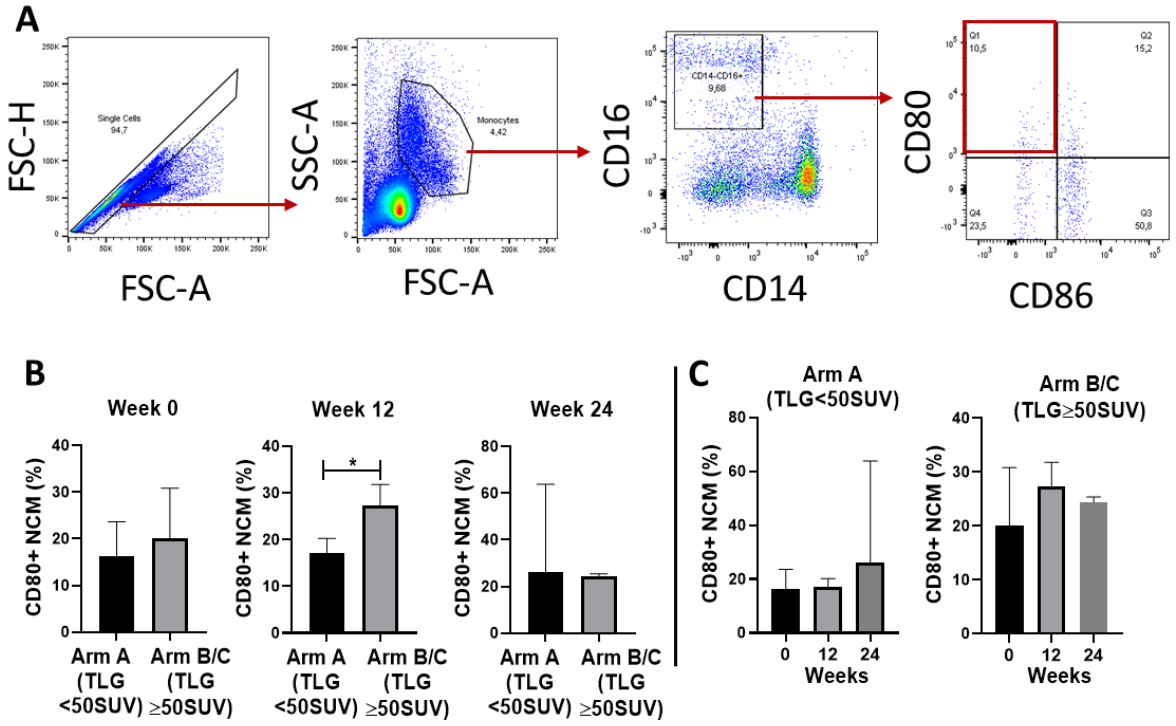

Figure 3.47. Evaluation of CD80+ non-classical monocyte (NCM) cell population between study Arm A (TLG < 50 SUV) (n=6) and study Arm B/C (TLG ≥ 50 SUV) (n=6) measured using flow cytometry after completion of anti-TB treatment. A. Flow cytometry gating strategy for identification of CD14-CD16+CD80+CD86- non-classical monocytes from PBMC; **B.** Comparison of CD80+ non-classical monocytes frequency (%) between study Arm A (TLG < 50 SUV) and study Arm B/C (TLG ≥ 50 SUV) at week 0, 12 and 24; **C.** Evaluation of frequency percentage changes within each study arm at different time points. Data is a representative of three independent experiments and shown as mean±SD. Data was analysed by Shapiro-Wilk test followed by Mann-Whitney t-test **(B)** or Kruskal-Wallis test followed by Dunn's multiple comparison test against week 0 time point **(C)**. Statistical significance is summarized as *p≤0.05. TLG= Total Lung Glycolysis, SUV= Standardized Uptake Value, FSC-H= Forward Scatter-Hight, FSC-A= Forward Scatter-Area, SSC-A= Side Scatter-Area.

3.7. *Ex-vivo* stimulation of PBMC from treated TB patients with atorvastatin modulate cell phenotypes

3.7.1. Evaluation of cell viability following *ex-vivo* atorvastatin stimulation and Mtb in human PBMC

Cell viability in atorvastatin-stimulated and unstimulated PBMC was evaluated using 7-aminoactinomycin D (7-AAD) at three-time points (1DPI, 3DPI, and 6DPI) after *ex-vivo* Mtb infection. Three Mtb strains were evaluated which included laboratory strain (H37Rv), and two clinical strains (HN878 and CDC1551). Results showed that cell viability remained above 80% in infected PBMC stimulated with 50µM and 100µM atorvastatin at 1DPI

regardless of Mtb strain. However, statistical analysis showed a significant reduction in cell viability with 200µM atorvastatin in all Mtb strain infections (Figure 3.48B-D) compared to control samples. Cell viability was significantly reduced below 80% at 3DPI and 6DPI regardless of Mtb strain and atorvastatin stimulation concentration. Collectively, this data shows that at 1DPI cell viability is not affected by infection regardless of Mtb strain in PBMC pre-stimulated with 50 µM or 100µM atorvastatin.

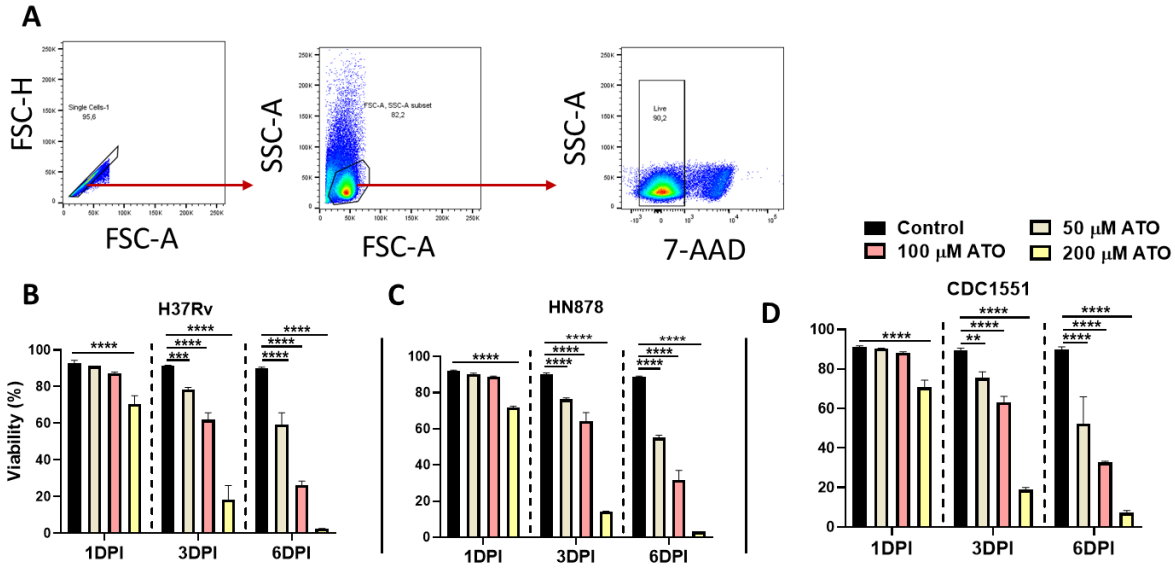

Figure 3.48. Evaluation of *ex-vivo* cell viability using flow cytometry from Mtb infected PBMC following 24 hours of atorvastatin stimulation with 50µM, 100µM, and 200µM. A. Flow cytometry gating to evaluate cell viability based on 7-aminoactinomycin D (7-AAD) binding where viable cells are shown by 7-AAD-; **B.** Cell viability in H37Rv infected PBMC at 1, 3 and 6 Days Post Infection (DPI); **C.** Cell viability in HN878 infection at 1, 3 and 6 DPI; **D.** Cell viability in CDC1551 infected PBMC at 1, 3 and 6DPI. Data is shown as a representative of three independent experiments and shown as mean±SD. Data was analysed using two-way ANOVA followed by Dunnett's corrected multiple comparisons against control samples; **p≤0.01, ***p≤0.001, and ****p≤0.0001. ATO= Atorvastatin, FSC-H= Forward Scatter-Hight, FSC-A= Forward Scatter-Area, SSC-A= Side Scatter-Area.

3.7.2. Investigating *ex-vivo* atorvastatin effects on cell phenotype changes relative to immune reconstitution following successful anti-TB treatment

Cell phenotype changes induced by *ex-vivo* stimulation with atorvastatin were evaluated with 10µM atorvastatin concentration and a single Mtb strain (hypervirulent clinical strain, HN878). Samples were isolated after completion of anti-TB treatment at two-time points (Week 0 and Week 12) after completion of anti-TB treatment and stimulated with atorvastatin for 24 hours prior to Mtb infection (24 hours). This aimed to collectively

evaluate *ex-vivo* effects on cell phenotype posed by atorvastatin pre-stimulation and Mtb infection in PBMC isolated after successful completion of anti-TB treatment.

3.7.2.1. Atorvastatin stimulation modulates different lymphocyte populations

Memory B-cell subsets were gated from the lymphocyte cell population and defined using CD21 and CD27 expression (Figure 3.49A.). A shown in Figure 3.49B., there were no significant reduction observed in memory B-cell (CD21+CD27+) population following atorvastatin stimulation and Mtb infection in unstimulated PBMC. However, atorvastatin stimulated-Mtb infected PBMC showed significant reduction of classical memory B-cell population at week 0 compared to control samples, whereas no significant changes were observed from PBMC isolated at week 12. In this study, atorvastatin stimulation significantly reduced the frequency of naïve B-cells defined by CD21+CD27- in PBMC isolated at both week 0 and week 12 after completion of anti-TB treatment. Additionally, naïve B-cell population showed a significant reduction following *ex-vivo* Mtb infection in unstimulated or stimulated PBMC (Figure 3.49C.).

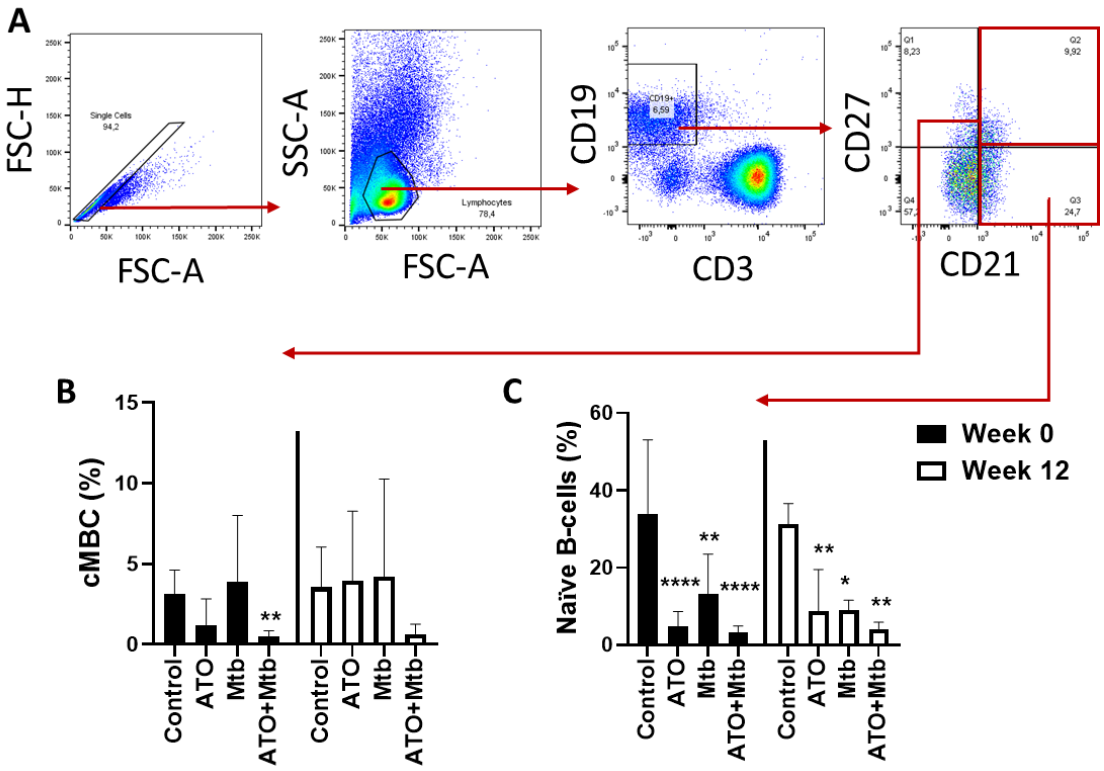

Figure 3.49. Evaluation of *ex-vivo* frequency (%) of classical memory B-cell (cMBC) and naïve B-cell population using flow cytometry in atorvastatin stimulated and Mtb infected PBMC isolated at week 0 (n=6) and week 12 (n=6) after anti-TB treatment completion. Four culture conditions were evaluated at each time point; control (unstimulated), 24hrs atorvastatin stimulated-uninfected, 24hrs unstimulated-infected and 24hrs atorvastatin stimulated+24hrs Mtb infection. **A.** Representative flow cytometry gating strategy for identifying B-cell subsets; **B.** Evaluation of CD19+CD21+CD27+ memory B-cells; **C.** Evaluation of CD19+21+CD27- naïve B-cells. Data is shown as a representative of three independent experiments and shown as mean±SD. Data was analysed using two-way ANOVA followed by Dunnett's corrected multiple comparisons against control samples, *p≤0.05, **p≤0.01, ****p≤0.0001. ATO= Atorvastatin (10µM), FSC-H= Forward Scatter-Hight, FSC-A= Forward Scatter-Area, SSC-A= Side Scatter-Area and Mtb=HN878 (MOI:0.5).

Memory phenotype in the T-cell population was evaluated from CD3+ lymphocyte cells and these were described based on CD45RA and CCR7 expression within both T-helper cells (CD4+) and cytotoxic T-cells (CD8+) (Figure 3.50A.). There were no significant differences observed within naïve (CD45RA+CCR7+), central memory (CD45RA-CCR7+), and effector memory (CD45RA-CCR7-) T-cell populations [104]. However, atorvastatin stimulation was shown to significantly reduce CD45RA+ effector memory T-cell population (CD45RA+CCR7-) [104] in both CD4+ and CD8+ PBMC isolated at week 12 after

completion of anti-TB treatment whereas there were no significant differences observed with PBMC isolated at week 0 in both T-cell subtype. Furthermore, Mtb infection of unstimulated and atorvastatin-stimulated PBMC showed no significant changes in T-cell memory phenotype in both CD4+ and CD8+ T-cells at both time points (Figure 3.50B-C.).

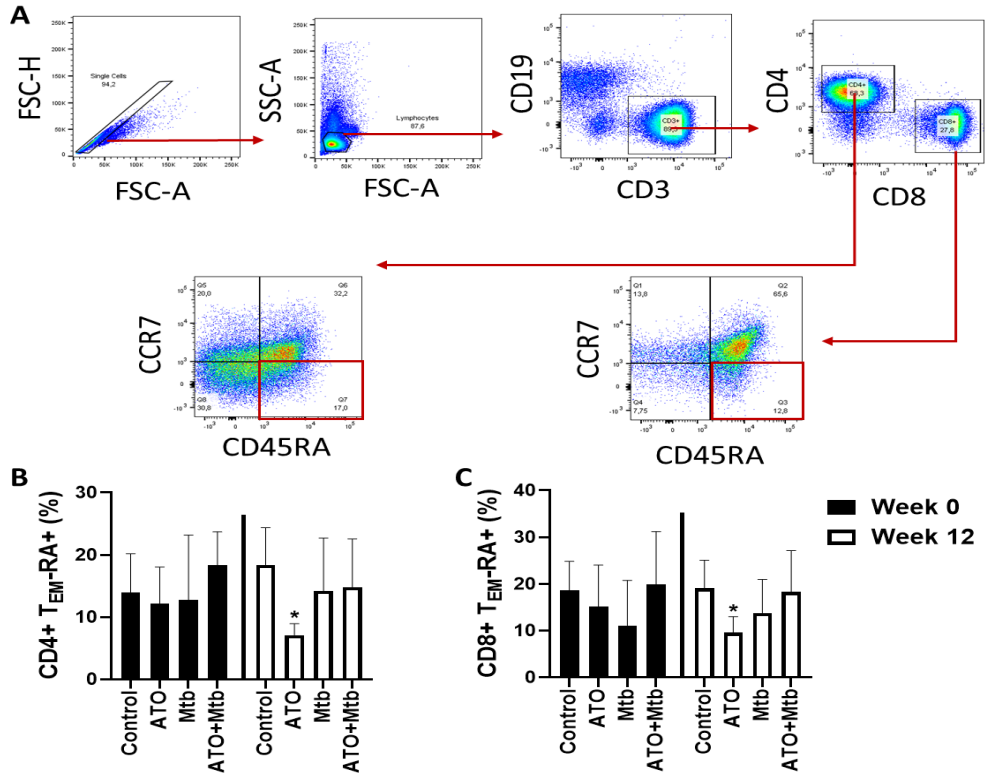

Figure 3.50. Evaluation of CD4+ effector memory-RA+ and CD8+ effector memory-RA+ T-cells in *ex-vivo* atorvastatin-stimulated-Mtb infected PBMC isolated at week 0 (n=6) and week 12 (n=6) after anti-TB treatment completion using flow cytometry. Four culture conditions were evaluated at each time point; control (unstimulated), 24hrs atorvastatin stimulated-uninfected, 24hrs unstimulated-infected, and 24hrs atorvastatin stimulated+24hrs Mtb infection. **A.** Representative flow cytometry gating strategy for identifying memory T-cell subsets; **B.** Evaluation of CD3+CD4+CD45RA+CCR7- effector memory-RA+ T-cells; **C.** Evaluation of CD3+CD8+CD45RA+CCR7- effector memory-RA+ T-cells. Data is shown as a representative of three independent experiments and shown as mean±SD. Data was analysed using two-way ANOVA followed by Dunnett's corrected multiple comparisons against control samples, *p≤0.05. ATO= Atorvastatin (10µM), FSC-H= Forward Scatter-Hight, FSC-A= Forward Scatter-Area, SSC-A= Side Scatter-Area and Mtb=HN878 (MOI:0.5).

Ex-vivo Mtb infection of unstimulated PBMC isolated from study participants after completion of anti-TB showed significant upregulation of conventional regulatory T-cells (CD25+FoxP3+) in PBMC samples isolated at week 12. However, there were no significant changes observed with PBMC isolated at week 0 compared to control samples (Figure 3.51B.). Unconventional regulatory T-cells (CD25-FoxP3+) showed significant reduction with atorvastatin stimulation in uninfected PBMC isolated at week 12 after completion of anti-TB treatment whereas there were no significant changes observed with PBMC isolated at week 0. Additionally, there were no significant differences observed in the frequency of both mature and unconventional regulatory T-cells with atorvastatin stimulated-Mtb infected PBMC at both time points compared to control samples (Figure 3.51C.). Collectively, these results show that atorvastatin stimulation does not affect the frequency of conventional regulatory T-cells, however, reduces the frequency of unconventional regulatory T-cells.

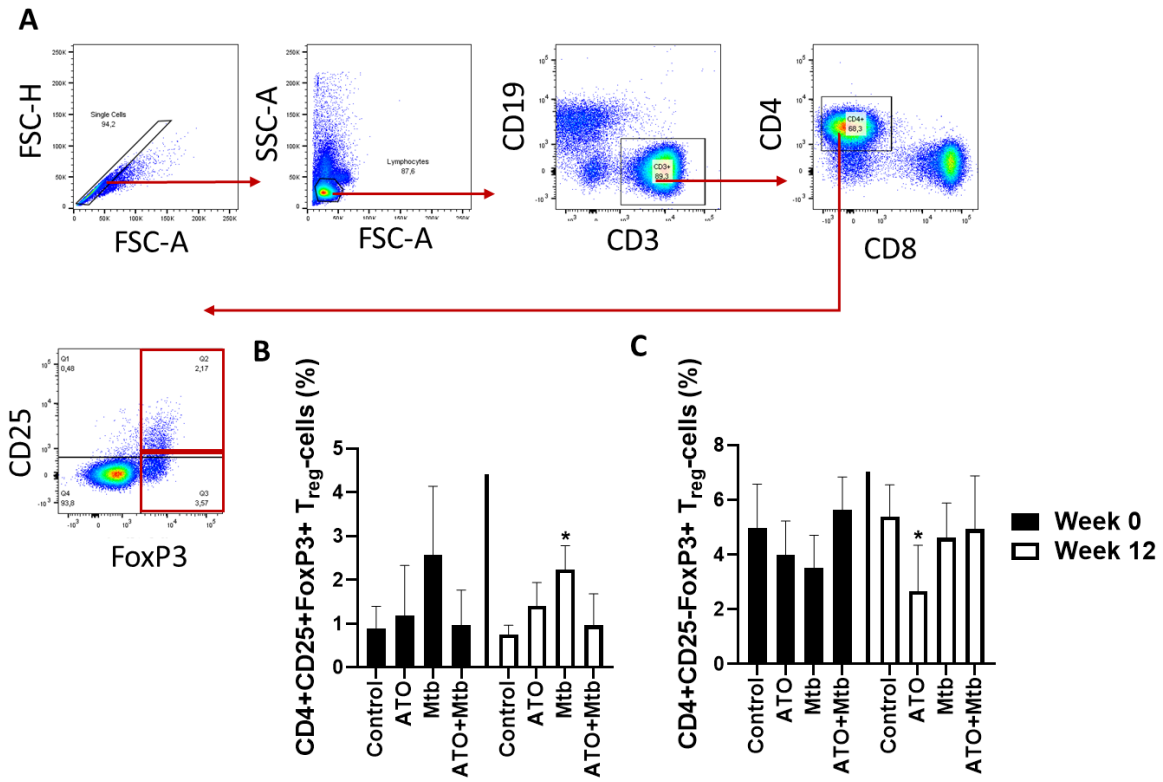

Figure 3.51. ***Ex-vivo*** **frequency (%) of conventional regulatory T-cells and unconventional regulatory T-cells measured using flow cytometry in uninfected and infected atorvastatin stimulated PBMC isolated at week 0 (n=6) and week 12 (n=6) after anti-TB treatment completion.** Four culture conditions were evaluated at each time point; control (unstimulated), 24hrs atorvastatin stimulated-uninfected, 24hrs unstimulated-infected, and 24hrs atorvastatin stimulated+24hrs Mtb infection. **A.** Representative flow cytometry gating strategy for identifying regulatory T-cell subsets; **B.** Evaluation of CD3+CD4+CD25+FoxP3+ conventional regulatory T-cells; **C.** Evaluation of CD3+CD4+CD25-FoxP3+ unconventional regulatory T-cells. Data is shown as a representative of three independent experiments and shown as mean±SD. Data was analysed using two-way ANOVA followed by Dunnett's corrected multiple comparisons against control samples, *p≤0.05. ATO= Atorvastatin (10µM), FSC-H= Forward Scatter-Hight, FSC-A= Forward Scatter-Area, SSC-A= Side Scatter-Area and Mtb=HN878 (MOI:0.5).

NK cells were evaluated based on CD16 and CD56 expression where activation was defined by NKp46 expression (Figure 3.52A.). This study showed significant upregulation of CD16+CD56-NKp46 NK subsets with both atorvastatin stimulation and Mtb infection of PBMC isolated at both week 0 and week 12 after completion of anti-TB treatment (Figure 3.52B). Additionally, CD16+CD56+ NK population showed significant upregulation with Mtb infection in PBMC isolated at week 12 whereas no significant changes were observed with PBMC isolated at week 0 compared to control samples (Figure 3.52C). Atorvastatin

stimulation showed to significantly increase activation within the CD16+CD56+ NK cell population through upregulated expression of NKp46 in PBMC isolated at both week 0 and week 12 after completion of anti-TB treatment (Figure 3.52D). This data shows that atorvastatin stimulation enhances activation of both CD16+CD56- and CD16+CD56+ NK cell populations through upregulation of NKp46 expression.

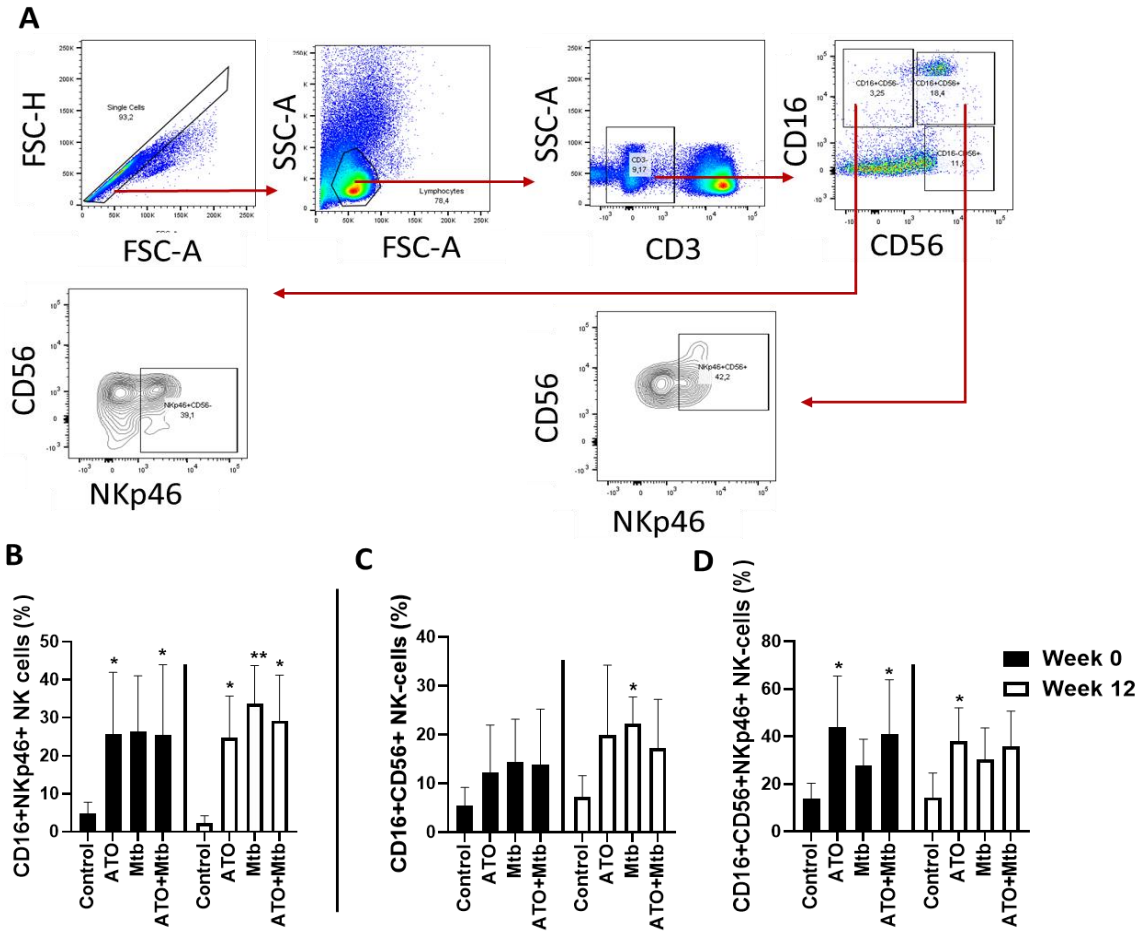

Figure 3.52. Representative plots showing changes in *ex-vivo* frequency (%) of Natural killer (NK) subsets measured using flow cytometry in uninfected and infected atorvastatin-stimulated PBMC isolated at week 0 (n=6) and week 12 (n=6) after anti-TB treatment completion. Four culture conditions were evaluated at each time point; control (unstimulated), 24hrs atorvastatin stimulated-uninfected, 24hrs unstimulated-infected and 24hrs atorvastatin stimulated+24hrs Mtb infection. **A.** Representative flow cytometry analysis for defining NK-cell subsets; **B.** Activated dysfunctional NK-cells defined as CD3-CD16+CD56-NKp46+; **C.** Evaluation of CD3-CD16+CD56+ conventional NK-cells; **D.** Activated conventional NK cells defined as CD3-CD16+CD56+ NKp46+. Data is shown as a representative of three independent experiments and shown as mean±SD. Data was analysed using two-way ANOVA followed by Dunnett's corrected multiple comparisons against control samples, *p≤0.05. ATO= Atorvastatin (10µM), FSC-H= Forward Scatter-Hight, FSC-A= Forward Scatter-Area, SSC-A= Side Scatter-Area and Mtb=HN878 (MOI:0.5).

Dendritic cells (DCs) were gated on the CD3- lymphocyte population and defined based on CD1c and CD11c expression where activation of CD11c DCs was evaluated through the expression of leukocyte receptor CD11b (Figure 3.53A.) [105]. Evaluation of CD11c+CD1c- DC subsets showed significant reduction with both atorvastatin stimulation and Mtb infection in PBMC isolated at both week 0 and week 12 compared to control samples (Figure 3.53B.). Additionally, atorvastatin stimulation of PBMC isolated at week 0 post-TB treatment showed a significant reduction of CD11b expression. However, there were no significant differences observed with both atorvastatin stimulation and Mtb infection of PBMC isolated at week 12 after completion of anti-TB treatment (Figure 3.53C).

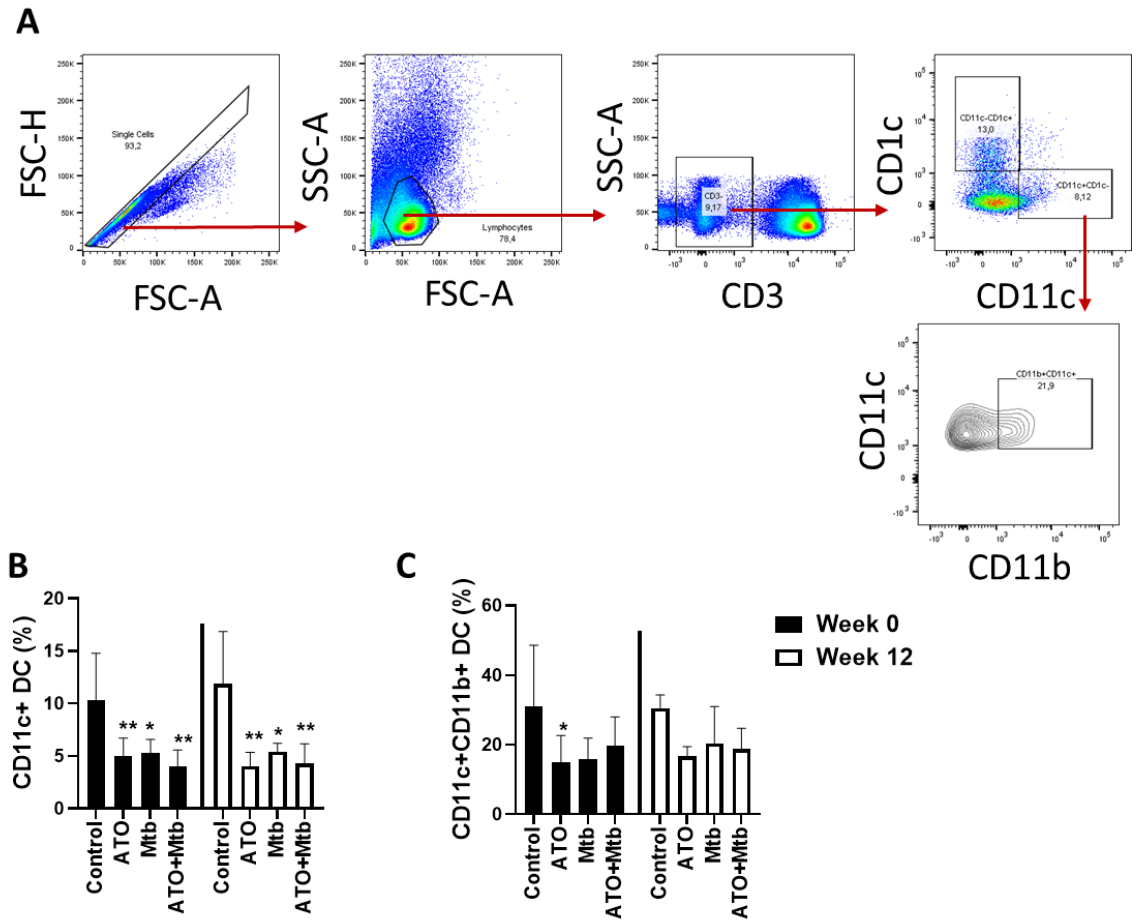

Figure 3.53. Changes in dendritic cells (DC) subsets in *ex-vivo* atorvastatin-stimulated-Mtb infected and uninfected PBMC isolated at week 0 (n=6) and week 12 (n=6) after anti-TB treatment completion measured using flow cytometer. Data is a representative of four culture conditions (control (unstimulated-uninfected), ATO (atorvastatin-stimulated-uninfected), Mtb (unstimulated-infected) and ATO+Mtb (atorvastatin-stimulated-Mtb infected). **A.** Representative flow cytometry gating strategy for identifying DC subsets; **B.** Evaluation of CD3-CD11c+CD1c- DCs; **C.** Evaluation of CD3-CD11c+CD1c-CD11b+ DCs. Data is shown as a representative of three independent experiments and shown as mean±SD. Data was analysed using two-way ANOVA followed by Dunnett's corrected multiple comparisons against control samples where significance is shown as, *p≤0.05, **p≤0.01. ATO= Atorvastatin (10µM), FSC-H= Forward Scatter-Hight, FSC-A= Forward Scatter-Area, SSC-A= Side Scatter-Area and Mtb=HN878 (MOI:0.5).

3.7.2.2. Atorvastatin modulates monocyte population

This study evaluated the modulation of the total monocyte (CD14+) cell population by atorvastatin stimulated in Mtb infected or uninfected PBMC isolated at week 0 and week 12 time points post-anti-TB treatment (Figure 3.54A). Significant reduction of the total CD14+ population was observed with Mtb infection of either stimulated or unstimulated PBMC isolated at both week 0 and week 12 after completion of anti-TB treatment (Figure 3.54B.).

Furthermore, evaluation of immune regulatory (M2) phenotype in CD14+ monocyte population through the expression of CD163 and CD206 showed a significant reduction of M2-monocytes (CD206-CD163+) with atorvastatin stimulation and Mtb infection of PBMC isolated at both week 0. However, there were no significant changes observed in PBMC isolated at week 12 after completion of anti-TB treatment (Figure 3.54C.). M2-like monocytes (CD206+CD163+) population showed no significant change with atorvastatin stimulation of PBMC isolated at both week 0 and week 12 time points after completion of anti-TB treatment. However, Mtb infection of either stimulated or unstimulated PBMC isolated after completion of anti-TB treatment showed a significant increase of M2-like monocytes. There were no significant changes observed with Mtb infection of unstimulated PBMC isolated at week 12 after completion of anti-TB treatment, whereas Mtb infection of stimulated PBMC showed significant upregulation of M2-like monocytes (Figure 3.54D.).

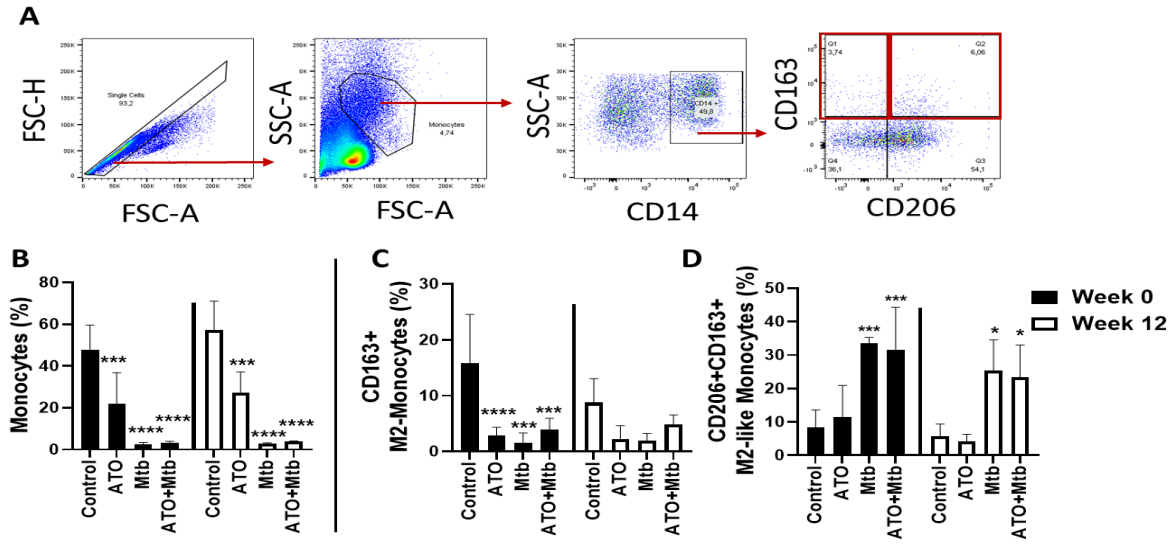

Figure 3.54. *Ex-vivo* frequency (%) of monocyte cell population, M2 monocyte subset, and M2-like monocytes in infected and uninfected PBMC isolated at week 0 (n=6) and week 12 (n=6) after anti-TB treatment completion. Four culture conditions were evaluated at each time point; control (unstimulated), 24hrs atorvastatin stimulated-uninfected, 24hrs unstimulated-infected and 24hrs atorvastatin stimulated+24hrs Mtb infection. **A.** Representative flow cytometry analysis for defining monocyte cells and M2 class switched monocyte subsets; **B.** Evaluation of CD14+ monocyte cells; **C.** Evaluation of CD14+CD206-CD163+ M2 monocyte subset; **D.** Evaluation of CD14+CD206+CD163+ M2-like monocyte cell population. Data is shown as a representative of three independent experiments and shown as mean±SD. Data was analysed using two-way ANOVA followed by Dunnett's corrected multiple comparisons against control samples where significance is shown as, *p≤0.05, ***p≤0.001, ****p≤0.0001. ATO= Atorvastatin (10µM), FSC-H= Forward Scatter-Hight, FSC-A= Forward Scatter-Area, SSC-A= Side Scatter-Area and Mtb=HN878 (MOI:0.5).

Monocyte subsets were classified based on CD14 and CD16 expression, where CD14-CD16+ represents non-classical monocytes, CD14+CD16- are classical monocytes and CD14+CD16+ are intermediate monocytes (Figure 3.55A.). There were no significant changes observed within the non-classical monocyte population. However, expression of co-stimulatory molecule CD86 in non-classical monocytes showed significant reduction with atorvastatin stimulation of PBMC isolated at both week 0 and week 12 after completion of anti-TB treatment. Additionally, Mtb infection of unstimulated PBMC showed a significant reduction of CD86 at week 12 whereas no significant change was observed with week 0 PBMC infection. Mtb infection of atorvastatin-stimulated PBMC showed a significant reduction of CD86 expression in PBMC isolated at both week 0 and week 12 (Figure 3.55B.). Evaluation of classical monocytes (CD14+CD16-) showed significant reduction with both atorvastatin stimulation and Mtb infection in PBMC isolated at both week 0 and week 12 after TB treatment completion. Furthermore, a significant reduction of the classical monocyte population was observed with infection of atorvastatin-stimulated PBMC at both time points. There were no significant changes observed in the frequency (%) of CD86+ classical monocytes with atorvastatin-stimulated PBMC isolated at both week 0 and week 12 after completion of anti-TB treatment. Mtb infection of unstimulated and atorvastatin-stimulated PBMC showed a significant reduction of CD86 expression in classical monocytes in PBMC isolated at both time points after TB treatment (Figure 3.55C.). There were no significant changes observed in the frequency of intermediate monocyte population with atorvastatin stimulation of PBMC at both week 0 and week 12 after completion of anti-TB treatment. However, Mtb infection of unstimulated PBMC showed a significant reduction on the frequency (%) of intermediate monocytes at week 0. The frequency of CD86+ intermediate monocytes showed no significant changes with atorvastatin stimulation at both week 0 and week 12 after completion of TB treatment. However, a significant reduction in the expression of CD86 was observed with Mtb infection of unstimulated and atorvastatin-stimulated PBMC isolated at week 12 whereas there were no significant changes observed with PBMC isolated at week 0 after TB treatment completion (Figure 3.55D.).

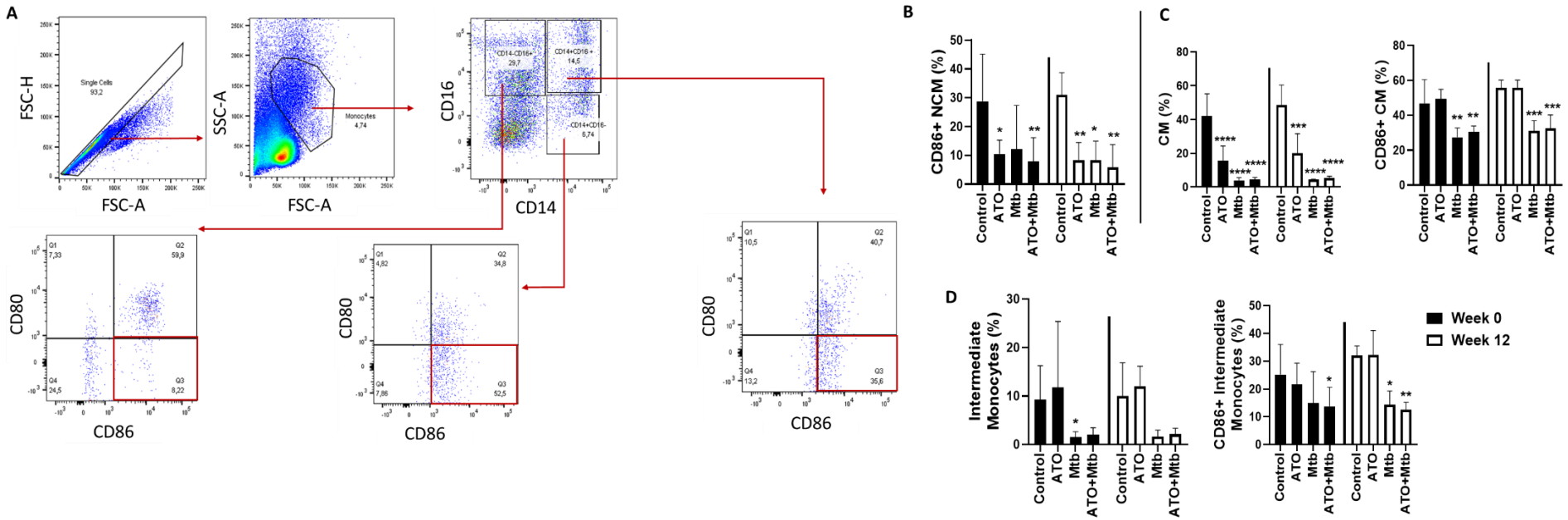

Figure 3.55. ***Ex-vivo*** **evaluation of monocyte subsets and expression of co-stimulatory molecules in classical, intermediate, and non-classical monocytes in uninfected and infected PBMC isolated at week 0 (n=6) and week 12 (n=6) after anti-TB treatment completion using flow cytometer.** Four culture conditions were evaluated at each time point; control (unstimulated), 24hrs atorvastatin stimulated-uninfected, 24hrs unstimulated-infected and 24hrs atorvastatin stimulated+24hrs Mtb infection. **A.** Representative flow cytometry analysis for defining monocyte subsets based on CD14/CD16 and expression of CD80/CD86 co-stimulatory molecules; **B.** Evaluation of CD14-CD16+CD86+ non-classical monocytes (NCM); **C.** Evaluation of CD14+CD16- and CD14+CD16-CD86+ classical monocytes (CM); **D.** Evaluation of CD14+CD16+ and CD14+CD16+CD86+ intermediate monocytes. Data is shown as a representative of three independent experiments and shown as mean±SD. Data was analysed using two-way ANOVA followed by Dunnett's corrected multiple comparisons against control samples where significance is shown as, *p≤0.05, **p≤0.01, ***p≤0.001, ****p≤0.0001. ATO= Atorvastatin (10µM), FSC-H= Forward Scatter-Hight, FSC-A= Forward Scatter-Area, SSC-A= Side Scatter-Area and Mtb=HN878 (MOI:0.5).

Chapter 4: Discussion and Conclusion

4.1. Successfully treated TB patients with persisting lung inflammation remain with elevated soluble inflammatory storm

Tuberculosis disease is listed among the deadliest diseases resulting from a single infectious agent, Mtb. Successful TB treatment has been mostly associated with resolved clinical symptoms, chest radiography, and negative sputum cultures presented at months 4 and 6 of anti-TB therapy. However, it has been shown that active TB disease is associated with tissue pathology which may remain unresolved after completion of anti-TB therapy, and this has been implicated in contributing to the growing percentage of recurrent TB [106]. Post-TB pulmonary damage represents a new challenge that remains unrecognized even though it has been suggested to be a risk factor for long-term respiratory impairment and reduced quality of life [107]. A study by Plit et al. (1998) reported an improved lung function in 54% of treated TB patients, whereas 24% showed restrictive pulmonary pattern, and 28% remained with residual airflow limitations suggesting that even though anti-TB therapy may improve pulmonary function post-TB treatment, a large proportion remain with persisting residual pulmonary impairment [108]. Even though soluble inflammatory mediators such as cytokines, chemokines, and growth factors play crucial roles in controlling TB disease outcomes. These mediators have been reported to contribute to chronic lung pathology due to excessive or uncontrolled secretion and increased expression of lung matrix-degrading proteases [107].

Using the Luminex multiplex platform, this study evaluated differences in the secretion profile of soluble immunological mediators from patients who have completed anti-TB therapy but presented with varying lung pathologies afterward. Patients were recruited from eight clinical facilities around Cape Town, South Africa. A total of 71 patients who met the study inclusion criteria were enrolled regardless of gender or HIV status. The recruited study participants' age ranged from 18-64 years old, with 19.71% being HIV-positive. All study participants were subjected to FDG PET/CT scan and classified into two study arms based on the severity of lung pathology. Study participants with TLG < 50 SUV included treated TB patients with no persisting lung inflammation (study Arm A), while those with TLG ≥ 50 SUV were described as having persisting lung inflammation (study Arm B/C).

Development of lung cavities during TB treatment has been associated with unfavourable disease outcomes such as delayed sputum conversion [106]. Here, a total of 20 soluble biomarkers were shown to be differently expressed between patients with persisting lung inflammation and those without persisting lung inflammation regardless of HIV status. Nine pro-inflammatory cytokines remained elevated in successfully treated TB patients with persisting lung inflammation. This data suggests aggravated residual inflammatory activity in treated TB patients with persisting lung inflammation mediated by activated macrophages, neutrophils, dendritic cells, and T-cells through elevated secretion of IL-1α, IL1β, IL-12p40, IL-16, IL-18, TNF-α, IL-2Rα, IL-17, and TRAIL. Previously, a strong association of soluble mediators with the development of lung cavities was highlighted in a study by Sigal et al. (2017) at the baseline of anti-TB treatment; however, these were reported to be significantly reduced over the treatment period [39]. This highlights the need to evaluate the activity of these biomarkers in the induction of tissue pathology, which will enhance the development of new therapies targeting individualized treatment [109], thus decreasing the prevalence of developing recurrent TB after treatment completion. Regulation of inflammatory responses has been suggested to be a hallmark in preventing progressive tissue damage during chronic diseases, including TB. In this study, anti-inflammatory profile was shown through upregulation of IL-4 in participants with persisting lung inflammation. However, the majority of the anti-inflammatory mediators that have been previously shown to be upregulated during TB disease, such as IL-1ra [110], IL-10, IL-13 [111], and MIF [112], were not detected in the enrolled study participants who have completed anti-TB treatment period. Additionally, upregulated expression of IL-10 and IL-13 during active TB treatment has been shown to be associated with better radiographic infiltration and prevention of cavity formation [111]. TB disease is known to induce lung fibrosis leading to cavitation, this has been speculated to further be exacerbated by host immune responses, such as elevated levels of matrix-degrading proteases which have been reported to be common during TB disease [107]. Growth factors represent crucial inflammatory modulators with functions ranging from induction of cell proliferation and migration to regulation of multicellular morphogenesis and differentiation during development and tissue healing [113]. This study identified five growth factors (Basic FGF, G-CSF, HGF, M-CSF, and SCGF-β) that were upregulated in participants with persisting lung inflammation. Evaluation of serum HGF has also been observed to be elevated in patients with active pulmonary tuberculosis, which further showed decrease with resolved disease state [114]. Furthermore, macrophages are known to play a crucial role in fibroproliferative response through upregulated secretion of basic FGF [115],

resulting in the accumulation of fibroblast and collagen deposition in the lungs [116]. In addition to the cytokine and growth factors storm that has been associated with pulmonary tissue damage, here we identified three chemokines (Gro-α, IP-10, and MIG) which are elevated in patients with persisting lung inflammation after successful anti-TB treatment. These are involved in pro-inflammatory immune responses through recruitment of other immune cells to the site of inflammation/infection. IP-10 and MIG has been shown to be involved in the recruitment of activated T-cells, NK-cells, macrophages, and dendritic cells whereas Gro-α is associated with the recruitment of neutrophils to the site of infection. It has been reported that increased levels of activated leukocytes, particularly the T-helper 2 cells (Th2 cells), may be associated with tissue necrosis, which leads to cavitation during pulmonary TB disease [70]. Elevated expression of these chemotactic mediators may be, in part, associated with exacerbated tissue necrosis and lung cavities after completion of anti-TB treatment.

This study further showed that successfully treated TB patients remain with elevated cytokine storm compared to healthy and latently infected individuals. Four biomarkers including Basic FGF, IL-4, IL-1α, and IL12p40 remained similarly elevated in successfully treated TB patients with minimal lung inflammation compared to both healthy (QFT-) and latently infected individuals (QFT+). However, G-CSF and MIP-1α were differentially regulated in QFT- and QFT+ individuals compared to treated TB patients with minimal lung inflammation. G-CSF is known for its role in enhancing neutrophil-related immunological functions during inflammatory state and further promote proliferation and differentiation of both mature neutrophils and neutrophil progenitors [117]. In this study, G-CSF secretion remained significantly upregulated in treated TB patients with no persisting lung inflammation compared to QFT- individuals. However, even though not statistically significant, it showed upregulation in QFT+ individuals compared to treated TB patients with no persisting lung inflammation. This implies that Mtb exposure prime G-CSF secretion to enhance neutrophil responses, which further remains elevated compared to Mtb unexposed individuals despite completion of anti-TB treatment or resolved lung inflammation. Furthermore, MIP-1α, which is a neutrophil-derived chemokine showed significant upregulation in QFT+ compared to treated TB patients with minimal lung inflammation. However, there was no significant difference observed between Mtb unexposed (QFT-) and treated TB patients with minimal lung inflammation. This data highlights the involvement of G-CSF and MIP-1α during the early stages of Mtb infection and further shows that their

secretion may be greatly affected by anti-TB therapy. Additionally, treated TB patients with persisting lung inflammation showed to remain with eight elevated biomarkers which includes IP-10, MIG, Basic FGF, IL-4, IL-1α, IL-1β, IL-12p40, and IL-17 compared to QFT- individuals. Comparison with QFT+ individuals showed six similar biomarkers, except for IL-1β and IP-10, which remained significantly elevated in treated TB patients with persisting lung inflammation with an addition of MIP-1α. Taken together, these results suggest a continued inflammatory activity of MIP-1α in treated TB patients with persisting lung inflammation compared to treated TB patients without persisting lung inflammation. The sustained elevated levels of MIP-1α in treated TB patients with persisting lung inflammation compared to QFT-, QFT+, and treated TB patients with no persisting lung inflammation may highlight beneficial MIP-1α functions such as enhanced wound healing and stem cell inhibition or detrimental MIP-1α functions such as continued inflammatory responses which include inflammatory cell recruitment and maintenance of effector immune responses in these patients [118].

Identification of biomarker signatures during TB disease represents a new platform which may enhance individualized treatment therapies and lead to better disease outcomes. Recent studies have focused on identifying soluble biomarker signatures that can distinguish between healthy individuals, those with latent TB infection (LTBI), and those with active TB. However, limited data is available on soluble biomarker signatures which may facilitate efficient identification of treated TB patients who remain with residual lung inflammation. Currently, evaluation of residual lung inflammation following anti-TB treatment is achieved through expensive techniques that are entirely based on chest radiography such as X-ray and FDG PET/CT scans. Although these techniques have been effective over the years, they may have other shortcomings, such as a lack of specificity in patients with comorbidities. Thus, further highlighting the need to identify host-specific responses that may be targeted to distinguish between treated TB patients with or without persisting lung inflammation. Using ROC curve analysis, this study identified a total of fourteen serum biomarkers that showed good potential to discriminate between the two groups following successful anti-TB treatment with an AUC > 0.70. These biomarkers were significantly elevated in treated TB patients with persisting lung inflammation and included seven pro-inflammatory cytokines such as IL-1α, IL-β, IL-2Rα, IL-12p40, IL-18, TNF-α, and TRAIL. Among these, five biomarkers (IL-1α, IL-2Rα, IL-12p40, TNF-α, and TRAIL) showed a significant correlation with TLG values, indicating their involvement in sustained lung inflammation despite

completion of anti-TB treatment. Three growth factors (HGF, M-CSF, and SCGF-β) showed high sensitivity and specificity to discriminate against treated TB patients based on residual lung inflammation, and these were significantly correlated with TLG values, with an addition of Basic FGF, which had a poor diagnostic potential. Furthermore, two pleiotropic mediators (LIF and IL-9) and three chemokines (Gro-α, IP-10, and MIG), which were significantly elevated in treated TB patients with persisting lung inflammation also showed significant correlation with TLG values. However, among these, the diagnostic potential to discriminate between successfully treated TB patients with minimal or persisting lung inflammation was only shown by LIF, IP-10, and MIG. This further implies that persisting lung inflammation in treated TB patients may be linked with aggravated secretion of soluble mediators during active TB disease which remains unresolved during anti-TB therapy. Additionally, the identification of biomarker signatures may represent a new platform to define effective biomarker combinations that can be used in the development of new techniques, such as point of care, to effectively identify residual lung inflammation after completion of anti-TB treatment.

HIV co-infection in TB patients has been reported to result in unfavorable clinical outcomes, leading to TB-immune reconstitution inflammatory syndrome (IRIS) and an increased risk of recurrent TB, which may be linked to systemic inflammation [119-121]. In this study, HIV stratification showed elevated levels of serum biomarkers in 2 growth factors (HGF and SCGF-β), 1 pleiotropic mediator (LIF), and 3 pro-inflammatory cytokines (IL-1α, il-12p40, and TRAIL) in both HIV-negative and HIV-positive participants with persisting lung inflammation, when compared to participants with minimal lung inflammation after completion of anti-TB treatment. Additionally, 13 biomarkers, including 3 chemokines (Gro-α, IP-10, and MIG), 3 growth factors (Basic FGF, M-CSF, and SCF), 6 pro-inflammatory cytokines (IL-1β, IL-2Rα, IL-16, IL-17, IL-18, and TNF-α), and 1 anti-inflammatory cytokine (IL-4), were significantly increased only in HIV-negative participants with persisting lung inflammation. This data may indicate that HIV co-infection does not alter the secretion of soluble host biomarkers; rather, these soluble inflammatory mediators may be associated with the developed lung inflammation post-anti-TB treatment. A study by Bal et al. (2005) reported that TB patients co-infected with HIV showed reduced levels of Th1 and Th2 cytokines [122]. However, these were measured during active TB disease and not stratified by TB-related lung inflammation. HIV co-infection in TB patients has been reported to as a risk factor for recurrent TB due to immunosuppression and exposure in areas

with high TB burden [123]. The prevalence rate of TB recurrence has been reported at 1.9 per 100 persons in HIV-negative, while in HIV-positive individuals, it is estimated at 4.5 per 100 person-years [124]. Particularly, a study by Pillay et al. (2021) showed the association of soluble inflammatory mediators with the development of recurrent TB in patients who have completed anti-TB treatment [121]. Furthermore, studies have reported that HIV-infected individuals are at an increased risk of pulmonary impairment despite TB infection [125, 126]. However, a study by Hnizdo et al. (2000) reported that both HIV-negative and positive patients co-infected with TB experienced similar pulmonary impairment [127].

4.2. *Ex-vivo* atorvastatin stimulation reduces pro-inflammatory cytokine profile in Mtb-infected PBMC

Evaluation of HDT candidates against infectious agents such as Mtb represents a growing platform for drug repurposing or identification of new effective drugs. Statins have been shown to exert lipid-independent pleiotropic effects through indirect inhibition of protein prenylation [78]. Additionally, statin use has been associated with decreased risk for active TB disease [128]. This study aimed to evaluate the immune-modulatory effects of atorvastatin on the secretion profile of pro-inflammatory cytokines following infection with different Mtb strains. It is reported that statins modulate the secretion of pro-inflammatory cytokines through inhibition of the NFκβ transcription factor. However, these compounds have shown differential effectiveness in blocking the NFκβ activation. A study by Hilgendorff et al. (2003) reported atorvastatin as the second most potent statin in blocking NFκβ activation with cerivastatin showing the most potency [129]. However, cerivastatin has been decommissioned from the world market [130]. Montero et al. (2000) reported an increased secretion of IL-1β in fluvastatin-stimulated human PBMC infected with Mtb [131]. Additionally, simvastatin stimulation was also reported by Guerra-De-Blas et al. (2019) to increase IL-1β secretion following Mtb infection in human PBMCs [95]. In contrast, this study showed that atorvastatin given as prophylaxis prior to Mtb infection significantly decreases IL-1β secretion in a dose-dependent manner from 1-day post-infection (DPI), regardless of Mtb strain. Mtb infection is known to induce IL-1β secretion by various monocyte cells through activation of Pathogen Recognition Receptors (PRRs) such as TLR-2 and NOD-2. Induction of IL-1β secretion is known to play a crucial role in priming pro-inflammatory responses and enhancing immune cell recruitment during Mtb infection. However, studies have reported that regulation of IL-1β secretion may be important for preventing immune pathology while ensuring host resistance to infection [132]. Furthermore,

elevated baseline levels of IL-6 secretion in patients with active TB disease have been associated with unfavorable TB treatment outcomes, which include treatment failure, recurrence, and mortality regardless of disease severity [133]. This study showed differential regulation of IL-6 and IL-8 in atorvastatin-stimulated PBMCs, which further showed to be dependent on Mtb strain virulence. Elevated IL-8 secretion is associated with susceptibility to TB pathogenesis through increased recruitment of inflammatory cells to the site of infection. This cytokine has been shown to be detected at high concentrations in patients who died from TB disease [134, 135]. Thus, further emphasizing the importance of evaluating additional HDT drugs which will facilitate a controlled secretion of these pathological pro-inflammatory cytokines. This study demonstrated that atorvastatin may be effective as an inflammation modulatory agent to reduce excessive secretion of pro-inflammatory cytokines; however, higher concentrations may be necessary for hyper-virulent Mtb strains.

4.3. Treated TB patients with persisting lung inflammation display reduces lymphocyte and monocyte frequencies with increased inflammatory monocytes

Innate and adaptive immune cells play a crucial role in regulating host immune responses against infectious agents such as Mtb [19]. T-cells are considered as the major regulators of Mtb containment during the early stages of infection, and they have been reported to migrate into the lungs, where they further regulate the secretion of soluble mediators [136]. A study by Deveci et al. (2006) showed a significant reduction in peripheral frequencies of total CD3+ lymphocytes and both CD4+ and CD8+ T-cells in patients with active pulmonary TB at diagnosis compared to healthy individuals [137]. Even though these are known to be reconstituted and return to baseline levels following anti-TB treatment, their reduction has been associated with disease severity and progression to lymphopenia [137-139]. Currently, no data has been reported on cell frequency differences in treated TB patients in relation to persisting lung inflammation. This study observed no significant differences in the frequency percentage of total CD3+ T-cells in treated TB patients with or without persisting lung inflammation at week 0 after anti-TB treatment completion. However, total CD3+ T-cells showed a significant reduction in treated TB patients with persisting lung inflammation (study Arm B/C (TLG $\geq$ 50 SUV)) at week 12 compared to treated TB patients without persisting lung inflammation (study Arm A). Additionally, T-cells have been suggested to regulate immune responses against Mtb infection through PD-1 expression on both CD4+ and CD8+ T-cells. Furthermore, PD-1 expression has been linked with increased activity of Mtb-specific CD4+ T-cells and has been shown to be elevated in smear-positive TB patients

[140]. In this study, there were no significant differences observed between study arms in the regulation of PD-1 expression on CD4+ T-cells. However, PD-1 expression on CD8+ cells was differentially regulated between study Arm A (TLG < 50 SUV) and study Arm B/C (TLG ≥ 50 SUV). PD-1 expression on CD8+ T-cells is a critical immune control point through the induction of cell death in Mtb-infected macrophages expressing PD-L1 [141]. A significant downregulation of PD-1 expression in CD8+ T-cells was observed in study Arm A (TLG < 50 SUV) between week 0, week 12, and week 24 after anti-TB treatment completion, whereas there were no significant changes observed within study Arm B/C (TLG ≥ 50 SUV). This data may suggest continued host-pathogen interaction in treated TB patients with persisting lung inflammation despite the completion of anti-TB treatment and negative sputum cultures. This was further shown by a significantly increased frequency of CD8+PD-1+ T-cells in study Arm B/C (TLG ≥ 50 SUV) compared to study Arm A (TLG < 50 SUV) at week 24 after completion of anti-TB treatment. There were no significant differences observed between the study arms in the frequency of the memory T-cell population indicated by CD45RA and CCR7 expression and the regulatory T-cell population through expression of CD25 and FoxP3.

B-cells are largely known for their antibody production, antigen presentation, and mounting memory responses against invading pathogens. Recently, it has been shown that active TB disease modulates B-cell population frequency through a significant reduction of total and naïve B-cell populations [24]. However, these populations were also shown to be reconstituted to baseline frequencies in treated TB patients. In this study, treated TB patients stratified based on residual lung inflammation following successful TB treatment showed no significant differences in the frequency percentage of naïve B-cells (CD19+CD21+CD27-) at time points week 0 and week 12. However, this cell population remained significantly upregulated in study Arm B/C (TLG ≥ 50 SUV) at week 24 compared to study Arm A (TLG ≥ 50 SUV), even though there were no statistically significant changes observed within each study arm at different time point visits. Furthermore, evaluation of B-cell memory showed a significant reduction in classical memory B-cells (CD19+CD21+CD27+) at week 0 time point in treated TB patients with persisting lung inflammation compared to treated TB patients with minimal lung inflammation, whereas no significant changes were observed at subsequent time points. Additionally, activated memory B-cells (CD19+CD21-CD27+) also showed no significant differences between study Arm A (TLG<50 SUV) and study Arm B/C (TLG ≥ 50 SUV) at week 0 time point; however, these cells showed a significant reduction in

study Arm B/C (TLG ≥ 50 SUV) at week 12. Collectively, this data shows that B-cell population are differentially regulated post-TB treatment, with classical memory B-cell activity suppressed in patients presenting with persisting lung inflammation. This may further be attributed to continued inflammatory responses inducing class-switching in the activated B-cell population in treated TB patients with persisting lung inflammation [142]. This notion has further been shown by Singh et al. (2022), where individuals with active TB disease displayed reduced frequencies of classical memory B-cells compared to healthy individuals [142].

During Mtb infection, dendritic cells (DCs) are known for their function in converting innate immune responses to adaptive immunity through interaction with various lymphocyte cells, including natural killer (NK) cells, NK-T-cells, T-cells, and γ^{δ}T-cells [143, 144]. DCs can be classified based on CD1c expression, which has been reported to present Mtb-derived lipid antigens [144]. In this study, conventional DC classified as CD3-CD1c+ showed no significant difference between the study arms at time week 0 and week 12, whereas a significant upregulation was observed in study Arm B/C (TLG ≥ 50 SUV) at week 24 when compared to study Arm A (TLG < 50 SUV). This was due to a significant reduction of the CD1c+ DC in study Arm A (TLG < 50 SUV) at week 24 compared to week 0 and week 12, whereas these cells remained elevated in study Arm B/C (TLG ≥ 50 SUV). This may indicate the presence of Mtb-lipid antigens in treated TB patients with persisting lung inflammation and a continued inflammatory response priming. This was further highlighted by the upregulation of NK cell populations that have cytotoxic functions. The significant upregulation of activated (CD16+CD56-NKp46+) NK cells observed in study Arm B/C (TLG ≥ 50 SUV) at week 24, may be due to a significant reduction of this cell population observed in study Arm A (TLG < 50 SUV) at week 24 compared to week 0 and week 12, which was not observed within study Arm B/C (TLG ≥ 50 SUV). Additionally, activated conventional NK cells (CD16-CD56+NKp46+) showed no significant differences between the study arms at respective time point visits, and these cells showed significant downregulation in both study arms at week 24 after the completion of anti-TB treatment. CD16+CD56- NK cells are regarded as dysfunctional NK cells and have been reported to have poor cell-to-cell induced cytotoxic functions due to the lack of Neural Cell Adhesion Molecule-1 (NCAM-1) expression [102]. However, they have been confirmed as NK cells through transcriptomics and proteomic evaluation and have been reported to mediate cytotoxic functions through antibody-related mechanisms such as antibody-dependent cell

cytotoxicity (ADCC), antibody-dependent respiratory burst (ADRB), engagement with complement receptor-3, or Fas/FasL interaction [102].

Monocytic cells are widely known for their immediate interaction with Mtb, and they have been shown to prime adaptive immunity through antigen presentation to T-cells [145]. These cells are classified into three principal classes based on CD14 and CD16 expression, which include classical (CD14+CD16-), intermediate (CD14+CD16+), and non-classical (CD14-CD6+) monocytes [26]. This study showed a significant reduction in total peripheral CD14+ monocyte cell population and classical monocytes (CD14+CD16-) at week 0 time point following successful anti-TB treatment in patients with persisting lung inflammation compared to patients with minimal lung inflammation. Expression of CD14 in monocytic APCs is associated with recognition of lipopolysaccharides (LPS) on the membrane of gram-negative bacteria, including Mtb [146]. Furthermore, these cells are known to migrate into the lung tissue where they aid in infection control during active TB state [147]. Additionally, using mice models, CD14-expressing monocytes were implicated in contributing to pulmonary inflammation and death during Mtb infection [148]. The reduced frequency of peripheral CD14+ monocytes observed in treated TB patients with persisting lung inflammation may further imply a continued migration of these cells into the lung space where they further prime inflammatory responses despite sputum culture conversion and completion of anti-TB treatment. Contrary to classical monocytes, non-classical monocytes (CD14-CD16+) were upregulated in Arm B/C (TLG ≥ 50 SUV) when compared to Arm A (TLG < 50 SUV) at week 0 and 24 after the completion of anti-TB treatment. This monocyte subpopulation has been suggested to mediate anti-inflammatory functions through increased production of IL-10 and the maintenance of vascular homeostasis [149, 150]. Furthermore, this study showed differential regulation of CD14-CD16+ non-classical monocytes in study Arm A (TLG < 50 SUV) at different time points, resulting in significant upregulation at week 12 compared to week 0 and a significant downregulation at week 24 compared to both week 0 and week 12, whereas no significant changes were observed within study Arm B/C (TLG ≥ 50 SUV).

Monocyte activation was evaluated based on CD80 and CD86 expressions, which are co-stimulatory molecules that induce T-cell response through binding to CD28 expressed on the T-cells [151]. There were no significant differences observed in the expression of both CD80 and CD86 in classical monocytes between study the study arms at week 0 and week 12. However, the expression of CD86 remained significantly elevated in study Arm B/C (TLG ≥

50 SUV) compared to study Arm A (TLG < 50 SUV), suggesting continued priming of T-cell responses in these treated patients. Activation in non-classical monocytes was highlighted by increased expression of CD80, CD86, or co-expression of both CD80 and CD86. Study Arm A (TLG < 50 SUV) showed significant upregulation of both CD14-CD16+CD86+ and CD14-CD16+CD86+CD80+ at week 12 compared to study Arm B/C (TLG ≥ 50 SUV). However, a significant upregulation of CD14-CD16+CD80+ was observed in study Arm B/C (TLG ≥ 50 SUV) at week 12 compared to study Arm A (TLG < 50 SUV). There were no significant changes observed in the regulation of CD14-CD16+CD80+ and CD14-CD16+CD80+CD86+ within either study arms at different time point visits. However, CD14-CD16+CD86+ showed significant reduction in study Arm A (TLG < 50 SUV) at week 24 compared to both week 0 and week 12. These results suggest that classical monocytes may contribute to the persisting lung inflammation observed in treated TB patients through suspected influx into the lung space, resulting in lower peripheral frequencies. Furthermore, the upregulation of CD80/CD86 co-stimulatory molecules within both classical and non-classical monocytes may further suggest a continued interaction between APCs and T-cells.

4.4. Atorvastatin modulated membrane-bound cell receptors *ex-vivo*

Statins have been suggested to mediate lipid-independent pleiotropic effect through interfering with protein prenylation, which is a crucial post-translational modification required for membrane proteins anchoring to the cell membrane [79]. Particularly, atorvastatin has been shown in COPD patient to mediated pulmonary anti-inflammatory effects by reduction CD45+ expressing cells and neutrophils in the lung [87]. This study showed in an *ex-vivo* model that atorvastatin stimulation had no effect on cell viability at 1 DPI following Mtb infection, despite high concentrations of atorvastatin. This study subsequently aimed to evaluate *ex-vivo* atorvastatin effects at a lower concentration (10µM) in PBMCs isolated from treated TB patients regardless of residual lung inflammation at the end of anti-TB therapy (week 0) and 12 weeks after completion of anti-TB treatment. Here, atorvastatin stimulation displayed immune modulatory effects on PBMCs isolated at week 0 and week 12 after completion of anti-TB treatment, demonstrating its potential as an HDT candidate to regulate immune cell populations, despite immune reconstitution or inflammatory state. A significant reduction in the frequency of naïve B-cells (CD21+CD27-), CD1c-CD11c+ dendritic cells, monocytes (CD14+), and classical monocytes (CD14+CD16-) was observed with atorvastatin stimulation at both week 0 and week 12 after completion of anti-TB treatment, regardless of residual lung inflammation in treated TB patients. However,

activated (NKp46+) NK cell subsets were significantly increased with atorvastatin stimulation. Additionally, Mtb infection of unstimulated PBMCs did not affect the frequency of classical memory B-cells (CD21+CD27+), which were significantly reduced with atorvastatin stimulation. This data may suggest that atorvastatin modulates inflammatory responses through reduction of immune activities mediated by APCs while enhancing cytotoxic activity through upregulation of NK cell activation, thus preventing the priming of adaptive immune responses. Furthermore, the reduction of secondary antibody response through reduced frequency of classical memory B-cells in Mtb infected, atorvastatin-stimulated PBMCs may highlight the ability of atorvastatin as an HDT agent to regulate priming of adaptive inflammatory responses. The expression of the co-stimulatory molecule CD86 was differentially regulated by atorvastatin stimulation on uninfected monocyte subsets, with a significant reduction in non-classical monocytes, whereas no changes were observed in both classical and intermediate monocytes. However, CD86 expression was significantly reduced in Mtb-infected unstimulated PBMCs, which was also not rescued by atorvastatin stimulation. This may suggest that atorvastatin mediates anti-inflammatory functions by repressing the expression of co-stimulatory molecules in monocytic cells, thus preventing antigen presentation and priming of adaptive immune responses. This is contrary to a study by Guerra-De-Blas et al. (2019), which evaluated simvastatin effects and reported an increased expression of co-stimulatory molecules CD80/CD86 by monocytes in Mtb-infected PBMCs following simvastatin stimulation [95]. Interestingly, there were no significant cell population changes observed at week 0 after anti-TB treatment completion in both uninfected and Mtb-infected, atorvastatin-stimulated PBMCs for different T-cell sub-populations, including conventional regulatory T-cells (Tregs) (CD25+FoxP3+), unconventional Tregs (CD25-Foxp3+), CD45RA effector memory T-helper (CD4+CD45RA+CCR7-), and CD45RA effector memory cytotoxic T-cells (CD8+CD45RA+CCR7-). However, atorvastatin stimulation significantly reduced unconventional Tregs, CD45RA effector memory T-helper, and CD45RA effector memory cytotoxic T-cells in uninfected PBMCs isolated at week 12 after anti-TB treatment completion. Furthermore, the frequency of classical M2 monocytes (CD14+CD206-CD163+) showed a significant reduction in infected PBMCs, whether stimulated with atorvastatin or not. However, atorvastatin stimulation in uninfected PBMCs isolated at week 0 and week 12 did not lead to any significant changes in the frequency of activated M2 monocytes (CD14+CD206+CD163+), which were significantly upregulated with Mtb infection in both unstimulated and stimulated PBMCs. Collectively, these data show that atorvastatin

modulates inflammatory response by inhibiting the activation of adaptive immune responses through reduced expression of co-stimulatory molecules in APCs.

4.5. Conclusion

This study demonstrated that a large portion of successfully treated TB patients remain with persisting lung inflammation as determined by FDG PET/CT scans. This work is part of the ongoing StatinTB clinical trial where participants in study Arm B/C (TLG ≥ 50 SUV) are shown to remain with persisting lung inflammation. These participants are subjected to either atorvastatin 40mg/day or placebo in a double-blinded fashion for a period of 12 weeks, followed by an observation period of 12 weeks. Despite the blinding in Arm B/C (TLG ≥ 50 SUV), this study confidently reports that treated TB patients with persisting lung inflammation remain with the elevated secretion of soluble mediators, which is evident from the week 0 time point following anti-TB treatment. Additionally, subsequent time point visits (week 12 and week 24) were collectively analysed in study Arm B/C (TLG ≥ 50 SUV) due to blinding and this further showed elevated soluble biomarkers in these patients. However, in a panel of 48 soluble biomarkers, 15 biomarkers were undetectable from the serum samples obtained from successfully treated TB patients and these include 10 pro-inflammatory biomarkers (IL-2, IL-3, IL-5, IL-6, IL-7, IL-12p70, IL-15, IFN-γ, and IFN-α2), 2 anti-inflammatory (IL-10 and IL-13), 2 growth factors (β-NGF and GM-CSF), and 2 chemokines (MCP-3 and VEGF). Furthermore, treated TB patients presenting with or without persisting lung inflammation showed no significant differences in the frequency of peripheral T-cell subsets, which include Tregs, memory T-cell subsets, and γ^{δ}T-cells at all time points. Atorvastatin demonstrated immunomodulatory effects in an *ex-vivo* model where the pro-inflammatory profile was reduced through modulation of either cell-mediated immunity or soluble immune mediators. However, intracellular mechanisms involved in the regulation of immune responses remain to be elucidated.

4.6. References

1. Cooper, A.M., *Cell-mediated immune responses in tuberculosis.* Annu Rev Immunol, 2009. **27**: p. 393-422.
2. Bermudez, L.E., et al., *The efficiency of the translocation of Mycobacterium tuberculosis across a bilayer of epithelial and endothelial cells as a model of the alveolar wall is a consequence of transport within mononuclear phagocytes and invasion of alveolar epithelial cells.* Infect Immun, 2002. **70**(1): p. 140-6.
3. Harding, C.V. and W.H. Boom, *Regulation of antigen presentation by Mycobacterium tuberculosis: a role for Toll-like receptors.* Nat Rev Microbiol, 2010. **8**(4): p. 296-307.
4. Vyas, S.P. and R. Goswami, *Striking the right immunological balance prevents progression of tuberculosis.* Inflamm Res, 2017. **66**(12): p. 1031-1056.
5. Ndlovu, H. and M.J. Marakalala, *Granulomas and Inflammation: Host-Directed Therapies for Tuberculosis.* Front Immunol, 2016. **7**: p. 434.
6. Flynn, J.L. and J. Chan, *Tuberculosis: latency and reactivation.* Infect Immun, 2001. **69**(7): p. 4195-201.
7. Orme, I.M., R.T. Robinson, and A.M. Cooper, *The balance between protective and pathogenic immune responses in the TB-infected lung.* Nat Immunol, 2015. **16**(1): p. 57-63.
8. Noss, E.H., et al., *Toll-like receptor 2-dependent inhibition of macrophage class II MHC expression and antigen processing by 19-kDa lipoprotein of Mycobacterium tuberculosis.* J Immunol, 2001. **167**(2): p. 910-8.
9. Yoshida, A., et al., *The role of toll-like receptor 2 in survival strategies of Mycobacterium tuberculosis in macrophage phagosomes.* Anticancer Res, 2009. **29**(3): p. 907-10.
10. Guler, R. and F. Brombacher, *Host-directed drug therapy for tuberculosis.* Nat Chem Biol, 2015. **11**(10): p. 748-51.
11. Wilburn, K.M., R.A. Fieweger, and B.C. VanderVen, *Cholesterol and fatty acids grease the wheels of Mycobacterium tuberculosis pathogenesis.* Pathog Dis, 2018. **76**(2).
12. Munoz-Elias, E.J. and J.D. McKinney, *Mycobacterium tuberculosis isocitrate lyases 1 and 2 are jointly required for in vivo growth and virulence.* Nat Med, 2005. **11**(6): p. 638-44.

13. Bloch, H. and W. Segal, *Biochemical differentiation of Mycobacterium tuberculosis grown in vivo and in vitro.* J Bacteriol, 1956. **72**(2): p. 132-41.
14. Pandey, A.K. and C.M. Sassetti, *Mycobacterial persistence requires the utilization of host cholesterol.* Proc Natl Acad Sci U S A, 2008. **105**(11): p. 4376-80.
15. Ortiz de Montellano, P.R., *Potential drug targets in the Mycobacterium tuberculosis cytochrome P450 system.* J Inorg Biochem, 2018. **180**: p. 235-245.
16. Russell, D.G., et al., *Foamy macrophages and the progression of the human tuberculosis granuloma.* Nat Immunol, 2009. **10**(9): p. 943-8.
17. BioRender.com. Available from: https://app.biorender.com/.
18. Rook, G.A., K. Dheda, and A. Zumla, *Immune responses to tuberculosis in developing countries: implications for new vaccines.* Nat Rev Immunol, 2005. **5**(8): p. 661-7.
19. Mayer-Barber, K.D. and D.L. Barber, *Innate and Adaptive Cellular Immune Responses to Mycobacterium tuberculosis Infection.* Cold Spring Harb Perspect Med, 2015. **5**(12).
20. Liu, C.H., H. Liu, and B. Ge, *Innate immunity in tuberculosis: host defense vs pathogen evasion.* Cell Mol Immunol, 2017. **14**(12): p. 963-975.
21. Chen, K. and J.K. Kolls, *T cell-mediated host immune defenses in the lung.* Annu Rev Immunol, 2013. **31**: p. 605-33.
22. Veenstra, H., et al., *Changes in leucocyte and lymphocyte subsets during tuberculosis treatment; prominence of CD3dimCD56+ natural killer T cells in fast treatment responders.* Clin Exp Immunol, 2006. **145**(2): p. 252-60.
23. Rodrigues, D.S., et al., *Immunophenotypic characterization of peripheral T lymphocytes in Mycobacterium tuberculosis infection and disease.* Clin Exp Immunol, 2002. **128**(1): p. 149-54.
24. Joosten, S.A., et al., *Patients with Tuberculosis Have a Dysfunctional Circulating B-Cell Compartment, Which Normalizes following Successful Treatment.* PLoS Pathog, 2016. **12**(6): p. e1005687.
25. Kirman, J.R., M.I. Henao-Tamayo, and E.M. Agger, *The Memory Immune Response to Tuberculosis.* Microbiol Spectr, 2016. **4**(6).
26. Kapellos, T.S., et al., *Human Monocyte Subsets and Phenotypes in Major Chronic Inflammatory Diseases.* Front Immunol, 2019. **10**: p. 2035.
27. Leon, B., M. Lopez-Bravo, and C. Ardavin, *Monocyte-derived dendritic cells.* Semin Immunol, 2005. **17**(4): p. 313-8.

28. Serbina, N.V., et al., *Monocyte-mediated defense against microbial pathogens.* Annu Rev Immunol, 2008. **26**: p. 421-52.
29. Lastrucci, C., et al., *Tuberculosis is associated with expansion of a motile, permissive and immunomodulatory CD16(+) monocyte population via the IL-10/STAT3 axis.* Cell Res, 2015. **25**(12): p. 1333-51.
30. Le, Y., et al., *Infection of Mycobacterium tuberculosis Promotes Both M1/M2 Polarization and MMP Production in Cigarette Smoke-Exposed Macrophages.* Front Immunol, 2020. **11**: p. 1902.
31. Atri, C., F.Z. Guerfali, and D. Laouini, *Role of Human Macrophage Polarization in Inflammation during Infectious Diseases.* Int J Mol Sci, 2018. **19**(6).
32. Lopez-Garcia, S., et al., *Macrophage Activation by Ursolic and Oleanolic Acids during Mycobacterial Infection.* Molecules, 2015. **20**(8): p. 14348-64.
33. Khan, A., et al., *Macrophage heterogeneity and plasticity in tuberculosis.* J Leukoc Biol, 2019. **106**(2): p. 275-282.
34. Castano, D., L.F. Garcia, and M. Rojas, *Increased frequency and cell death of CD16+ monocytes with Mycobacterium tuberculosis infection.* Tuberculosis (Edinb), 2011. **91**(5): p. 348-60.
35. Domingo-Gonzalez, R., et al., *Cytokines and Chemokines in Mycobacterium tuberculosis Infection.* Microbiol Spectr, 2016. **4**(5).
36. Dunlap, M.D., et al., *A novel role for C-C motif chemokine receptor 2 during infection with hypervirulent Mycobacterium tuberculosis.* Mucosal Immunol, 2018. **11**(6): p. 1727-1742.
37. Nouailles, G., et al., *CXCL5-secreting pulmonary epithelial cells drive destructive neutrophilic inflammation in tuberculosis.* J Clin Invest, 2014. **124**(3): p. 1268-82.
38. Flynn, J.L. and J. Chan, *Immune evasion by Mycobacterium tuberculosis: living with the enemy.* Curr Opin Immunol, 2003. **15**(4): p. 450-5.
39. Sigal, G.B., et al., *Biomarkers of Tuberculosis Severity and Treatment Effect: A Directed Screen of 70 Host Markers in a Randomized Clinical Trial.* EBioMedicine, 2017. **25**: p. 112-121.
40. Shi, R., N. Itagaki, and I. Sugawara, *Overview of anti-tuberculosis (TB) drugs and their resistance mechanisms.* Mini Rev Med Chem, 2007. **7**(11): p. 1177-85.
41. Garg, K., et al., *Isoniazid mono-resistant tuberculosis: Time to take it seriously.* Indian J Tuberc, 2019. **66**(2): p. 247-252.

42. Faksri, K., et al., *Comparisons of whole-genome sequencing and phenotypic drug susceptibility testing for Mycobacterium tuberculosis causing MDR-TB and XDR-TB in Thailand.* Int J Antimicrob Agents, 2019.
43. Chaisson, R.E. and G.J. Churchyard, *Recurrent tuberculosis: relapse, reinfection, and HIV.* J Infect Dis, 2010. **201**(5): p. 653-5.
44. Malherbe, S.T., et al., *Persisting positron emission tomography lesion activity and Mycobacterium tuberculosis mRNA after tuberculosis cure.* Nat Med, 2016. **22**(10): p. 1094-1100.
45. Gadoev, J., et al., *Recurrent tuberculosis and associated factors: A five - year countrywide study in Uzbekistan.* PLoS One, 2017. **12**(5): p. e0176473.
46. Glynn, J.R., et al., *High rates of recurrence in HIV-infected and HIV-uninfected patients with tuberculosis.* J Infect Dis, 2010. **201**(5): p. 704-11.
47. Vree, M., et al., *Survival and relapse rate of tuberculosis patients who successfully completed treatment in Vietnam.* Int J Tuberc Lung Dis, 2007. **11**(4): p. 392-7.
48. Sun, Y., et al., *Impact of Multidrug Resistance on Tuberculosis Recurrence and Long-Term Outcome in China.* PLoS One, 2017. **12**(1): p. e0168865.
49. Narayanan, S., et al., *Impact of HIV infection on the recurrence of tuberculosis in South India.* J Infect Dis, 2010. **201**(5): p. 691-703.
50. Gopal, R., R.R. Rapaka, and J.K. Kolls, *Immune reconstitution inflammatory syndrome associated with pulmonary pathogens.* Eur Respir Rev, 2017. **26**(143).
51. Urbanowski, M.E., et al., *Cavitary tuberculosis: the gateway of disease transmission.* Lancet Infect Dis, 2020. **20**(6): p. e117-e128.
52. Elkington, P., et al., *MMP-1 drives immunopathology in human tuberculosis and transgenic mice.* J Clin Invest, 2011. **121**(5): p. 1827-33.
53. Price, N.M., et al., *Unopposed matrix metalloproteinase-9 expression in human tuberculous granuloma and the role of TNF-alpha-dependent monocyte networks.* J Immunol, 2003. **171**(10): p. 5579-86.
54. Parks, W.C., C.L. Wilson, and Y.S. Lopez-Boado, *Matrix metalloproteinases as modulators of inflammation and innate immunity.* Nat Rev Immunol, 2004. **4**(8): p. 617-29.
55. de Melo, M.G.M., et al., *Imbalance of NET and Alpha-1-Antitrypsin in Tuberculosis Patients Is Related With Hyper Inflammation and Severe Lung Tissue Damage.* Front Immunol, 2018. **9**: p. 3147.

56. Squeglia, F., A. Ruggiero, and R. Berisio, *Collagen degradation in tuberculosis pathogenesis: the biochemical consequences of hosting an undesired guest.* Biochem J, 2018. **475**(19): p. 3123-3140.
57. Allwood, B.W., et al., *Post-Tuberculosis Lung Disease: Clinical Review of an Under-Recognised Global Challenge.* Respiration, 2021. **100**(8): p. 751-763.
58. Singh, S., et al., *Immunologic and imaging signatures in post tuberculosis lung disease.* Tuberculosis (Edinb), 2022. **136**: p. 102244.
59. Gai, X., B. Allwood, and Y. Sun, *Post-tuberculosis lung disease and chronic obstructive pulmonary disease.* Chin Med J (Engl), 2023. **136**(16): p. 1923-1928.
60. Pasipanodya, J.G., et al., *Pulmonary impairment after tuberculosis.* Chest, 2007. **131**(6): p. 1817-24.
61. Mosser, D.M. and J.P. Edwards, *Exploring the full spectrum of macrophage activation.* Nat Rev Immunol, 2008. **8**(12): p. 958-69.
62. Fan, J.M., et al., *Interleukin-1 induces tubular epithelial-myofibroblast transdifferentiation through a transforming growth factor-beta1-dependent mechanism in vitro.* Am J Kidney Dis, 2001. **37**(4): p. 820-31.
63. Ameglio, F., et al., *Post-treatment changes of six cytokines in active pulmonary tuberculosis: differences between patients with stable or increased fibrosis.* Int J Tuberc Lung Dis, 2005. **9**(1): p. 98-104.
64. Christine, T., A.P. Tarigan, and F.R. Ananda, *The Correlation between Levels of Transforming Growth Factor-beta with Pulmonary Fibrosis in Post Pulmonary Tuberculosis in Medan, North Sumatera - Indonesia.* Open Access Maced J Med Sci, 2019. **7**(13): p. 2075-2078.
65. Lasco, T.M., et al., *Evaluating the role of tumor necrosis factor-alpha in experimental pulmonary tuberculosis in the guinea pig.* Tuberculosis (Edinb), 2005. **85**(4): p. 245-58.
66. Singh, S., et al., *Antimycobacterial drugs modulate immunopathogenic matrix metalloproteinases in a cellular model of pulmonary tuberculosis.* Antimicrob Agents Chemother, 2014. **58**(8): p. 4657-65.
67. Wang, C.H., et al., *MMP-1(-1607G) polymorphism as a risk factor for fibrosis after pulmonary tuberculosis in Taiwan.* Int J Tuberc Lung Dis, 2010. **14**(5): p. 627-34.
68. Ong, C.W., et al., *Neutrophil-Derived MMP-8 Drives AMPK-Dependent Matrix Destruction in Human Pulmonary Tuberculosis.* PLoS Pathog, 2015. **11**(5): p. e1004917.

69. Wangoo, A., et al., *Contribution of Th1 and Th2 cells to protection and pathology in experimental models of granulomatous lung disease.* J Immunol, 2001. **166**(5): p. 3432-9.
70. Mazzarella, G., et al., *T lymphocyte phenotypic profile in lung segments affected by cavitary and non-cavitary tuberculosis.* Clin Exp Immunol, 2003. **132**(2): p. 283-8.
71. Davies, J.T., et al., *Current and Emerging Uses of Statins in Clinical Therapeutics: A Review.* Lipid Insights, 2016. **9**: p. 13-29.
72. Schachter, M., *Chemical, pharmacokinetic and pharmacodynamic properties of statins: an update.* Fundam Clin Pharmacol, 2005. **19**(1): p. 117-25.
73. Zvizdic, F., et al., *Impact of Different Types of Statins on Clinical Outcomes in Patients Hospitalized for Ischemic Heart Failure.* Med Arch, 2018. **72**(6): p. 401-405.
74. Manzoni, M. and M. Rollini, *Biosynthesis and biotechnological production of statins by filamentous fungi and application of these cholesterol-lowering drugs.* Appl Microbiol Biotechnol, 2002. **58**(5): p. 555-64.
75. Subhan, M., R. Faryal, and I. Macreadie, *Exploitation of Aspergillus terreus for the Production of Natural Statins.* J Fungi (Basel), 2016. **2**(2).
76. Toth, P.P. and M. Banach, *Statins: Then and Now.* Methodist Debakey Cardiovasc J, 2019. **15**(1): p. 23-31.
77. Kalliokoski, A. and M. Niemi, *Impact of OATP transporters on pharmacokinetics.* Br J Pharmacol, 2009. **158**(3): p. 693-705.
78. Stancu, C. and A. Sima, *Statins: mechanism of action and effects.* J Cell Mol Med, 2001. **5**(4): p. 378-87.
79. Hottman, D.A. and L. Li, *Protein prenylation and synaptic plasticity: implications for Alzheimer's disease.* Mol Neurobiol, 2014. **50**(1): p. 177-85.
80. Yang, J., et al., *Intensive Atorvastatin Therapy Attenuates the Inflammatory Responses in Monocytes of Patients with Unstable Angina Undergoing Percutaneous Coronary Intervention via Peroxisome Proliferator-Activated Receptor gamma Activation.* Inflammation, 2015. **38**(4): p. 1415-23.
81. Lazzerini, P.E., et al., *Simvastatin inhibits cytokine production and nuclear factor-kB activation in interleukin 1beta-stimulated synoviocytes from rheumatoid arthritis patients.* Clin Exp Rheumatol, 2007. **25**(5): p. 696-700.
82. Yilmaz, A., et al., *Differential effects of statins on relevant functions of human monocyte-derived dendritic cells.* J Leukoc Biol, 2006. **79**(3): p. 529-38.

83. Romano, M., et al., *Inhibition of monocyte chemotactic protein-1 synthesis by statins.* Lab Invest, 2000. **80**(7): p. 1095-100.
84. Schramm, R., et al., *Statins inhibit lymphocyte homing to peripheral lymph nodes.* Immunology, 2007. **120**(3): p. 315-24.
85. Sabeel, S., et al., *Protocol for systematic review and meta-analysis: impact of statins as immune-modulatory agents on inflammatory markers in adults with chronic diseases.* BMJ Open, 2020. **10**(8): p. e039034.
86. *<EACS. European AIDS Clinical Society. version 9.1. www.eacsociety.orgfiles2018_guidelines-9.1-english.pdf.pdf>.*
87. Mroz, R.M., et al., *Anti-inflammatory effects of atorvastatin treatment in chronic obstructive pulmonary disease. A controlled pilot study.* J Physiol Pharmacol, 2015. **66**(1): p. 111-28.
88. *Global tuberculosis report 2022. Geneva World Health Organization; 2022. Licence CC BY-NC-SA 3.0 IGO. https://www.who.int/teams/global-tuberculosis-programme/data.*
89. Shah, N.S., et al., *Worldwide emergence of extensively drug-resistant tuberculosis.* Emerg Infect Dis, 2007. **13**(3): p. 380-7.
90. Ehlers, S. and U.E. Schaible, *The granuloma in tuberculosis: dynamics of a host-pathogen collusion.* Front Immunol, 2012. **3**: p. 411.
91. Wang, J.Y., et al., *Mixed infection with Beijing and non-Beijing strains in pulmonary tuberculosis in Taiwan: prevalence, risk factors, and dominant strain.* Clin Microbiol Infect, 2011. **17**(8): p. 1239-45.
92. Jo, K.W., et al., *Risk factors for 1-year relapse of pulmonary tuberculosis treated with a 6-month daily regimen.* Respir Med, 2014. **108**(4): p. 654-9.
93. Lovewell, R.R., C.M. Sassetti, and B.C. VanderVen, *Chewing the fat: lipid metabolism and homeostasis during M. tuberculosis infection.* Curr Opin Microbiol, 2016. **29**: p. 30-6.
94. Parihar, S.P., et al., *Statin therapy reduces the mycobacterium tuberculosis burden in human macrophages and in mice by enhancing autophagy and phagosome maturation.* J Infect Dis, 2014. **209**(5): p. 754-63.
95. Guerra-De-Blas, P.D.C., et al., *Simvastatin Enhances the Immune Response Against Mycobacterium tuberculosis.* Front Microbiol, 2019. **10**: p. 2097.
96. Dutta, N.K., et al., *Adjunctive Host-Directed Therapy With Statins Improves Tuberculosis-Related Outcomes in Mice.* J Infect Dis, 2020. **221**(7): p. 1079-1087.

97. Skerry, C., et al., *Simvastatin increases the in vivo activity of the first-line tuberculosis regimen.* J Antimicrob Chemother, 2014. **69**(9): p. 2453-7.
98. Oliviero, B., et al., *Expansion of atypical memory B cells is a prominent feature of COVID-19.* Cell Mol Immunol, 2020. **17**(10): p. 1101-1103.
99. Portugal, S., et al., *B cell analysis of ethnic groups in Mali with differential susceptibility to malaria.* Malar J, 2012. **11**: p. 162.
100. Breton, G., et al., *Human dendritic cells (DCs) are derived from distinct circulating precursors that are precommitted to become CD1c+ or CD141+ DCs.* J Exp Med, 2016. **213**(13): p. 2861-2870.
101. Mavilio, D., et al., *Characterization of CD56-/CD16+ natural killer (NK) cells: a highly dysfunctional NK subset expanded in HIV-infected viremic individuals.* Proc Natl Acad Sci U S A, 2005. **102**(8): p. 2886-91.
102. Forconi, C.S., et al., *A New Hope for CD56(neg)CD16(pos) NK Cells as Unconventional Cytotoxic Mediators: An Adaptation to Chronic Diseases.* Front Cell Infect Microbiol, 2020. **10**: p. 162.
103. Ulevitch, R.J. and P.S. Tobias, *Receptor-dependent mechanisms of cell stimulation by bacterial endotoxin.* Annu Rev Immunol, 1995. **13**: p. 437-57.
104. Geginat, J., A. Lanzavecchia, and F. Sallusto, *Proliferation and differentiation potential of human CD8+ memory T-cell subsets in response to antigen or homeostatic cytokines.* Blood, 2003. **101**(11): p. 4260-6.
105. Li, H., et al., *CD11c+CD11b+ dendritic cells play an important role in intravenous tolerance and the suppression of experimental autoimmune encephalomyelitis.* J Immunol, 2008. **181**(4): p. 2483-93.
106. Johnson, J.L., et al., *Shortening treatment in adults with noncavitary tuberculosis and 2-month culture conversion.* Am J Respir Crit Care Med, 2009. **180**(6): p. 558-63.
107. Ravimohan, S., et al., *Tuberculosis and lung damage: from epidemiology to pathophysiology.* Eur Respir Rev, 2018. **27**(147).
108. Plit, M.L., et al., *Influence of antimicrobial chemotherapy on spirometric parameters and pro-inflammatory indices in severe pulmonary tuberculosis.* Eur Respir J, 1998. **12**(2): p. 351-6.
109. Thompson, E.G., et al., *Host blood RNA signatures predict the outcome of tuberculosis treatment.* Tuberculosis (Edinb), 2017. **107**: p. 48-58.
110. Zhang, H., et al., *Serum level of IL-1ra was associated with the treatment of latent tuberculosis infection in a Chinese population.* BMC Infect Dis, 2020. **20**(1): p. 330.

111. Mortazavi Moghaddam, S.G., et al., *The sequential assay of interleukin-10 and 13 serum levels in relation to radiographic changes during pulmonary tuberculosis treatment.* J Res Med Sci, 2020. **25**: p. 63.
112. Yamada, G., et al., *Elevated levels of serum macrophage migration inhibitory factor in patients with pulmonary tuberculosis.* Clin Immunol, 2002. **104**(2): p. 123-7.
113. Ren, X., et al., *Growth Factor Engineering Strategies for Regenerative Medicine Applications.* Front Bioeng Biotechnol, 2019. **7**: p. 469.
114. Imaizumi, T., *[Hepatocyte growth factor(HGF) in lung tuberculosis]*. Kekkaku, 1996. **71**(10): p. 587-9.
115. Henke, C., et al., *Macrophage production of basic fibroblast growth factor in the fibroproliferative disorder of alveolar fibrosis after lung injury.* Am J Pathol, 1993. **143**(4): p. 1189-99.
116. Burnham, E.L., et al., *The fibroproliferative response in acute respiratory distress syndrome: mechanisms and clinical significance.* Eur Respir J, 2014. **43**(1): p. 276-85.
117. Robinson, R.T., *T Cell Production of GM-CSF Protects the Host during Experimental Tuberculosis.* mBio, 2017. **8**(6).
118. Bhavsar, I., C.S. Miller, and M. Al-Sabbagh, *Macrophage Inflammatory Protein-1 Alpha (MIP-1 alpha)/CCL3: As a Biomarker*, in *General Methods in Biomarker Research and their Applications*. 2015. p. 223-249.
119. Worsley, C.M., et al., *Multi-analyte profiling of ten cytokines in South African HIV-infected patients with Immune Reconstitution Inflammatory Syndrome (IRIS).* AIDS Res Ther, 2010. **7**: p. 36.
120. Lanzafame, M. and S. Vento, *Tuberculosis-immune reconstitution inflammatory syndrome.* J Clin Tuberc Other Mycobact Dis, 2016. **3**: p. 6-9.
121. Pillay, K., et al., *Plasma Biomarkers of Risk of Tuberculosis Recurrence in HIV Co-Infected Patients From South Africa.* Front Immunol, 2021. **12**: p. 631094.
122. Bal, A.M., et al., *Dysregulation of proinflammatory and regulatory cytokines in HIV infected persons with active tuberculosis.* Cytokine, 2005. **30**(5): p. 275-81.
123. Vega, V., et al., *Recurrent TB: a systematic review and meta-analysis of the incidence rates and the proportions of relapses and reinfections.* Thorax, 2021. **76**(5): p. 494-502.

124. Korenromp, E.L., et al., *Effects of human immunodeficiency virus infection on recurrence of tuberculosis after rifampin-based treatment: an analytical review.* Clin Infect Dis, 2003. **37**(1): p. 101-12.
125. Gingo, M.R., et al., *Pulmonary function abnormalities in HIV-infected patients during the current antiretroviral therapy era.* Am J Respir Crit Care Med, 2010. **182**(6): p. 790-6.
126. Gingo, M.R., et al., *Contributors to diffusion impairment in HIV-infected persons.* Eur Respir J, 2014. **43**(1): p. 195-203.
127. Hnizdo, E., T. Singh, and G. Churchyard, *Chronic pulmonary function impairment caused by initial and recurrent pulmonary tuberculosis following treatment.* Thorax, 2000. **55**(1): p. 32-8.
128. Lai, C.C., et al., *Statin treatment is associated with a decreased risk of active tuberculosis: an analysis of a nationally representative cohort.* Thorax, 2016. **71**(7): p. 646-51.
129. Hilgendorff, A., et al., *Statins differ in their ability to block NF-kappaB activation in human blood monocytes.* Int J Clin Pharmacol Ther, 2003. **41**(9): p. 397-401.
130. Furberg, C.D. and B. Pitt, *Withdrawal of cerivastatin from the world market.* Curr Control Trials Cardiovasc Med, 2001. **2**(5): p. 205-207.
131. Montero, M.T., et al., *Hydroxymethylglutaryl-coenzyme A reductase inhibition stimulates caspase-1 activity and Th1-cytokine release in peripheral blood mononuclear cells.* Atherosclerosis, 2000. **153**(2): p. 303-13.
132. Silverio, D., et al., *Advances on the Role and Applications of Interleukin-1 in Tuberculosis.* mBio, 2021. **12**(6): p. e0313421.
133. Gupte, A.N., et al., *Baseline IL-6 is a biomarker for unfavourable tuberculosis treatment outcomes: a multisite discovery and validation study.* Eur Respir J, 2022. **59**(4).
134. Friedland, J.S., et al., *Inhibition of ex vivo proinflammatory cytokine secretion in fatal Mycobacterium tuberculosis infection.* Clin Exp Immunol, 1995. **100**(2): p. 233-8.
135. Ma, X., et al., *Association between interleukin-8 gene alleles and human susceptibility to tuberculosis disease.* J Infect Dis, 2003. **188**(3): p. 349-55.
136. Hoft, S.G., et al., *The Rate of CD4 T Cell Entry into the Lungs during Mycobacterium tuberculosis Infection Is Determined by Partial and Opposing Effects of Multiple Chemokine Receptors.* Infect Immun, 2019. **87**(6).

137. Deveci, F., et al., *Lymphocyte subpopulations in pulmonary tuberculosis patients.* Mediators Inflamm, 2006. **2006**(2): p. 89070.
138. Montes Santiago, J., et al., *[Cellular immune response in tuberculosis: analysis of T-lymphocytes and their subsets, B-lymphocytes and natural cytotoxic cells in different tuberculosis states and body fluids].* Rev Clin Esp, 1996. **196**(4): p. 223-7.
139. Jones, B.E., et al., *CD4 cell counts in human immunodeficiency virus-negative patients with tuberculosis.* Clin Infect Dis, 1997. **24**(5): p. 988-91.
140. Day, C.L., et al., *PD-1 Expression on Mycobacterium tuberculosis-Specific CD4 T Cells Is Associated With Bacterial Load in Human Tuberculosis.* Front Immunol, 2018. **9**: p. 1995.
141. Suarez, G.V., et al., *PD-1/PD-L1 Pathway Modulates Macrophage Susceptibility to Mycobacterium tuberculosis Specific CD8(+) T cell Induced Death.* Sci Rep, 2019. **9**(1): p. 187.
142. Singh, K., et al., *Distinct and shared B cell responses of tuberculosis patients and their household contacts.* PLoS One, 2022. **17**(10): p. e0276610.
143. Reschner, A., et al., *Innate lymphocyte and dendritic cell cross-talk: a key factor in the regulation of the immune response.* Clin Exp Immunol, 2008. **152**(2): p. 219-26.
144. Kim, H. and S.J. Shin, *Pathological and protective roles of dendritic cells in Mycobacterium tuberculosis infection: Interaction between host immune responses and pathogen evasion.* Front Cell Infect Microbiol, 2022. **12**: p. 891878.
145. Adane, T., et al., *Accuracy of monocyte to lymphocyte ratio for tuberculosis diagnosis and its role in monitoring anti-tuberculosis treatment: Systematic review and meta-analysis.* Medicine (Baltimore), 2022. **101**(44): p. e31539.
146. Shams, H., et al., *The CD14 receptor does not mediate entry of Mycobacterium tuberculosis into human mononuclear phagocytes.* FEMS Immunol Med Microbiol, 2003. **36**(1-2): p. 63-9.
147. Lavalett, L., H. Ortega, and L.F. Barrera, *Infection of Monocytes From Tuberculosis Patients With Two Virulent Clinical Isolates of Mycobacterium tuberculosis Induces Alterations in Myeloid Effector Functions.* Front Cell Infect Microbiol, 2020. **10**: p. 163.
148. Wieland, C.W., et al., *CD14 contributes to pulmonary inflammation and mortality during murine tuberculosis.* Immunology, 2008. **125**(2): p. 272-9.
149. Shahzad, F., et al., *Decreased classical monocytes and CD163 expression in TB patients: an indicator of drug resistance.* Braz J Microbiol, 2021. **52**(2): p. 607-617.

150. Narasimhan, P.B., et al., *Nonclassical Monocytes in Health and Disease.* Annu Rev Immunol, 2019. **37**: p. 439-456.
151. Fuse, S., et al., *CD80 and CD86 control antiviral CD8+ T-cell function and immune surveillance of murine gammaherpesvirus 68.* J Virol, 2006. **80**(18): p. 9159-70.

Chapter 5: Study relevance and future Prosperity

5.1. Relevance

TB diseases remain a global threat with increasing percentages of recurrent TB in successfully treated TB patients due to various factors including persisting lung inflammation. Evaluation of additional HDT drugs which can be proven to exert beneficial effects in resolving persisting inflammatory states in treated TB patients represents a growing platform. This will further enhance curbing the growing percentage of TB recurrence. This study demonstrates immune modulatory effects mediated by atorvastatin as an HDT candidate to reduce inflammatory responses.

5.2. Novelty

Recent studies have associated immune responses with early development of pulmonary inflammation during TB disease and treatment. These inflammatory mediators are reported to return to baseline levels comparable to TB diagnosis after completion of anti-TB treatment. This study demonstrates that treated TB patients with persisting lung inflammation remain with elevated inflammatory responses. Furthermore, atorvastatin as an HDT candidate may reduce the inflammatory state in treated TB patients.

5.3. Study Strengths and Limitations

This study is part of the ongoing StatinTB clinical trial which is a randomized, double-blind, placebo-controlled clinical trial aimed at investigating the safety and efficacy of atorvastatin as a host-directed therapy (HDT) to reduce post-TB lung inflammation in TB patients who have completed standard anti-TB treatment. Participants with persisting lung inflammation (Arm B/C (TLG $\geq$ 50 SUV)) after completing anti-TB treatment are randomized to either atorvastatin (40mg/day) or a matching placebo for 12 weeks, followed by an observation period of 12 weeks. However, participant randomization and lipid profile during the trial remain currently blinded. This approach is taken to maintain clinical trial blinding and prevent involuntary unblinding, despite randomization to atorvastatin or a matching placebo. Thus, for the purpose of this thesis work, the evaluation of host serum biomarkers and cell phenotypes at weeks 12 and 24 in study Arm B/C are collectively analysed as a single study arm. In contrast, at week 0, participants are not yet randomized and this represents base-line analysis post-anti-TB treatment relative to lung inflammation. This study combines lung inflammation measured by DFG PET/CT with both soluble and cellular inflammatory mediators after completion of anti-TB treatment. A broad panel of soluble

mediators/biomarkers covering different immunological functions were evaluated from study participants while also stratified by HIV. Cell phenotype analysis using flow cytometry analysis covered both lymphocyte and monocyte populations. However, it is important to note that flow cytometry analysis was not stratified by HIV status. Evaluation of e*x-vivo* atorvastatin immunomodulatory effects covered Mtb strains with different virulence and immunogenicity. However, it is of note that atorvastatin stimulation concentration may not be a direct reflection of systemic atorvastatin concentration in StatinTB clinical trial participants due to variation in metabolism and bioavailability.

5.4. Future prospective

In the StatinTB clinical trial, participant recruitment is still ongoing and lung inflammation is evaluated using FDG PET/CT scan at week 0 and week 12 post-anti-treatment. Additionally, participants are tested for lung function using spirometry while biochemical parameters are used for monitoring safety profiles during the trial. PBMC and serum samples are continuously processed and stored, these will be analysed in batches. Luminex multiplex assay and flow cytometry will be performed on additional clinical samples that have completed specified time points in the StatinTB clinical trial. Stored serum samples will further be used for metabolomics using mass spectrometry. PAXgene blood RNA tubes which are collected during study participants' time point visits will be used for transcriptional profiling using RNA-seq. In addition, *ex-vivo* atorvastatin immunomodulatory effects on phagosome maturation will be assessed using confocal microscopy targeting phagosome markers such as ras-related protein-7 (Rab7), lysosome-associated membrane glycoprotein-3 (LAMP-3), Cathepsin D, and microtubule-associated protein 1 light chain 3B (LC-3B). Following the study unblinding on participants' lipid profile and Arm B/C randomization to atorvastatin or matching placebo, this data will be used to evaluate the safety and efficacy of atorvastatin as an intervention HDT candidate to resolving pulmonary inflammation after completion of anti-TB treatment.